Politecnico di Torino

Master degree in Energy and Nuclear Engineering, Renewable Energy Systems
A.a. 2023/2024
Sessione di Laurea Luglio 2024

Optimization tool for offshore wind farm in Mediterranean area

Relatori:
Prof. Bracco Giovanni
Giorgi Giuseppe
Ghigo Alberto
Petracca Ermando

Candidato:
Bellomo Marcello, 303278

Abstract

Nowadays decarbonisation process and clean energy expansion are in full development era and increasing trend for future are encouraging.Through the numerous typologies of renewable technologies offshore wind has been estimated to have good opportunity of increasing in gross installed power for its large potential, possibility of exploit large maritime areas and cost that are in decreasing trend. All these advantages place this technology in a relevant role for worldly energy market share, not only for electric energy perspective, but with more innovative green H2 production or Power-to-X.

Offshore wind farms nowadays are mostly located in China and Northern Europe countries but most exploitable areas such as Mediterranean basin see more difficulties in development of this technology because of economic and technological issues. However numerous projects have been already presented to governments of countries facing Mediterranean sea, among countries that have already a renewable program and countries that rely still on conventional energy sources to "clean" their energy mix.

This thesis work claims to investigate, through a specifically designed tool in Python language, the optimization of a floating offshore wind farm in Mediterranean basin with the aim of help spreading offshore wind projects in the area where this technology is unexploited. The objective is to provide an overview of the possible optimal configuration of the wind turbine farm, the energy balance, and the costs that will be faced, taking into account some constraints defined by the final user. The tool has been created and carried on internally at MOREenergy Lab.

Reached results demonstrate that tool is accurate and can firstly simulate, through fluid dynamic and economical models, and then optimize a wind farm for chosen position in Mediterranean basin. Numerical results, obtained through a case study of a 900 MW farm located 10 km from the coast, show for optimized farms better performance in terms of annual produced energy with less wake effects and an improvement in economic indicators (-3% of LCOE from 104.9 to 101.8 €/MWh) following also minor Capex costs that lead to better investments. On the other hand, a larger reduction of the visual impact, (-46% passing from 171.3 to 92.8 cm^2) measured in occupied horizon area, visible from nearest coast can improve social acceptance. Finally, the economic model validation and the evaluation of optimization tool through a convergence study are done.

The presented work has the potential to significantly increase the sustainability and economic viability of wind energy projects. It also evidence the limits in utilisation of this instrument for example in restricted grid resolution to let user better understand how much simulations are reliable. This approach has the potential to significantly increase the sustainability and economic viability of wind energy project towards the untapped Mediterranean basin.

Keywords: *Offshore wind, Optimization, Visual impact, Python, Genetic algorithm*

Summary

List of figures

List of tables

Chapter 1

Introduction

Offshore wind farm with its big potential and versatility have been starting to spread all around the world with the stimulus of increasing in energy demand. Nowadays energy production market has to deal also with low environmental impact rules and the occupation of exploitable land that, with increasing in population, has to be split accurately between human residencies, food production and economical activities including the fundamental energy generation. For these reasons go floating to exploit portion of sea has been an attractive idea in last 10 years with large investments of governments and big companies in energy sector.

The attractiveness of offshore wind in particular in Mediterranean area has inspired a tool creation and all the work for this and other thesis [1] [2] developed inside MOREnergy Lab [3].

Considering the developing of this thesis work firstly, the state of the art and the development of offshore wind technology will be explained with a focus on the Mediterranean area, highlighting its increasing importance in recent years for the decarbonisation targets of the EU for 2030 and 2050, along with a view on current technology development.

Then the optimization tool will be presented, explaining the dataset input that has been utilized, followed by site selection, the model creation and description for fluid-dynamic, economic and visual impact evaluations in highlighting the functions used in the Python environment.

1.1 Renewables energy in Europe and Mediterranean

In the world we live that must face many future challenges, overpopulation and climate change on top, Renewable energy production plays a relevant role. Clean energy can be considered a breakpoint between the carbon era (the twentieth century) and the new century, with all world countries moving rapidly towards energy transition in order to avoid rise of global temperature above 2° C from preindustrial era. Clean energy market worth 1.77 trillion dollars in 2023 [4], of which electric energy production is only a part,and also include electrification of transport, heat and energy storage, grid upgrades, and hydrogen production.

Talking about Eu-27 data are positive with 360 billion invested in 2024 [4], total that is overcome only by China. All this money invested are visible through data about energy production: in EU total production of 2797 TWh in 2022 is covered at 38% from renewable energy in all his forms with respect to the 16% from fossil carbon [5], 20% from natural gas and 22% from nuclear source and so the hoped

scenario is finally occurred in fact the energy production by renewables overcome the one by traditional carbon source as shown in Figure 1 below.

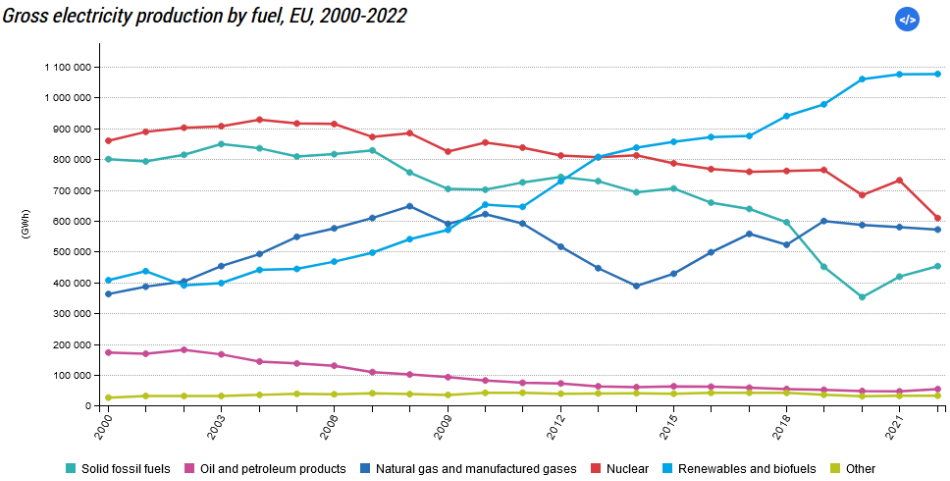

Figure 1 Gross energy production by fuel 2000-2022

The share of renewable energy has risen considerably in the last ten years, setting a trend that follows the EU directives on energy production and greenhouse gas emissions (EU Green Deal) [6], which aims to reduce greenhouse gas emissions by 55% in 2030 compared to 1990 levels and climate neutrality in 2050. It's claimed that for his climate friendly policy EU is considered a world leader.

Another launched program is Repower EU, which represents a strategy to make Europe independent from fossil fuel imports. The plan, with various strategies, has been funded with 300 billion euros, which will partially boost the expansion of renewables [7].

In this scenario wind energy represent a big contribute to the European energy mix with 272 GW of already connected power [8] and a trend of installation that is continuously growing: 18,3 GW of new plant in Europe in 2023 of which 3,8 GW are offshore installation as visible in Figure 2.

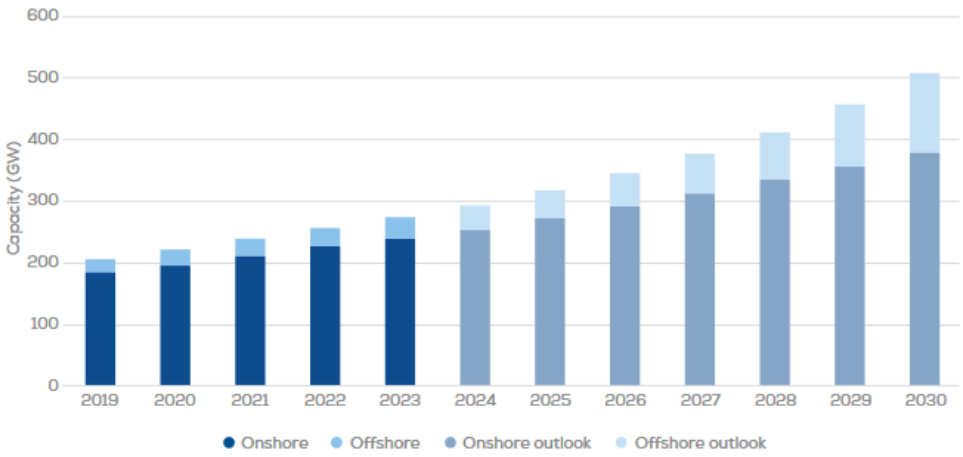

Figure 2 Wind power installed by typology in EU-27

Focusing on Mediterranean primary energy supply, as shown in Figure 3 [9], countries situation is divided into: Northern countries (e.g. Albania, Italy, Spain, Montenegro) that invest strongly on renewables such solar PV, wind and hydroelectric and Southern and Eastern countries (north African countries above all) in which the energy mix is only composed by oil and natural gas due to large deposits of this assets.

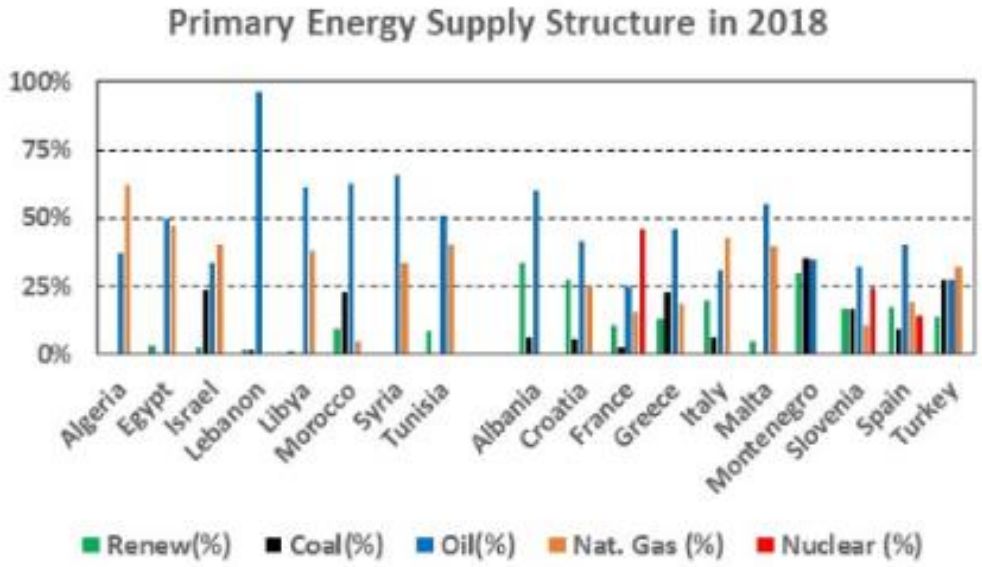

Figure 3 Primary energy supply in Mediterranean area in 2018

Using Mediterranean unexploited large areas with energy plants like offshore wind and wave energy converter could be a great opportunity for countries to enlarge or in such case begin renewable share in energy mix not only for with conventional usage but with perspectives of innovative utilization such green hydrogen production, Power-to-X and also energy for desalinization purpose that can resolve the problem of scarcity of clean water for countries affected by desertification.

1.2 State of art of offshore wind turbines farms

Offshore wind technology starts with the idea of placing wind turbines in water surfaces that can be sea or also lake to resolve issues and improve the already existing and well-known wind technology for energy production onshore.

Offshore wind turbines have many advantages comparing with onshore wind fields:

- Exploiting undisturbed and more consistent wind energy with no terrain obstacles.
- Vaste portion of marine area can be used with less constraints specially for floating type.
- Visual impact is less relevant with respect to onshore turbines.
- Possibility to give electricity for energy disadvantaged zones like minor islands.

Beside advantages also drawbacks can be underlined since offshore technology cannot be defined mature yet:

- Major costs with respect to onshore counterparts related to transportation of structures and substructures and grid connection.
- Technology issues with submarine structures or buoyancy structures as well be seen below and electric energy transportation on land.
- Dependency on large ports facilities and requirement of heavy vessels for the heavy structures.
- Environmental impact on marine vegetal and animal species not very well studied yet.

Among the offshore plant seabed fixed plant and floating plant are distinguished as shown in Figure 4 [10]. While bottom fixed use structure anchored to seabed and so can be installed in location with width up to 60 meters, floating type has not foundation and are docked to the seabed through anchoring system and cables and so can be placed at farther distance and deeper depth also permitting to exploit stronger wind, to be less visual impacting, to be less environmental impact for the marine life and also to reduce conflict with other economic activities that are normally performed near coast.
Both technology permit to exploited large turbines up to 15 MW (since constraints of occupied area, hub height and noise control are relaxed compared to onshore installations) that have better performance with respect to lower size in utilize also relatively low wind speed and can offer better power density in optimized maritime areas.

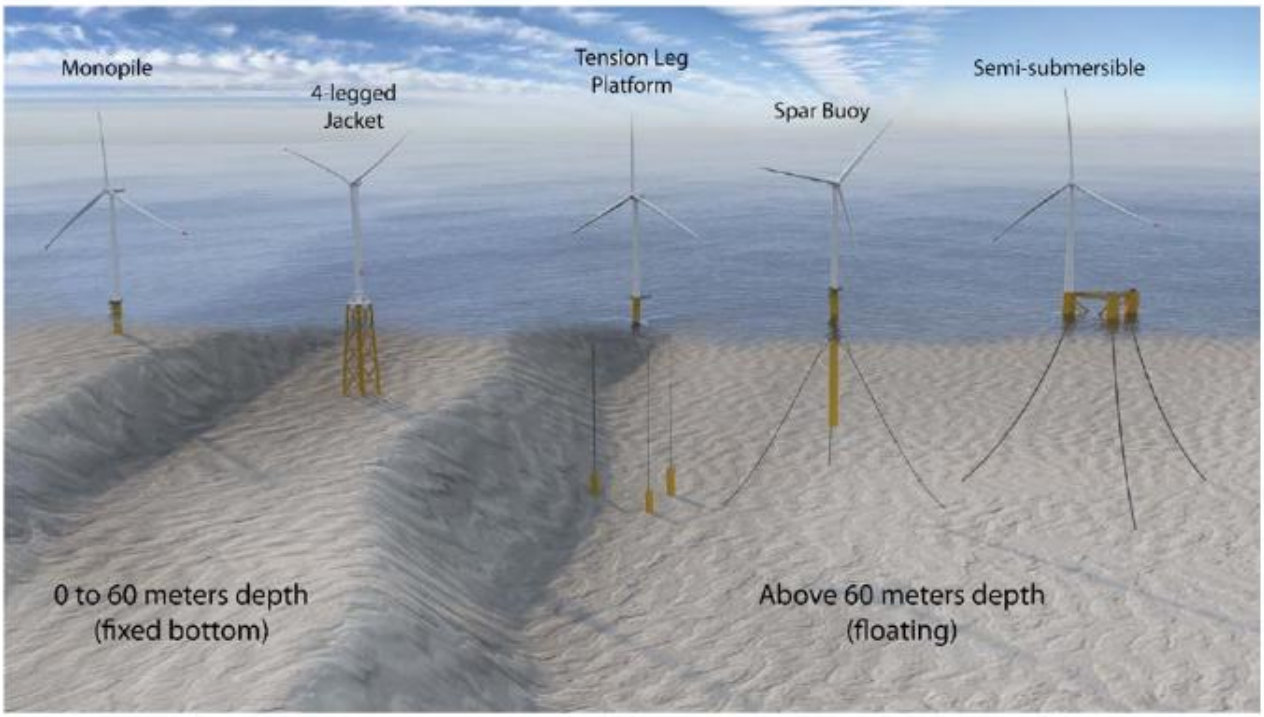

Figure 4 Offshore wind developed technology

Bottom fixed is an already mature technology that permit to stabilize with basement wind turbines also for though conditions of sea and wind, but it suits only for relatively shallow water.

Floating offshore, on the contrary, is a promising technology non totally came out from development stage but that will allow to exploit all wind potential also far from the coast. Substructures for floating offshore wind nowadays are of three types, they are chosen among vantages and disadvantages depending on height and size of turbines to be installed, cost, type of seabed, sea and wind conditions, difficulties of transportation and assembling.

An overview of the three different technology is showed in Table 1 below.

Table 1 Substructure typology comparison [10]

Substructure	Advantages	Disadvantages
SPAR	• Low cost • Low platform motion • Low wave profile	• Wide anchor footprint • Difficult assembly • Deep draft required
SEMI-SUBMERSIBLE	• Potentially low platform motion • Static stability for assembly and towing	• Wide anchor footprint • Corrosion potential • Wave exposure at waterline
TENSION LEG PLATFORM	• Small anchor footprint • Low cost • Low platform motion • Low wave profile	• Unstable without mooring system • High vertical load moorings

As well as the substructure mooring and anchoring system must be well designed for floating type. While catenary and Semi-taut mooring are simplest but with weight and overlapping problems, taut and tension leg made with synthetic ropes are more compact and suitable for deep seabed applications. Example is showed in Figure 5.

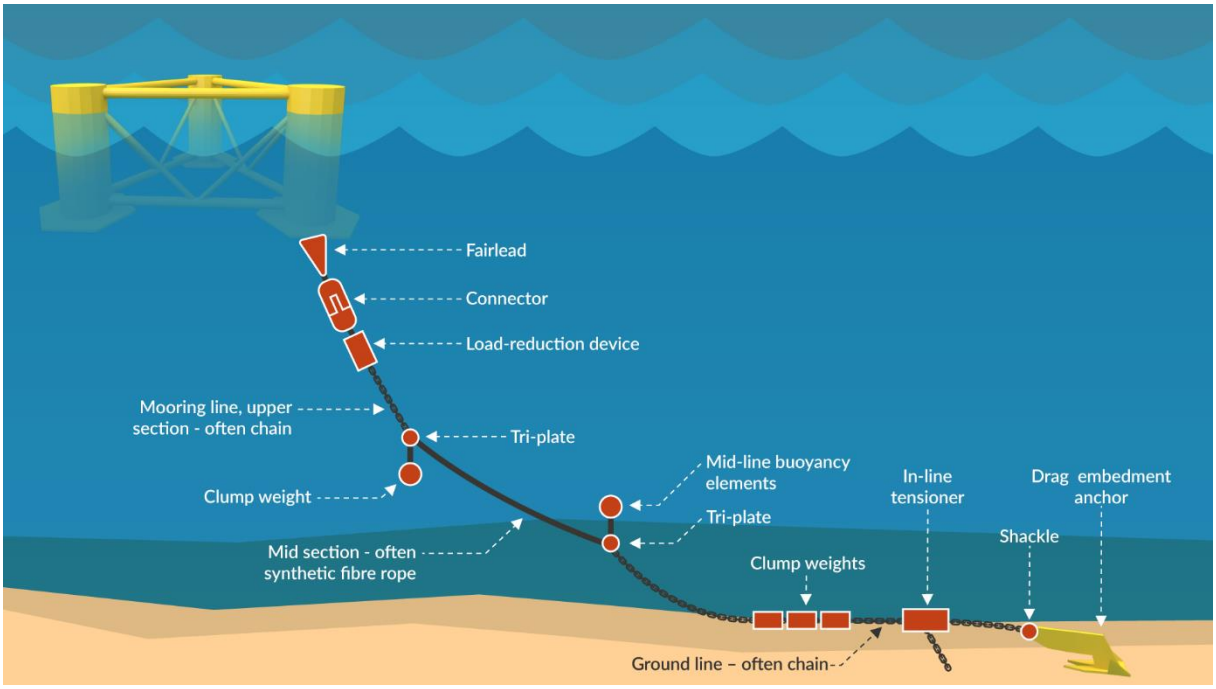

Figure 5 Mooring and anchorage system

To connect all generated energy coming from every array of turbines a well projected system of sub marine cables and substations is needed. Typical schemes involve the utilization of medium voltage cables of 33 kV AC to connect turbines to each other and all arrays to an offshore substation that has the role of rise voltage up to 132 – 220 kV AC, to avoid cable losses, and finally send electricity onshore. In some case utilizing DC current when the farm is very farm from coast is desirable to minimize cable losses, this option require two additional substation (one offshore and one onshore) to operate pre and post current conversion. In Figure 6 [11] an example of cable connection is showed enlightening cables and substations.

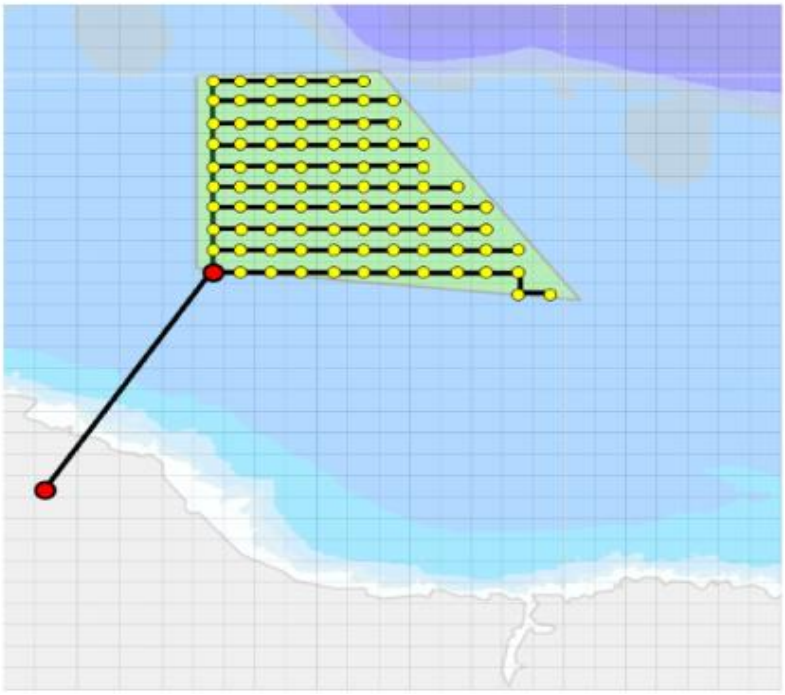

Figure 6 Example of cable connection

1.3 Spatial layout of offshore wind farms

Spatial distribution for offshore wind farms requires well design to satisfy many objectives: costs reduction and produced energy enhancement that have the aim of maximize the investment but in such case also visual impact reduction from the coast perspective has to be considered. Principal variable is the main wind direction that must be stated both with sea conditions (current and waves height) and sea depth.

Containing the costs can tend to closer layout in order to minimize cables, installation and maintenance costs, maximize efficiency and produced energy can lead to wide layout to avoid disturbance in air stream (shade effect) and more wake losses. Another parameter is also the authorized area and the sea conditions that frequently lead to non-regular layout.

Below a list of typical design layout is reported:

- Rectangular layout [12]: the simpler and easier to project layout with equidistance between turbines has the cons of not taking into account shade effects in respect with other configuration but simplify maintenance and installation operations.
- Staggered layout: Figure 7 [13] shows rectangular base with staggered arrays that permits a better control on wake losses but require longer project time and more accurate wind studies.

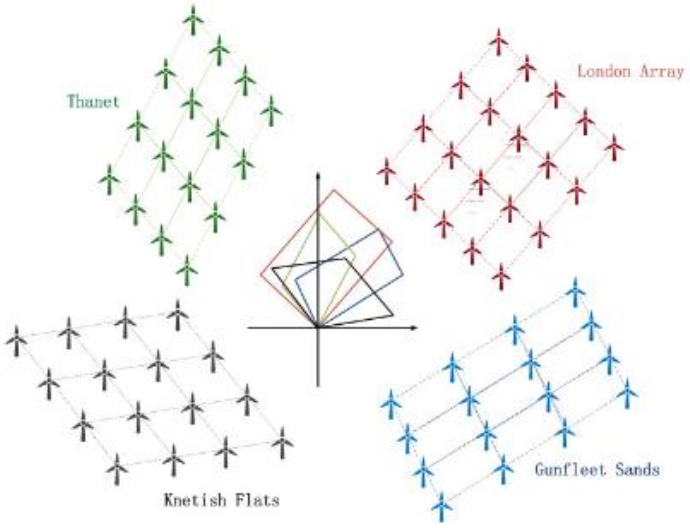

Figure 7 Example of staggered layout

- Radial layout [14]: regular layout form that can lead to maximize space occupation, has the pros of intercept wind coming from several directions and to simplify maintenance and installation operations because offshore energy collecting substation is placed at the centre of the farm with branches that collect every radial array of turbine to the centre. In this way cables lengths are controlled to avoid electric losses and maintenance is easier.

- Non regular layout: well projected layout that maximize energy production or more than one objective utilising specific optimization algorithms. Irregular or sparse layout can lead to more difficult cables connect and less efficient installation and maintenance operations with a more difficult project phase but can ensure economic and fluid dynamic efficiency.

In the following paragraph an account of layout optimization algorithms is treated.

1.4 Optimization algorithms for offshore wind farm

Layout optimization of offshore wind farms has been investigated by multiples sectorial studies in order to give an help in project phase about pursuing different objectives that can be economical, energetic or also from environmental impact point of view.

Implemented optimization algorithms used for searching best layout for offshore wind farms can be divided into three main types according to [15]: Calculus based methods, heuristics methods and metaheuristics methods. For specific characteristics of problem such as number of objectives, applied constraints and available computing power, one method has to be chosen rather than others. For simplicity and effectiveness in many applications Genetic Algorithm, that will be presented below, is the most utilised method and has been much tested, so other methodologies often are compared with it in terms of efficiency as it is enlightened below.

Below an overview of different existing method are reported with reference to sectorial studies.

- Calculus based methods: called also gradient-based optimizations, this algorithms implement deterministic, non-deterministic and iteratives methods that rely on the first and second order derivative of the objective function to find the optimal solution. Examples can be found in [16] in which a comparison has been made with Genetic algorithm overperforming it and in [17] that has develop a better layout of Horns Rev 1 wind farm of about 7.3% in power gain. Algorithms of this type are not so popular for various issues including their high computational cost, they are not suitable for non-derivative functions, have problems with non-convex solutions area and not handle constraints very well.

- Heuristics methods: since exact optimized solutions obtained with gradient methods are difficult to be computed heuristics methods are defined as approximate methods since they made a trade-off between the final solution quality and spent computational time because they implement semi empirical rules. Heuristics are classified in two different groups: constructive and iterative. Constructive heuristics build a complete solution by performing multiple sequential deterministic or non-deterministic assemblies of the involved variables while considering all defined constraints. Iterative heuristics attempt to improve a complete solution (that can be

obtained from a constructive heuristic) by doing a controlled evaluation of the local search space of each of the involved variables. Examples of application are Random Search (RS) presented in [18] in which the model has performed well in reduction of computational time with respect to common wind optimization software in the market, Greedy Heuristic Algorithm (GHA) studied in [19] that assess capability of algorithm to perform better than Genetic Algorithm in placing turbines with different hub heights in the same farm, Monte Carlo Method presented in [20] that has showed to perform better in such case than Genetic algorithm. Despite the relative velocity of this methods compared to gradient based not always computed solutions are optimal.

- Metaheuristics methods: metaheuristics are evolution of heuristic algorithm since they are more efficient. They are computational methods that implement usage of nature-based optimization strategies and are suitable for nearly every type of problems and so also for large farms since they are very easy to implement. Since they can manage also complex problems their utilisation in optimal layout research for wind farm has been deeply studied. Some examples are Genetic Algorithm (GA) [21] based on evolutionary survival of species, that study affirm the effectiveness of the method and the optimization of variables number to obtain a less time consuming solution, Simulated Annealing Algorithm (SAA) [22] based on concept of lowering energy in solids this study affirm the effectiveness of this method giving optimal but different layout comparing with other metaheuristics method, Particle Swarm Optimization (PSA) [23] in which a strategy inspired by social behaviour of fish is utilised combined with local search strategy to optimize micro siting problems.

Table 2 below sum up different methods.

Table 2 Optimization methods comparison

Optimization method	Nominal power [MW]	Technology	Ref
Gradient based	90-360	1.8 MW	[16]
Sequential convex programming	160	2 MW	[17]
Local search	735.5	2.5 MW Onshore turbine	[18]
Greedy algorithm	7.6-13.3	Turbines with hub height between 50/78 m	[19]
Monte Carlo simulation	156-192	6 MW	[20]
Genetic Algorithm	14-32	-	[21]
Simulate Annealing	14-34	-	[22]
Particle Swarm Optimization	27.2	850kW	[23]

1.5 Economic perspective of offshore wind sector

Since the first offshore farm has been installed in Denmark in 1991 (Vindeby), this technology has been spread all over the world in the last 30 years. Major investors in this technology are North Europe countries (UK, Germany, Netherlands) and China. Chinese market has reached up the 50% of offshore wind share in 2023 (as showed in Figure 8) with enlarging in the last years government funding. [24]

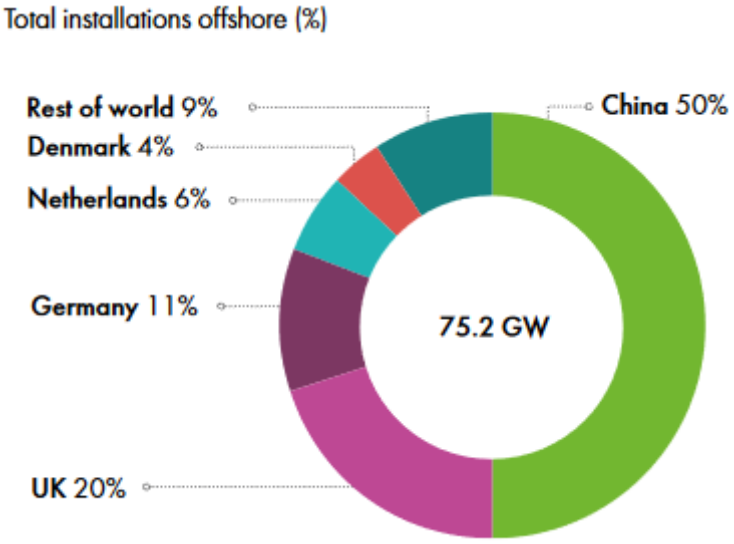

Figure 8 Offshore wind world market share

Countries leaders in this field for Europe, as above mentioned, are northern Europe countries that take advantage of strong wind of North Sea in particular five countries have invested a lot in this sector in the last years (UK, Denmark, Netherlands, Germany, Belgium) accounting for 96% [8] of offshore wind capacity in Europe that account for 34 GW or 4% in Europe energy mix [8].

In Mediterranean Sea most of the offshore wind potential due to bathymetry conformation is conveniently exploitable only by floating platforms technology of which 207,3 GW [25] only in Italy that has great offshore potential along Sicily and Sardinia coast. The following map in Figure 9 shows areas that can be potential be profitably exploited considering distance and depth limitations in a study of EU [26].

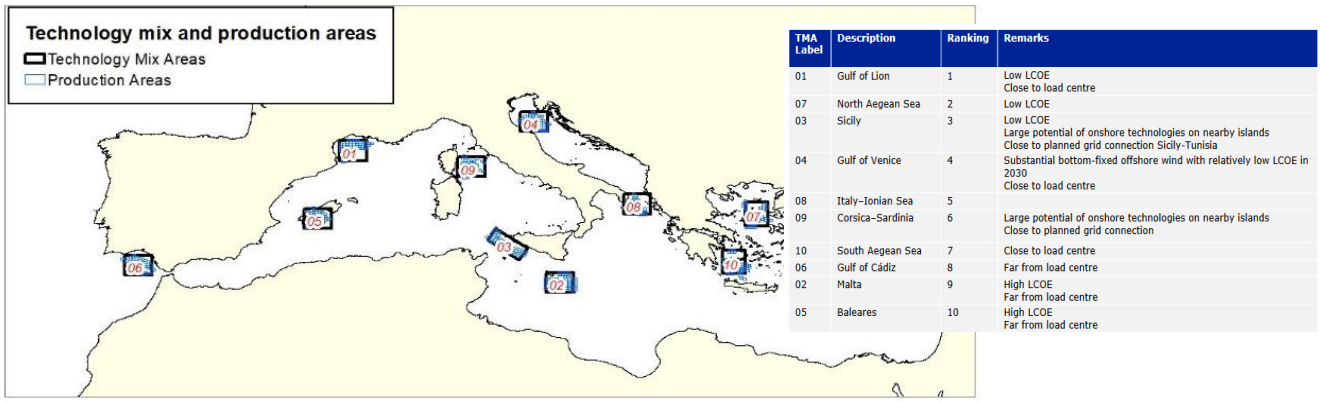

TMA Label	Description	Ranking	Remarks
01	Gulf of Lion	1	Low LCOE Close to load centre
07	North Aegean Sea	2	Low LCOE
03	Sicily	3	Low LCOE Large potential of onshore technologies on nearby islands Close to planned grid connection Sicily-Tunisia
04	Gulf of Venice	4	Substantial bottom-fixed offshore wind with relatively low LCOE in 2030 Close to load centre
08	Italy–Ionian Sea	5	
09	Corsica–Sardinia	6	Large potential of onshore technologies on nearby islands Close to planned grid connection
10	South Aegean Sea	7	Close to load centre
06	Gulf of Cádiz	8	Far from load centre
02	Malta	9	High LCOE Far from load centre
05	Baleares	10	High LCOE Far from load centre

Figure 9 Exploitable area for offshore wind in MED region

In the Mediterranean area numerous offshore wind projects are already presented and submitted for approval, however due to lower wind resource and the prohibitive seabed depth comparing to North Sea leading to more technical issues and less profitable investments, several projects have been cancelled or delayed. Companies that have resources to invest in the offshore wind sector complain about inadequate infrastructures, unclear regulatory frameworks and lengthy permitting procedures operated by countries. Social acceptance (NIMBY effects) and conflict with several sea uses are other restrictions to spreading. Mediterranean offshore potential for these reason is nowadays nearly unexploited despite the large number of presented projects [27] in different countries as shown in Table 3 below (N.B France and Spain projects are also located in Atlantic Ocean).

Table 3 Offshore projects presented in MED area

Country	Nr. of projects	Total capacity	Status	Updates
Albania	1	539 MW	cancelled	Offshore wind resource mapping ongoing (EBRD)
Croatia	2	840 MW	cancelled	Non-binding target of 0.5 GW
Cyprus	1	44 MW	cancelled	
France	46	20883 MW	Pre/under construction (2506 MW), dev. zone (13980 MW)	In March 2023, France awarded 1 GW capacity to be installed along the coast of Normandy
Greece	59	9280 MW	Only 2600 MW in dev. zone	New NECP presented (2.7 GW by 2030)
Italy	122	84338 MW	Early planning (74324 MW), cancelled/dormant	Terna provided technical concession solutions for a total of 95 GW by end 2022
Malta	4	636 MW	cancelled/ dormant	Various studies undertaken – a min of 50 MW according to Energy Minister
Portugal	19	15310 MW	About 430 MW cancelled	Auction for projects of 1 GW capacity by end 2023; aiming at 10 GW by 2030
Spain	127	26156 MW	Early planning (17885 MW), cancelled/dormant	Offshore Wind and Marine Energy Roadmap 2022 (1-3 GW by 2030)
Tunisia	1	NA	cancelled	Feasibility study ongoing
Türkiye	1	1200 MW	dormant	1st tender announced in 2018 – new ToRs for the investigation of sites in the Marmara sea published in June

Nowadays only Italy and France has operating offshore wind farms but only in pilot projects or in relatively small scale, Beleolico project in Taranto (Italy) [28] a 30 MW bottom fixed field is one of them.
In literature can be found an high number of presented project e.g.:

- Provence Grand Large [29] 25 MW floating offshore wind project is situated 40 km west of Marseille and it's been already connected to grid (FR)
- EolMed [30] presented project in advanced status 30 MW offshore wind farm (3 wind turbines) 15 km off the coastal town of Gruissan (FR)
- MedWind [31] a 2,8 GW presented project in advanced approval status placed near Egadi islands (IT)
- Atis Floating Wind [32] 864 MW project presented far from Tuscany coast (IT)
- Olbia-Tibula [33] offshore wind farm a 975 MW project 25 km away from Olbia coast of Sardinia (IT)
- Nereus [34] a projected farm of 1800 MW near Barletta coast (IT)

To also consider offshore investment trend price of technology should be evaluated. The world cost for floating type is about 145 $/MWh [35] (136 €/MWh) but for Mediterranean area this value can be higher due to non-optimal site and lack of infrastructure and dedicated industry in the interested country but it is forecast to became smaller in the following years.

Nevertheless, with the progress in technology and the policy of governments we will see soon offshore turbine in Mediterranean area and so work done in this thesis want to be a small contribute to floating offshore wind spread all over the area.

1.6 Methodology for offshore wind farm simulation tool building

Like every energy production facility, an offshore wind farm in project phase must consider optimization to maximize generated energy, maximize exploitation of allowed area, minimize time of investment recovery and initial costs, minimize impacts of constructions on surrounding ecosystems and human activities.

With estimation of wind resource and optimization purpose for offshore wind farm many studies have been carried out. From the work estimation of Mediterranean bathymetry and wind resource presented in [2], a specific tool has been developed in [1] to join energy producibility, cost estimation and wake effects study for every point of Mediterranean sea.

Studying of wake effects is beneficial in pursuing optimization and analysing wind farms. Wake showed in Figure 10, so interaction between every wind turbine to each other in deflecting main air stream as visible, impact spacing of arrays in wind farm and it is crucial to optimize energy production. Beside spacing optimization also the optimal allowed area exploitation and the optimal turbine size is object of study in project step as done in [36].

Figure 10 Wake effects visualization

Also from economical perspective many works has been carried out to characterize every voice of cost from initial to operational costs in order to estimate LCOE (Levelized cost of energy) and return of investment for projects as seen in [37] and [11].

Since is known that renewables have lower energy density than conventional technologies, the issue of large occupied areas and visual impact of plants can influence heavily new projects. For offshore wind the mean energy density has been estimate in range between 4.9 and 5.9 MW/km^2 [38], this means occupied area that, according to nominal power, can reach tens of square kilometres. Big issues with this occupied area, despite located far from coast, is the visibility for near population and so the visual impact has to be considered in initial phase of projects as assessed in [39].

The focus of this thesis work is the implementation of an optimization algorithm for offshore wind farms with multiple objectives concerning balancing between the social acceptance and technoeconomic objectives. The chapters will include the Genetic Algorithm implemented for optimization purpose and its convergence study, the visual impact function created to provide an overview of how the wind turbine farms will be perceived from the coast and how they can impact the citizens view, the added constraint regarding site selection to avoid high maritime route density areas, and an accurate characterization of cost functions for calculation of LCOE by considering the distance from the selected site to the nearest port facility that affects installation costs.

In Figure 11 below an overview of tool working is showed with synthetic explanation of arguments that will be investigated through body of thesis.

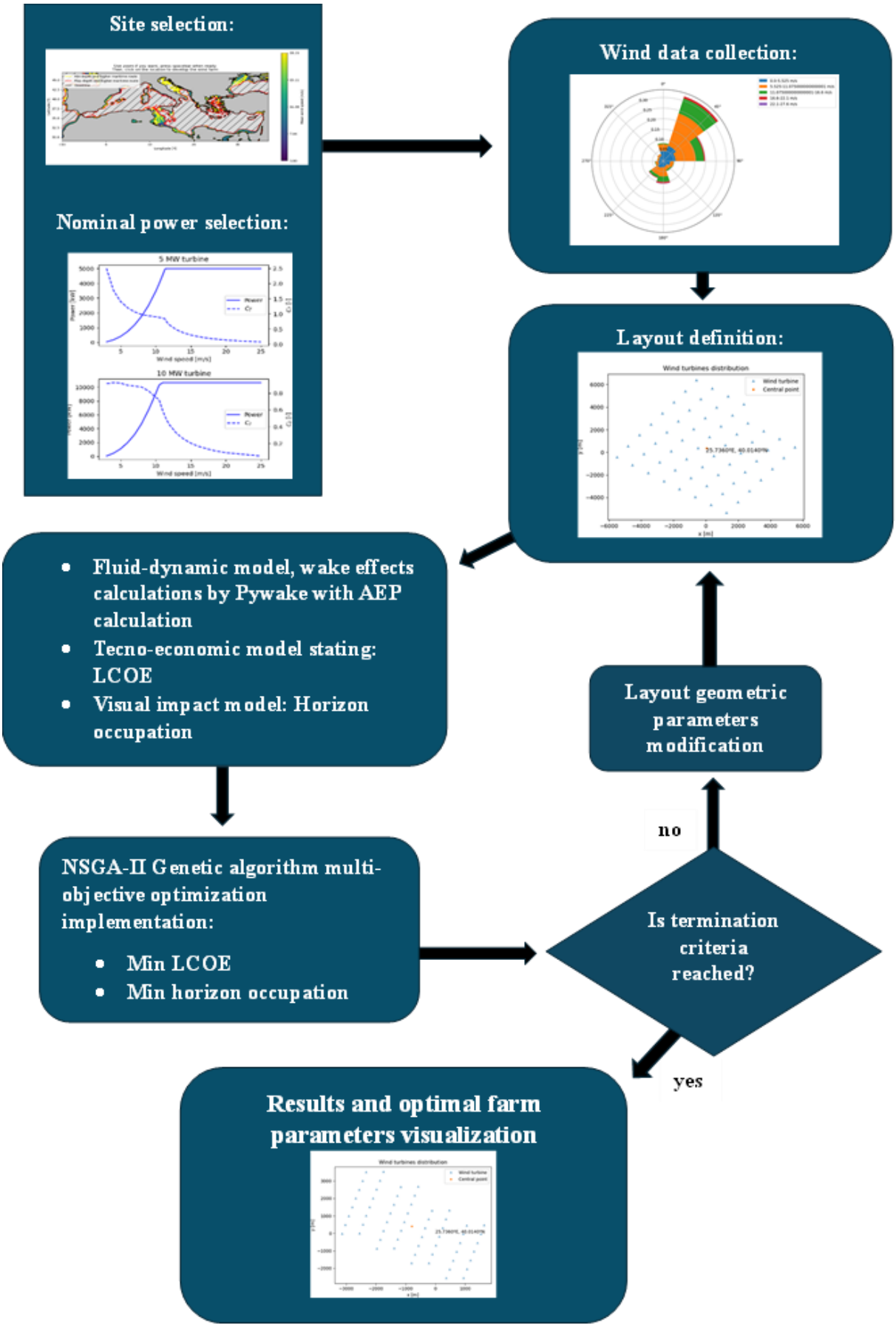

Figure 11 Workflow of applied method

To better understand functioning of tool every step is then explained with a resume of insights that will constitute every next chapter.

- Size selection and siting: as will be explained in 2.1, through Python terminal user is asked to give as input the nominal power and the size of turbines (or alternatively max sea area and power density value) in wind farm that he would simulate. Then user is asked to furnish limitations in their environmental choice: min and max sea depth, min and max distance from coast and max acceptable value of maritime route allowed. Coordinates selection is then performed as input by user. Every pair of coordinates in Mediterranean basin can be chosen, within limitations imposed before, trough manual writing or trough selection in a created map.

- Data collection: trough implemented function in Python environment explained in 2.1, for selected point, data for bathymetry status, wind speed and direction condition, distance from nearest port facility and power curve for selected turbine size are searched and elaborated. This step is a little bit time consuming for the large number of data to be elaborated.

- Farm layout implementation: following the site choice and collection of data then layout parameters are selected so space between turbines in wind and crosswind direction and angle between array that will be changed during the optimization process as it's outlined in 3.1. These parameters are crucial because influence farm wake losses and so energy production as well as visibility of entire farm from the coast.

- Implementation of models: as it will be explained in 2.2, 2.3, 3.2 models for this type of simulation are primarily fluid dynamic type. Following different equations strategies (*BastankhahGaussian, Jensen*) different models for modelling wakes and interferences can be chosen of which some are less accurate but with less resources required, and some are more precise but more computational time consuming. Computing these parameters the tool will give user the amount of energy produced AEP and also the losses for chosen farm. Then economic model is considered with evaluation of many parameters such as distance from nearest port and from nearest coast, the union of multiple factors permit the tool to give an account of the estimated initial cost and the LCOE for the project divided by cost voice. Finally visual impact model is considered with an estimation of how the project that will be simulated impact on citizens visual perspective.

- Optimization algorithm: as will be seen in 4 optimization process in this case is the pursuit of two objectives minimize the LCOE so abate cost and rise the energy production and reduce visual impact perceived. Farm best layout is achieved by implementing a genetic algorithm. Genetic algorithms give good results in term of variability of solutions and are very adaptable in case like this where there are more than on object to optimize and more variable to consider. GA has been implemented in this tool using Pymoo a Python library.

- Optimal layout visualizations and results: last point of tool work is the representation of results and choice of best layout that can optimize the farm. Presented plot start with a convergence study of the GA, then continue with the optimal layout including wakes plot, then wind conditions in the area and power curve of turbine are plotted and finally an LCOE breakdown and a realistic visualization of visual impact are shown in 5.

In order to show tool working, some case studies will be considered to demonstrate, with numerical results and figures, how the tool works in selecting different locations. Conclusions finally are explained.

Chapter 2

Offshore wind turbine farm simulation tool

Thesis writer and researchers of MORE [1] [2] initially developed a specific tool written in Python language to offer to a final user the possibility to simulate an installation of an offshore wind farm in all Mediterranean area.

Starting considering wind conditions, bathymetry data and the characteristics of turbines, to the user is given the opportunity to of setting various parameters such as the total nominal power or alternatively the maritime area that is willing to occupy, the minimum and maximum seabed depth, the minimum distance from the coast and also the fluid dynamic model that is set during the simulation.

2.1 Analysis input data

Firstly, choice of site is performed by tool user that can choice to manually input coordinates or chose from an interactive map. Then chosen point data for bathymetry and wind condition are extracted from the datasets presented below as well as turbine data according to user size input. Datasets utilized to run properly wind farm simulations are three:

- Speed and direction wind data
- Bathymetry data of Mediterranean Sea
- Turbine data depending on size

Speed and direction wind data considered have been obtained from the CERRA (Copernicus European Regional ReAnalysis) data sets [40] that is provided by European commission and European space agency that utilise either satellite observation and terrestrial station to collect data. These data sets provide a wide range of weather-related historical parameters as wind speed, temperature, relative humidity or pressure and contain data from 1984 to 2021. The wind database used in this study is a grid (the spatial resolution is 0,01°x0,01°) in which every point represents a coordinate (latitude, longitude) following a Lambert conformal conic projection of the Earth surface and give a value both for wind speed and wind direction every 3 hours for every day.
The wind speed and direction are used as inputs for calculating key data such as annual energy production, total power coefficient and the Levelized Cost of Energy (LCOE). For simulations and case studies presented in this report simulation between 10 years are performed (2011-2021). Coordinates grid limitations for wind data are visible in Table 4. It can be noticed how longitude is accounted with a

360° system so values before Greenwich meridian are not negative with reference to east direction as they are in the bathymetry grid descripted below.

Table 4 Wind data coordinates threshold

	MIN	**MAX**
Longitude	301.8949° E	74.1051º E
Latitude	20.2923° N	75.3468° N

Bathymetry of Mediterranean area has been obtained from the data set GEBCO [41] Grid (General Bathymetric Chart of the Oceans). In this case grid is created starting from latitude and longitude and to each position a level of elevation in meter is assigned with a resolution of 15 arc second following SRTM15+ dataset [42] generating a grid that measure (15600x4080) pixel that has the following threshold resumed in Table 5:

Table 5 Bathymetry data coordinates threshold

	MIN	**MAX**
Longitude	-9.9979° E	37.9979° E
Latitude	30.0021° N	46.9979° N

Specifically, Figure 12 illustrates that by using this grid one out of every ten point has been selected for simulation. This approach significantly reduces the computational burden without major losses in accuracy.

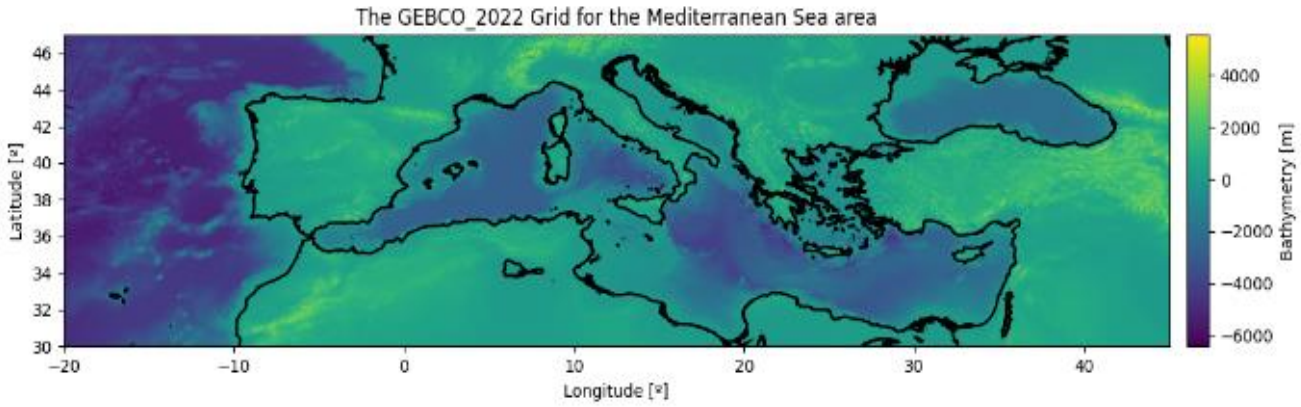

Figure 12 Bathymetry grid

The superposition of these two grids (wind and bathymetry) is not straightforward due to their differing sizing, resolutions and coordinates definitions. Consequently, a specific function has been developed for this tool to identify the nearest point in each grid for every set of input coordinates.

Either for wind and bathymetry grid due to the very large amount of data that must be computed the way is to use is netCDF file that is common for this type of work and are utilized for geographical, metereological and oceanographic study purposes and allowed an easy access to all data that otherwise can be difficult to manage. NetCDF is opened in python with a dedicated library [43] [44] [45] [46].

In site chosen beyond the depth constraint that is selectable manually by user also maritime route constraint are considered and visible through the map. Vessel routes must be considered because nowadays offshore wind farm can reach up to hundreds of square kilometres of extension and can represent an obstacle to economic maritime exploitation such as fishing activities. Maritime routes are only one of multiple constraints that a feasibility study must take into account other are military zone, protected area (e.g Natura 2000 sites), maritime zone assigned to hydrocarbons extraction.

In this study used data are collected by European commission [47] that furnish data of routes in *routes per square kilometers* per year visible in Figure 13.

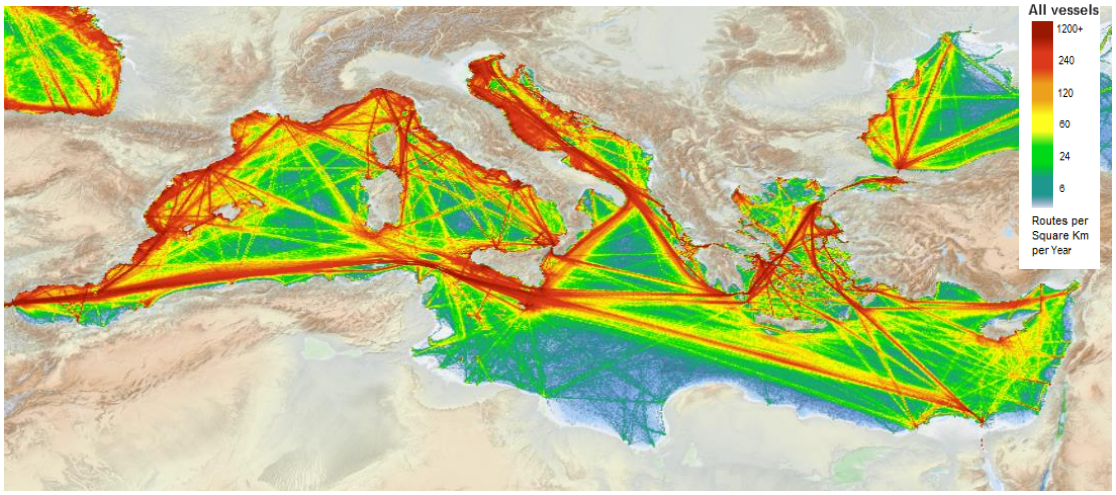

Figure 13 Maritime routes in MED sea

Data from EU site can be downloaded in raster grid type. Raster is a typical way to store geo data information but is useless without georeferentiation that for this study has been done with Qgis software [48]. Georeferencer starting from a map projection (EPSG:4326 [49]) assign to every pixel a coordinate of longitude and latitude that has been taken directly from the bathymetry grid in order to overlap together two type of information and give an overview of every constraint in one map. In the Figure 14 below an example of constraints shows depth level from 50 to 200 m and a threshold of 100 routes per square per year only coloured area respect constraints.

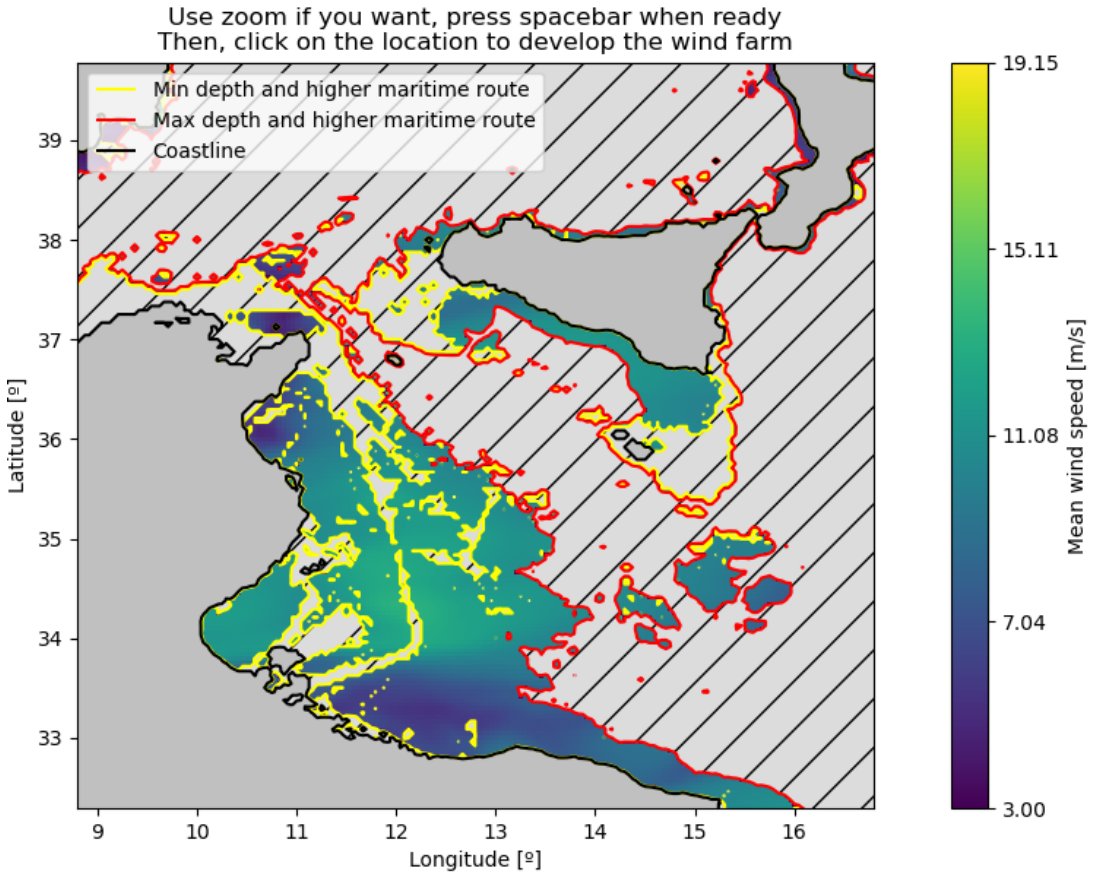

Figure 14 Feasible region with applied constraints

Another parameter that is given to simulation as input is the turbine typology that can be chosen from various size [5, 8, 10, 15 MW] for applications in various case and that are also the most common commercially sizes. The models that include geometrical, mass and functional characteristics written in .csv format are all Reference Wind Turbine models (RWT) this means they are theoretical models created for analysis and concept studies but in a way of trace market main sold existing turbines. The source of this data is either National Renewable Energy Laboratory (NREL) [50] for 5-10-15 MW size and LEANWIND project inside EU FP7 [51] for 8 MW size.

Parameters to value a wind turbine performance are typically the Power curve that represent how much power can be extracted depending on wind velocity based on following equation.

Equation 2.1 Power curve equation

$$P = 0.5 * C_p * \rho * \pi * R^2 * V^3$$

Where ρ is air density, R is blade length V is wind speed. C_p is computed as follow:

Equation 2.2 Cp equation

$$C_p = \frac{P}{\frac{1}{2}\rho A V^3}$$

In the curve in Figure 15 [1], generated according to power data for each turbine, we can recognize two typical point that are cut in speed that is namely minimal speed 3 or 4 m/s for energy production and cut off speed that is speed typically around 25 m/s at which turbine is stopped to preserve mechanical parts.

C_T represent thrust coefficient that is a dimensionless parameter characterizing each turbine computed as Equation 2.3 where T is thrust, ρ is the air density, A is the area of the wind turbine, and V is the wind speed:

Equation 2.3 Ct equation

$$C_t = \frac{T}{\frac{1}{2}\rho A V^2}$$

These two parameters descripted above change with turbine power size as well as height of tower and length of blades.

The Figure 15 below shows aerodynamic performances for various size used in work [1]: Power and C_T in varying wind speed.

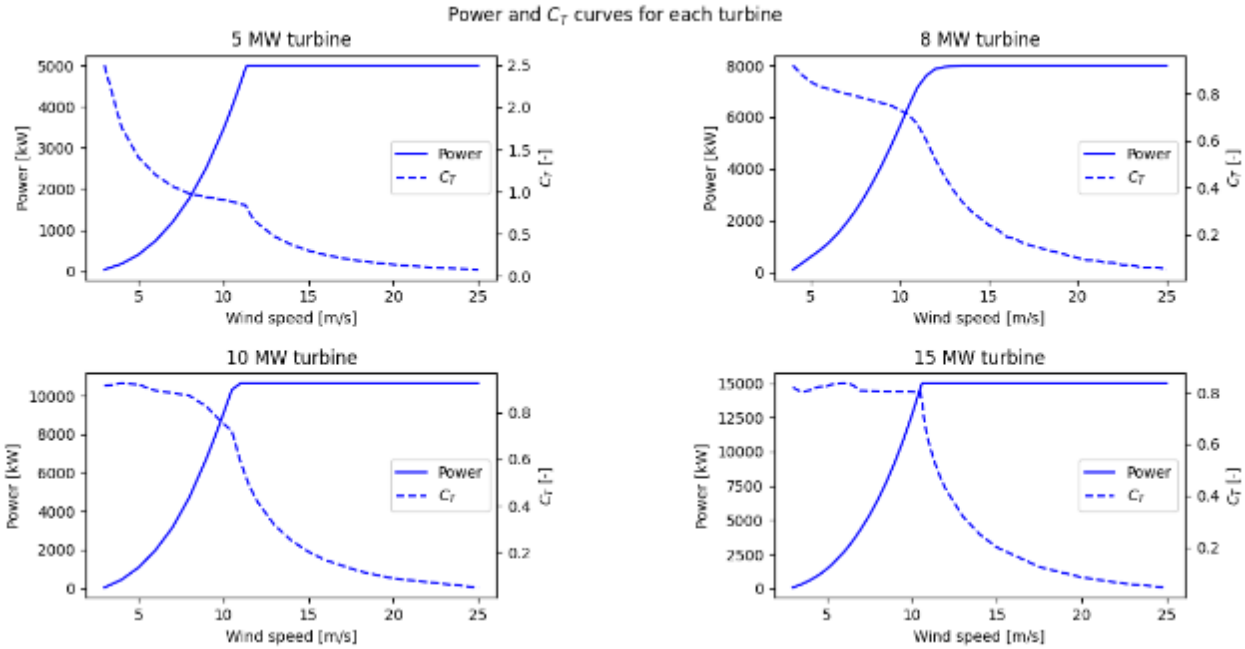

Figure 15 Power and Ct curves for various turbine size

2.2 Site and fluid dynamic models

To simulate properly the performance of the entire farm through Phyton PyWake is utilized. PyWake [52] is an open-source and Python-based wind farm simulation tool developed at DTU (Technical University of Denmark) capable of computing flow fields, power production of individual turbines as well as the Annual Energy Production (AEP) of a wind farm. The software can create a fluid-dynamic model starting from variables that has to be specified.

- Site model: defined among different choice depending on terrain type (roughness) and the way wind data are taken into account. For this study a Weibull distribution is chosen. Weibull distribution is commonly utilised in wind simulations to fit probability of finding a certain wind speed during time considered in a defined area. The equation of distribution is [53] Equation 2.2:

Equation 2.4 Weibull distribution equation

$$f(v) = \frac{k}{A}\left(\frac{v}{A}\right)^{k-1} * \exp\left(-\left(\frac{v}{A}\right)^{k}\right)$$

where parameters A is the Weibull scale parameter (m/s in case of wind speed) a measure for the characteristic wind speed of the curve so the velocity to which tend the distribution; A is also proportional to the mean wind speed. K is the Weibull form parameter, it specifies the shape of a Weibull distribution and specify the position of the peak and the initial and final slope.

An example of wind distribution is reported below in Figure 16:

Class	Frequency in %
0 - 1 m/s	2.75
1 - 2 m/s	7.80
2 - 3 m/s	11.64
3 - 4 m/s	13.79
4 - 5 m/s	14.20
5 - 6 m/s	13.15
6 - 7 m/s	11.14
7 - 8 m/s	8.72
8 - 9 m/s	6.34
9 - 10 m/s	4.30
10 - 11 m/s	2.73
11 - 12 m/s	1.62
12 - 13 m/s	0.91
13 - 14 m/s	0.48
14 - 15 m/s	0.24
15 - 16 m/s	0.11
16 - 17 m/s	0.05
17 - 18 m/s	0.02
18 - 19 m/s	0.01
19 - 20 m/s	0.00
Sum	100.00

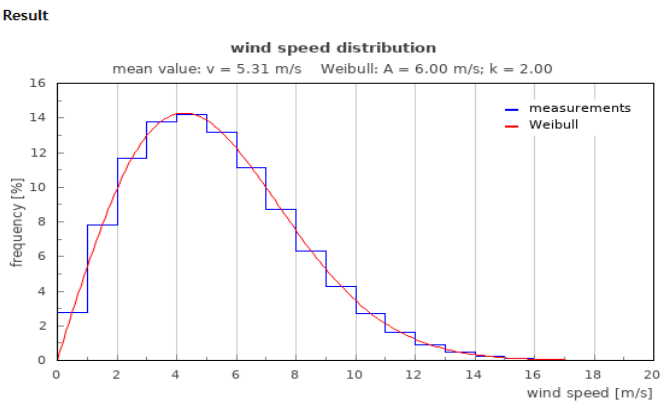

Figure 16 Example of Weibull speed distribution

To run this simulation firstly the wind rose that goes from 0° to 360° has been divided in 10 sectors with equal size (according to a previous study [54]), for each position in Mediterranean grid data for velocity and direction are collected as previously explained and every value is collocated in a sector, the frequency of each sector is then computed as well as main wind direction, then through velocity distribution in one of each ten sector Weibull parameters A end k has been calculated.

Data previously obtained are used in PyWake site model function as showed in Figure 17 (defined as XRSite [55] for this study) together with a turbulence parameter that is set to 0,04.

```
def site_mod(ti, k, f_sectors, A, wd):
    ds = xr.Dataset(data_vars={'Sector_frequency': ('wd', f_sectors),
                               'Weibull_A': ('wd', A),
                               'Weibull_k': ('wd', k),
                               'TI': ti},
                    coords={'wd': wd})
    site_model = site.XRSite(ds=ds)
    return site_model
```

Figure 17 Code snippet relative to site definition

– Turbine model: turbine geometrical and power characteristics are given as input to the simulation and data are taken as descripted in 3.1 accordingly to chosen size.

Fluid dynamic models are descripted below however for each parameters below a user choice can be made:

– Wind farm model: is the first choice that can be made between three different models presented in Pywake: *PropagateDownWind, All2AllIteratives and PropagateUpDownIterative*.[56]

  The first one is the choice if an approximation has to be made in order to avoid a long computational time since it iterates over all turbines in downstream order. In each iteration it calculates the effective wind speed at the current wind turbine as the free stream wind speed minus the sum of the deficit from upstream sources. Based on this effective wind speed, it calculates the deficit caused by the current turbine on all downstream destinations. This method doesn't take into account the blockage deficit model that, as is explained below, is an effect that act from the downwind turbine up to the arrays before in disturbing the wake.
  In the example below at the iteration 1 the wind velocity in front of each turbine is computed and is clearly visible that the first turbine "sees" 10 m/s of wind that is the freestream velocity while its effect disturbs the air flow for the others two downwind turbines. In iteration 2 deficit from the second turbine affect the third turbine front velocity. This process is repeated for every turbine in the farm as showed in Figure 18.

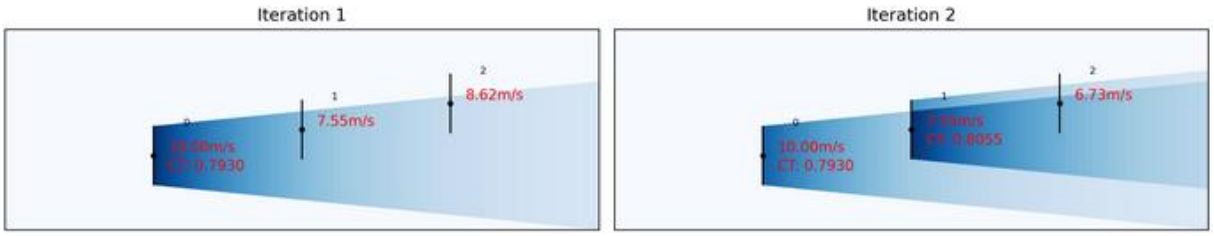

Figure 18 Example of application of PropagatedDownwind

All2AllIterative is a more accurate method that however require more computational resource and time. It handles the Blockage effect and so it iterates for the entire farm to find best solution with a certain converging tolerance that has to be specified. In the following example in Figure 19 is clearly visible as assessed before that the blockage effect influence also the wind velocity upstream so the first turbine will not see any more the freestream velocity but influenced by downstream two turbines it see a minor stream.

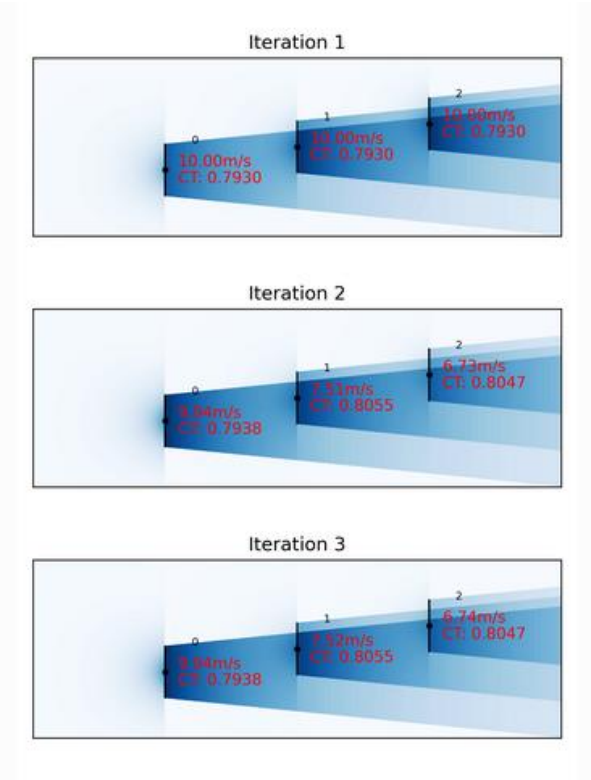

Figure 19 Example of application of All2AllIterative

Last method that can be used is *PropagateUpDownIterative* that is a good mix of the other two. Beside the wind farm model that is the base for the dynamic model the other implemented model will be descripted deeply only if will be implemented in the case study for this work of thesis to not to step outside the main topic.

- Wake deficit model: shows how the wind line stream is affected by upwind turbine in a row so how the velocity of the wind change for the turbine that is below another.
  This model choice is very important for the calculation of produced energy and so to evaluate the performance of wind farm. Proposed models are several, but they converge in three fundamentals: GaussianDeficit, Top-Hat, FugaDeficit.

    - Top-hat models: the simplest and also the less accurate one that models the uniform velocity into the wake in a circular form.
    - Gaussian models: more accurate but more computational expensive than the previous that model the wake with a bell-shaped Gaussian distribution.
    - Fuga models: the most accurate but most computational expensive among the three that since use RANS (Reynolds-Averaged Navier Stokes) solvers.

According to [1] and Pywake developers (DTU) that have made a study on reliability of different wake model utilising real data (SCADA) of existing wind farm in order to give users an overview of the differences [57] between models, *BastankhahGaussianDeficit* model has performed better than *NOJDeficit* in efficiency calculations, the first one present a relative error of only 3% efficiency in relation to real data while *NOJDeficit* arrive to 11% and so this model will be used in simulation for this thesis work. *FugaDeficit* since is not mentioned in the comparison has been discarded for lack of information.

To give a general idea to the GaussianDeficit model the first of this type is then explained the *BastankhahGaussianDeficit* model [58] from which the other are only evolution. Explanation of other can be found in Pywake documentation.

According to *BastankhahGaussianDeficit* the velocity downstream is calculated as:

Equation 2.5 Downstream velocity equation

$$\frac{\Delta U}{U_\infty} = C(x)e^{-\frac{x^2}{2\sigma^2}}$$

With the maximum velocity deficit at the wake center calculated as:

Equation 2.6 Wake center max velocity

$$C(x) = 1 - \sqrt{1 - \frac{C_T}{8\left(\sigma/d_0\right)^2}}$$

While the wake width is computed as:

Equation 2.7 Wake width expression

$$\frac{\sigma}{d_0} = k * x/d_0 + e$$

Where k represents the wake expansion parameter and e = 0,2 * β where β is a parameter that depend on turbine's C_t.

- Superposition model: it adds the effect of the different wind turbines wakes and deficits from other sources to obtain a realistic effective wind speed at any point of the wind farm. Among different models presented

  - *LinearSum*: this choice just sums linearly the effect of the wake effects in the downwind direction. Special attention should be given to negative speeds with this sum model. It does not have boundary for negative values and so with many turbines aligned in the wind direction, it could happen that the added wake ends up causing negative speeds.
  - Squared Sum: as its name denotes, it calculates the wake addition with an squared sum of its components ($\sqrt{x^2 + y^2}$).
  - *MaxSum*: with this sum model, only the largest wake deficit is considered downwind.
  - *WeightedSum*: in this case, a weighted sum is performed. The weights are determined according to the ratio between the mean convection velocity and the convection velocity of the combined wake. This model is capable of conserving momentum in the stream wise direction.

The one chosen for simulations is SquaredSum since avoid negative speed.

- Rotor-average model: this object discretizes the wind velocity through the rotor geometry in defining different speed at different point of the rotor. Several types of rotors are available, following different geometry patterns for the selected points: grid distributions, polar distributions. Some incompatibilities may arise between the rotor-average model and the wake deficit model.
    - *AreaOverlapAvgMode*l: it calculates the fraction of the downstream rotor that is covered by the wake from an upstream wind turbine. It can only be used with top-hat wake deficit models.
    - *GaussianOverlapAvgModel*: it computes the integral of the Gaussian wake deficit over the downstream rotor. Normally, the results of the integrals are taken from look-up tables for speeding up the process. It can only be used with Gaussian wake deficit models.
    - *CGIRotorAvg*: Circular Gauss Integration (CGI) with a chosen number of points among 4, 7, 9 and 21.
    - *EqGridRotorAvg*: it consists in a equidistant NxN grid defined in cartesian coordinates.
    - *GridRotorAvg*: it is a custom grid defined in cartesian coordinates.
    - *PolarGridRotorAvg:* it is a custom grid defined in polar coordinates.
    - *RotorCenter*: it only includes one point at the centre of the rotor.
    - *WSPowerRotorAv*g: recently included and still under development

Since the utilization of Gaussian model for wake deficit the *GaussianOverlapAvg* model has been selected for simulations. The plot below in Figure 20 show some absolute errors for different approaches in rotor model simulation.

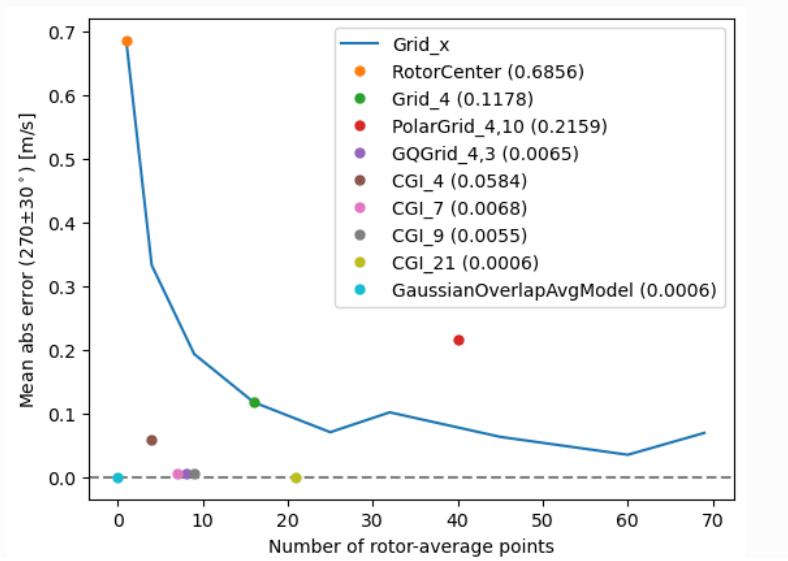

Figure 20 Rotor average model comparison

– Deflection model: model that is applied when turbine is under yaw control and so is misaligned from the main wind direction. This condition can easily be real in an optimization approach where maybe only front array can see free-stream main wind direction while to others an angle from main direction can be applied to mitigate wake effects.
Type of model in Pywake are:

  – *JimenezWakeDeflection*: based on LES (Large Eddy Simulation) so resolution of Navier Stokes Equations for downwind to characterize the turbulence behind a wind turbine given the wake deflection created by different yaw angle and thrust coefficient settings. Example is given in Figure 21.
  – *FugaDeflection*
  – *GCLHillDeflection*

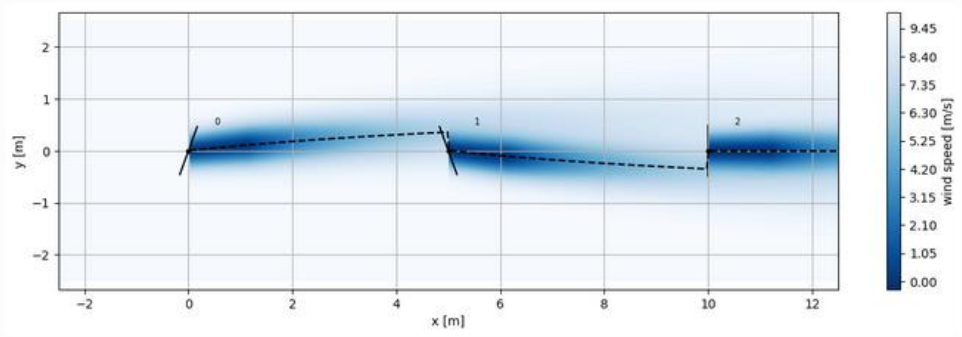

Figure 21 Example of JimenezWakeDeflection

- Turbulence model: model for accurate study of air flow behind the rotor that in nominal situation is not implemented but is helpful for example in case of fatigue load studies.

- Blockage deficit model: object that model upstream wake effect so can be applied only in case of *All2All* wind farm model since adding this model give more accurate simulation but slow down computational time. However, is negligible in study that concern in macro-scale large wind farms.

2.3 Tecno-economical model

To evaluate the feasibility of the investment economic models must be more reliable as possible. Starting from a study at internal study at MOREenergy Lab the economic model has been elaborated from the original one in implementing this present work.

Fundamental parameter to evaluate feasibility of investment is LCOE (Levelized Cost of Energy) is the amount of money at which theoretically the energy produced by the field can be sold to make profit in a certain period. LCOE has been defined in [€/MWh] according to [59]:

Equation 2.8 Levelized cost of energy

$$LCOE = \frac{Life\ cicle\ cost}{Electrical\ energy\ provided} = \frac{C_0 + \sum_{t=1}^{n} \frac{O\&M_t}{(1+r)^t} + \frac{D_n}{(1+r)^n}}{\sum_{t=1}^{n} \frac{E_t - L_t}{(1+r)^t}}$$

The life cycle cost (LCC), at numerator of previous equation, includes all costs occurring in the lifetime of the plant such as the capital cost (C0) for the initial investment that include several voices that will be treated in detail below, the cost during the operation and the maintenance phase (O&Mt) as well as the decommissioning cost (Dn) at the end of lifetime. The energy provided refers to a balance between the generated energy (Et) during the lifetime minus the energy losses (Lt) that occur in generation, collection and transmission of the energy. Since the costs occur in different years (t) they have to be discounted to their present value. The discounting of cash flows (discount rate (r)) is based on the concept that money has different values in time so nowadays invested money will change their value in future, it's difficult to make an accurate estimation of this value because it depends on economic situation and also on hypothetic energy benefits given by countries. According to [60] this value has been estimated in 8%.

Capex cost or capital expenditure includes various voice:

- Project development: cost not only related to barely project design engineering and project management but also to develop campaign of collecting data such as seabed and wind data. The costs at this stage are related also to marketing, licenses, environmental impact assessment, government authorization. As stated in [11] the value for this cost has been approximated in: 180,9*NP [M€] where NP is the total nominal power in kW.

- Turbine cost: this value is the major voice of cost in the total cost breakdown because it covers not only the cost of blade tower and nacelle but also the internal components as visualized in Figure 22. As it is stated in study of [61] this cost it's been set to 1,3 [M€/MW].

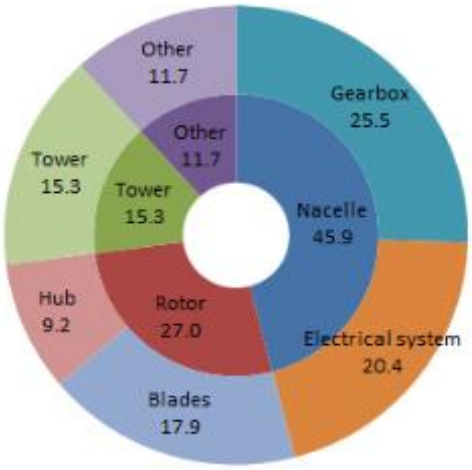

Figure 22 Cost breakdown of an offshore wind turbine

- Platform cost: it depends on the technology utilised. Due to typical seabed depth of the Mediterranean area for this study Spar buoy technology has been chosen. The spar-type platform, visible in Figure 23 [c], is a deep-draft vertical cylinder, which provides buoyancy. Roll/pitch stability is maintained by placing the centre of gravity sufficiently below the centre of buoyancy [62] .

  Choose of platform technology in offshore wind is carried out taking into account seabed depth, but also wave height in the area because this component give stability to all structure. Furthermore, the technology utilised influence also other cost voices primarily the installation cost because the weight and the strategy of installation of different platform require different vessels but also the as well the mooring type. As stated in [63] this price has been set to 0,51 [M€/MW].

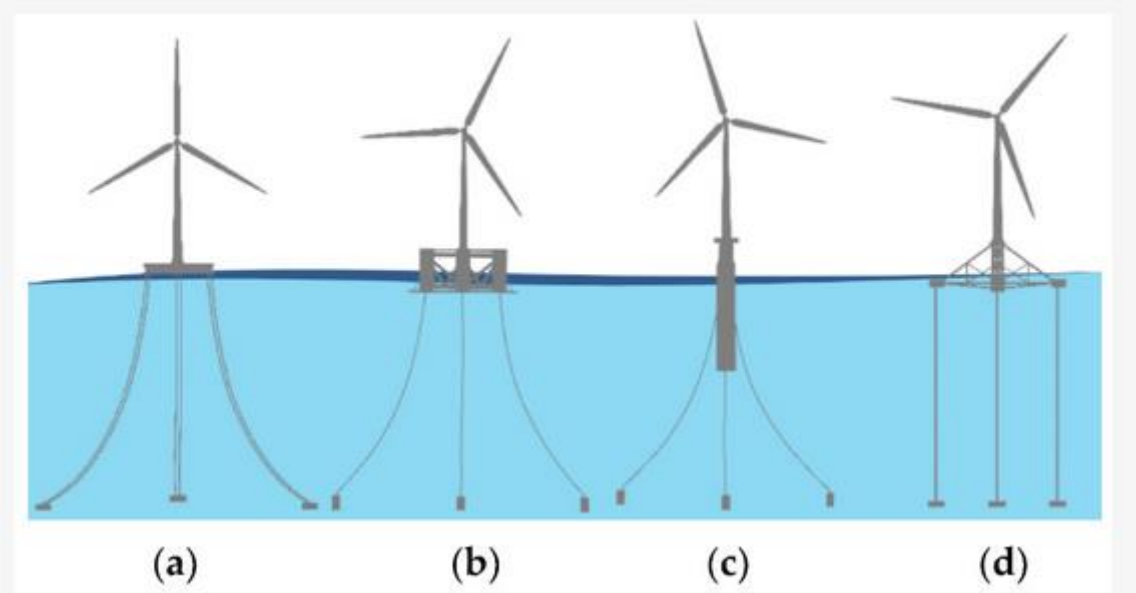

Figure 23 Platform type for offshore wind application

- Mooring cost: as well as the platform the choose of mooring depends on preliminary study on seabed typology and also on the platform that has to be anchored. Mooring can be different in chosen material: chain, fibre and rope depending on level of elasticity requested but also anchorage that are drag embedment or suction pile anchors varies with fixing requirements: normal, vertical or taut leg.

  Typer of mooring varies a lot according to the chosen site so to make a simplification in this study three catenary mooring has been selected [62] with three regular anchorage.

  According to [11] and Equation 2.9 cost of mooring has been computed following this equations where W_d indicates the water depths in the selected point and N_{lines} the number of mooring, while $N_{anchors}$ the number of seabed anchorage computed:

Equation 2.9 Cost function for mooring

$$Chain = 600 * W_d * N_{lines}$$

$$Anchor_{regular} = 114000 * N_{anchors}$$

- Cable cost: cost of connection is an important cost voice to take into account when simulate a wind farm. Cables are divided in inter array cables that connect together turbines in strings and pass energy to an offshore station that collect current and send it to shore with export cable. Typically used cable for inter array purpose are 33 kV in medium AC voltage, then with a

substation that contains transformers voltage is risen up to value typically of 132 or 220 kV High Voltage AC and finally the export cable transport the electricity to shore substation [64]. For high distanced farm the collected electricity is converted from AC to DC with the purpose of reduce cable losses, this transformation is operated inside the offshore substation that rise voltage up to values between 320 kV and 880 kV DC however that option is economically valuable only for distance far than 110 km [37] as visible in inflexion point in Figure 24. Another special case is distance less than 8 km from onshore for which medium voltage is economically favourable.

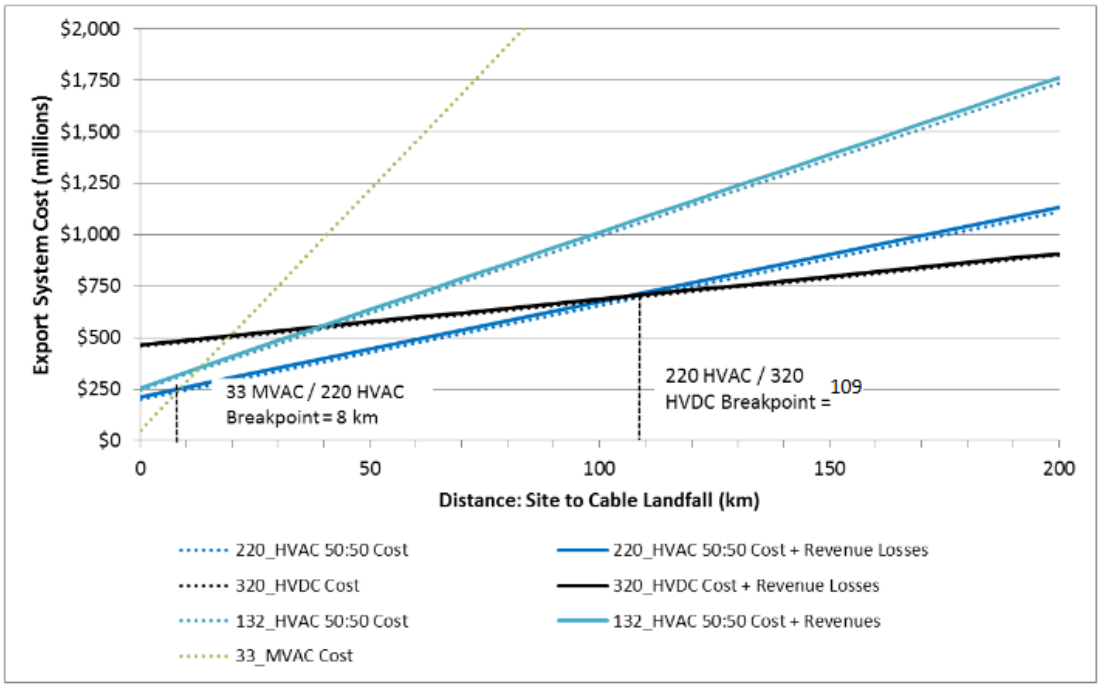

Figure 24 Export cable cost in function of farm distance

In this analysis three case are considered in varying the type of cable used in function of the coast distance in km as shown in Table 6. $D_{offshore\ substation}$ is the distance in km between every turbine and the offshore substation that for the simulations tool presented in this report is located at the centre of the farm. In real case study the substation (that can be more than one) is located in a way that allow to be cost effective for cable connection. D_{shore} is the distance in km between the offshore substation and the onshore substation. WFC is the nominal farm power in MW. Difference in price of substation between case 1 and the other two are for the presence of transformer that are useless if there is only medium voltage utilisation. [11]

Table 6 Cable and substation cost function relate to different coast distance [11]

Coast distance	Cable cost	Offshore Substation
D < 8 km	$MVAC - 33kV = 299600 * D_{offshore\ substation}$	$AC\ collector\ substation_{offshore} = 185000 * WFC\ [MW]$ $Substation_{onshore} = 107417 * WFC\ [MW]$
8 km < D < 110 km	$MVAC - 33kV = 299600 * D_{offshore\ substation}$ $HVAC - 132KV = 651250 *\ D_{shore}$	$Substation_{offshore} = 245318 * WFC[MW]$ $Substation_{onshore} = 107417 * WFC\ [MW]$
D > 110 km	$MVAC - 33kV = 299600 * D_{offshore\ substation}$ $HDVC - 275kV = 1200000 *\ D_{shore}$	$Substation_{offshore} = 245318 * WFC[MW]$ $Substation_{onshore} = 107417 * WFC\ [MW]$

Other cost related to cables are the onshore cable, substation, fees and other infrastructures that must link the farm to distribution system of the country. Every specific case must be considered depending also on legislation of different countries to make a precise estimation, but this is beyond the scope of this thesis.

- Installation cost: these costs cover the assembling and transport of all turbine components as well as electric components and infrastructure. Depending on type of platform used the assembly of tower and platform can be performed onshore and be towed offshore or performed on site. According to [60] in general, offshore assembly of the turbines is three to four times more expensive than inshore assembly and towing of the complete structure.
  Installation cost so depend on the type of used vessels that transport physically all structures, on the employed workforce so on hours of works, on the distance to the nearest port facilities that can accommodate the vessel and all substructures, on the water depth of the site and of course on the size of plant.

Starting port has a key role in offshore wind installation for the local supply chain, logistics and supporting infrastructure (e.g. storage of components). Ports are where operation and maintenance of offshore wind farms are run, where all offshore wind turbines and other equipment get transported, and where floating turbines are assembled [65]**.** Not every port in Mediterranean Sea can be exploitable to installation or maintenance operation so to assess cost a list **APPENDIX B** with ports with proper offshore wind facilities has been drafted for nearly every Mediterranean country. In Figure 25 ports are showed with right coordinates.

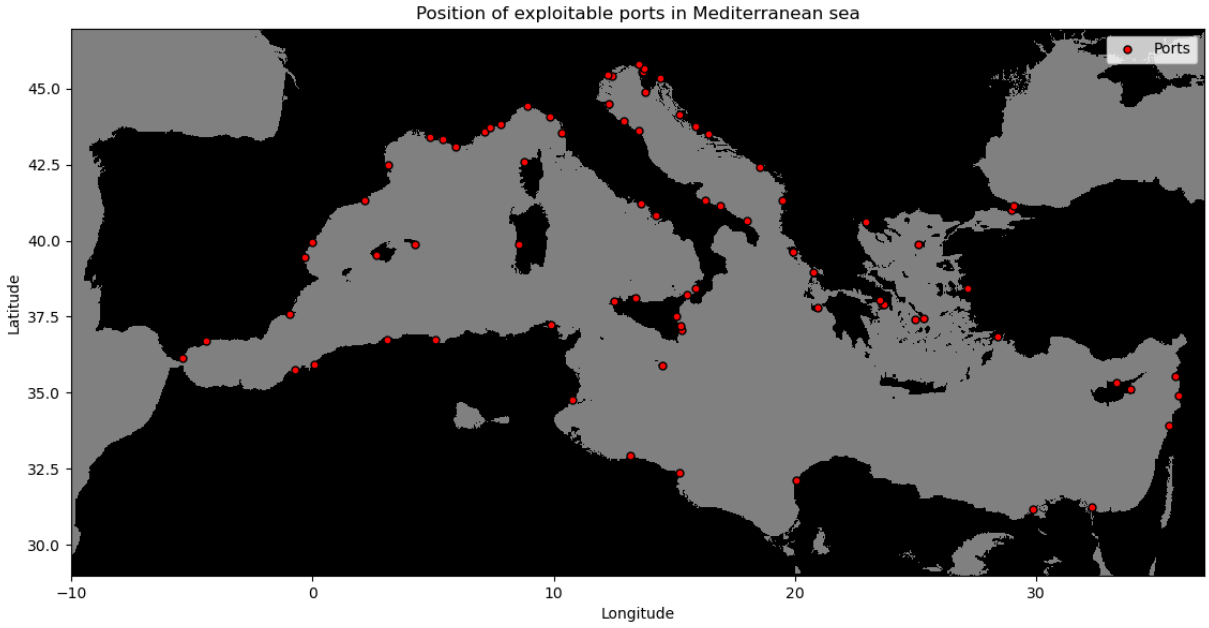

Figure 25 Map of Mediterranean exploitable ports

In order to compute the minimum distance from each point in the grid to every possible port the geographical straight-line method was not accurate at all because it signifies to taking into account every piece of land between the farm and the port causing misleading results in terms of distance. Optimum chosen algorithm is named Dijkstra [66], this algorithm is exploited to find the minimum distance between two points that are not directly linked and it's applicable to various network (e.g road map, hydraulic network, telecommunication).

Algorithm use graph method building a network of vertex and edge, every vertex is linked to the next one with an edge to which a value of weight is assigned, the algorithm then will look for the shortest path between one starting point and one final point in adding weight of path for each crossed edge at the end the minimum value of weight is chosen that corresponds to the

shortest path. Example is shown in Figure 26 [67] where shortest path between point 1 and point 9 is computed.

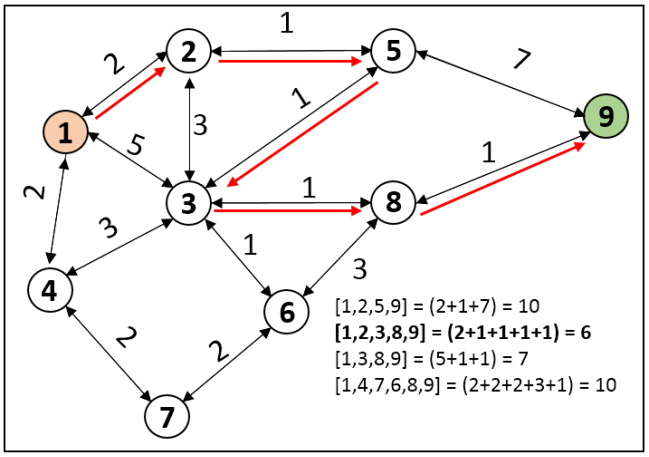

Figure 26 Dijkstra algorithm example

To implement this type of algorithm in Python language Networkx library [68] has been applied. Starting from bathymetry grid that has been presented before in 2.1 Analysis input data value has been assigned to each point to identify position (0 to point that are inland, 1 to marine point, 2 to port coordinate).

Subsequently, a graph was created for every point that represent a pair of coordinates in the grid (except for the previously identified inland points). Edges were placed linking each node to the adjacencient nodes in all directions: left, right, bottom, top, bottom left, bottom right, top left and top right in order to consider every possible path. Each edge was assigned the value of the actual geographic distance between the two coordinates using the *Geopy* [69] library. Finally, a specific function already available in the library will find path to every reachable port and the shortest path is chosen.

The construction of this function is not perfect due to the grid resolution and the considered points (as mentioned earlier only one out of ten point of coordinate points is considered). Therefore, a certain tolerance on the path is documented in **APPENDIX A**, along with a sensitivity analysis that asses the precision of computed distance within a 10% of error,

- Decommissioning cost: according to Equation 3 decommissioning cost is considered in LCOE calculation, these costs cover the de-assembling of the entire structure and infrastructure (also cables and substation) at the end-of-life cycle of wind farm that is considered 25 years in the tool calculation but can reach up to 30 years. All parts are sent to land and the site is cleaned. This cost are approximately 62000 €/MW [70].

- Operation and maintenance: O&M cost account for operation in lifespan of the farm from standard maintenance to replacement of main subsystem. Many aspects are taken into account: failure rate of components and cable, deployed vessel , insurance, port facilities cost, workforce in specialized workers as assessed in [60]. This voice of cost is approximately in 0.09 M€/MW.

In taking into account all the costs expressed above for every tool simulation, a plot visible in Figure 27 is generated to give an idea of how costs are distributed, considering an hypothetical wind farm of 100 MW and 10 MW single turbines with the centre of the farm at 25.56 km from the nearest coast. As already discussed, the turbine cost is the major voice in cost breakdown foe every simulation.

It is emphasized that is only an estimated cost layout. In real scenarios, additional cost factors must be considered such as port facilities and operational cost, as well as grid connection costs. These may include substructure and reinforcement to the grid to facilitate connection to the national electric grid. Such costs are challenging to estimate with a general tool like that one developed, as they can vary significantly depending on specific location and countries.

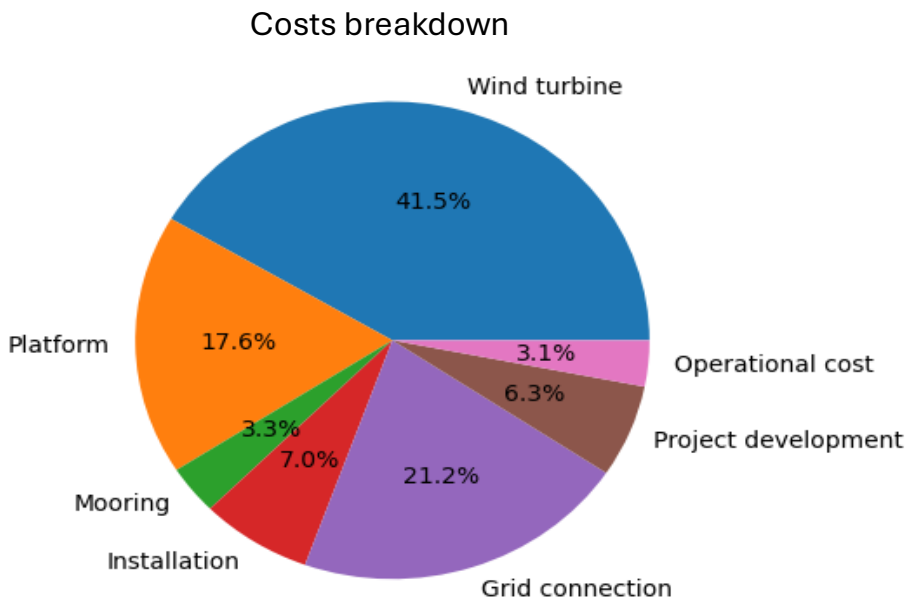

Figure 27 Example of cost breakdown

Chapter 3

Optimization parameters definition

This tool aims also to investigate the optimal layout for farms of floating offshore wind. Optimization of wind farm is a key factor for future spreading of this technology, energy yield has to be maximized avoiding fluid dynamic losses and consequently initial cost has to be recovered in order to make investments in this sector profitable. Best parameter that can assess if one layout is better than another is LCOE that as view before in is a total overview of how economic 'efficient' the farm is in considering energy produced and total cost, the lower is the LCOE the better the investment to make. Another important aspect of wind farm or in general for every energy infrastructure is the visual impact, the more a new construction is integrated in the surrounding environment and not visually imposing from citizen perspective the more easy will be to receiving permitting and to be perceived as good from public opinion.

So, the optimization implemented in this tool will pursue these two objectives:

- Minimum LCOE
- Minimum visual impact from the nearest coast point

In next paragraphs after optimization objectives decision, optimization variables will be explained.

3.1 Layout parameters

In this tool working turbines layout is build starting from main wind direction and so to position the hub facing it that in first approach its proven to ever guarantee a good energy production over a year.

However, distances between arrays and disposition are not negligible issues and have to be considered for every wind condition.

The wind turbines can interfere with each other. In fact, by converting the wind speed into rotational kinetic energy, they disturb the wind speed field, reducing it and creating turbulent zones. This phenomenon is called wake effect and is fundamental to study the energy production in a farm, the model used has been descripted in 2.2 Site and fluid dynamic models.

To attenuate wake effects it will be easy to put turbine array far from each other in order to avoid interferences but this solution is not economical sustainable because the more the distance between arrays the more is the cost of cable and connection losses that will lead to major costs and also the power density will decrease [MW/km^2] and so the space will be not optimized.

In study [71] and in publication [72], which simulated various layout using Large Eddy simulation (a fluid dynamic model based on Navier Stokes equations) of offshore farm of Lillgrund in Sweden, several layouts, generated by staggering rows, increasing streamwise (in wind direction) and/or spanwise (perpendicular to wind direction) spacings, and simultaneously staggering and increasing spacings, were evaluated. Wind farm layouts were shown to affect the performance up to 33%.

To find parameters that can describe optimal layout geometrical parameters are taken from Geometry-based models as assessed in [71]. These are statistical models that utilize geometric quantities associated with wind farm layouts to predict power generation and are developed through regression analyses using data from large-eddy simulations (LES) of wind farms. By considering parameters like blockage ratio, blockage distance, and their combinations, these models can accurately estimate the relative power generated by wind turbines in different layouts and conditions. Parameters are descripted below and visible in Figure 28:

- SY distance in wind direction
- SX distance in crosswind direction
- Sdy distance between two adjacent vertical arrays
- β angle between two adjacent horizontal arrays

These three parameters combined can change layout to farms in forming different shape: rectangular shape in Figure 28 (a,b) and staggered in Figure 28 (c).

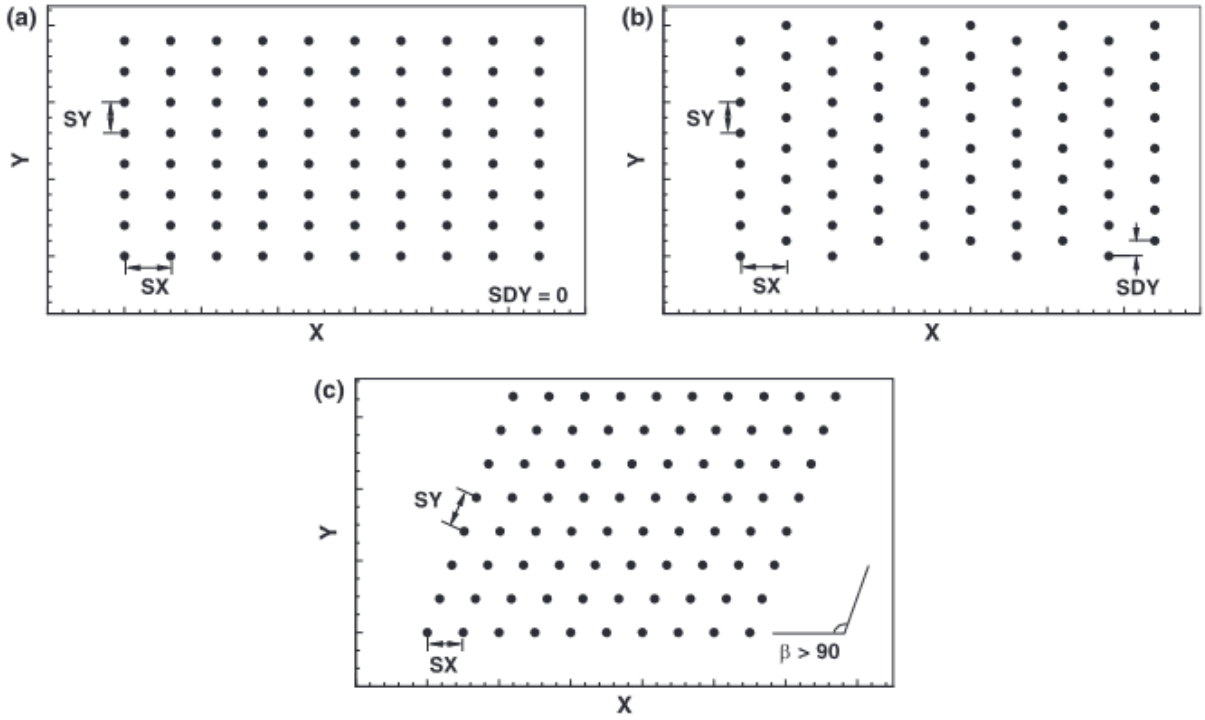

Figure 28 Visualization of layout optimization parameters

Generally, to describe the layout wind farm, the reference distance is expressed as a multiple of the rotor diameter *D* so range chosen for variables are SX ∈ [3D, 10D], SY ∈ [3D, 10D], SDY ∈ [0<SY<0.83] and β ∈ [-20°,+20°] that differ from the article reference [71] because in the tool the reference axis in Y axes that represent 0°.

In varying these quantities in the chapter below also energy yield, Ct parameters and finally LCOE will be computed in order to find best optimum.

3.2 Visual impact

Visual impact is a big issue among the RES outlook, the lower energy density compared to other conventional energy sources has the result that res plants occupy vast portion of territory either on land or maritime. This issue, combined with the fact that wind turbines can exceed 100 meters in hub height can create a substantial visual impact for residents in the affected areas or even for passerby. Social opposition, often referred to as NIMBY (Not In My BackYard), is one of the major obstacles to the expansion of wind energy leading to be abandonment of even most ambitious projects.

Offshore wind farms do not deal with typical onshore farms issues (i.e. space, noise, shadow flicker) and, thanks to their offshore distance, can offer advantages from the visual problem point of view. However, offshore projects are not economically feasible to be placed too far from the cost mainly for important costs of the connection cables and rise in electricity losses. Coast proximity, on the other hand, can lead to more visible plants, especially for Mediterranean area that present large coastal city and so highly populated areas.

It's challenging to determine visibility parameters that can describe the phenomenon because the problem depend on angle of view and the distance from the observer. Additionally, it’s important to consider local population density and the height of buildings located near shore. The scope of this thesis and of the presented tool is giving a general description of the phenomenon and so the density of population in specific place is not taken into account and can be an argument for future works. The analysis is carried out based on wind farm characteristics, the position and the angle of viewer view will be considered constant. The assess of visual impact will be carried out following this scheme showed in Figure 29 following the reference article [39].

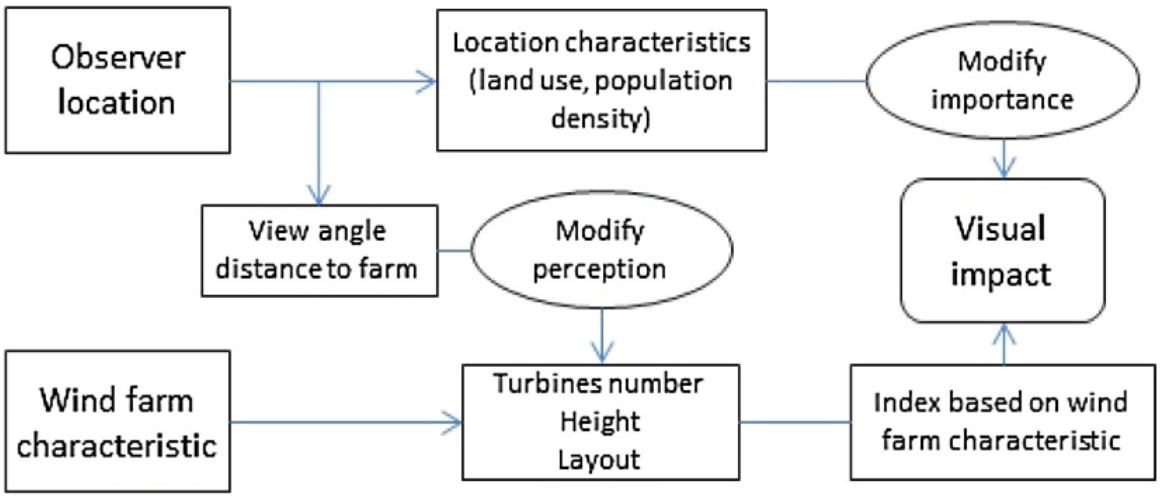

Figure 29 Visual impact definition scheme

Parameters chosen to define visual impact objective function in this work are horizon occupation area and distinguishable turbines that are defined under perfect visibility so clear sky hypothesis.

- Horizon occupation: considering the wind farm as the whole object of study. The spatial distribution of the wind turbines is considered as a convex polygon. This polygon constitutes the object whose visual occupation is to be estimated. The considered area for the horizon surface occupation is the one derived by the polygon projection on a perpendicular sight direction plan located at one meter of the observer this area has been estimated in 130-135º in vertical direction and 200-220º in horizontal [73] so combined give an approximate area of 55200 cm^2 at 1 m from the viewer.

  The sight is supposed in the direction of the farm centre with an average height of the observer of 1.7m. The apparent height of the turbine is derived from basic trigonometry equations in function of tower distance considering the actual hub height which a hidden part has been removed due to the Earth curve when the turbines are located above the horizon distance as showed in Figure 31. The surface occupied by the farm on the horizon is defined by the area delimited by a convex curve joining the turbine hubs placed at the polygon visible edges. The horizon occupation, HO, is defined as the surface below the convex envelop as in Figure 30 [39].

Figure 31 Apparent height visualization

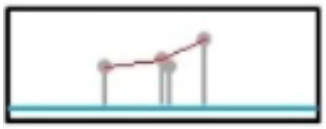

Figure 30 Horizon occupation

- Distinguishable turbine: at high distance the human eye cannot perceive good distance between near object and perspective plain the real distance between turbine that cannot be distinguished in visual depth. Apparent distance between every adjacent hub is computed as the apparent hub height with basic rule of trigonometry in function of distance from the object.

  With assessment of apparent distance the rule to determine how many turbine human eye can distinguish the sensibility has set in one minute of arc between the two adjacent objects [74] to be separated seen. Finally, parameter *Dt* is computed as a ratio between the visible hub and the total present in the farm.

Equation 3.1 Dt parameter definition

$$Dt = {}^{Visible\ turbine}/_{Total\ turbine}$$

For optimization purpose the chosen parameter is the area of horizon occupation that can give a deeper idea of how wind farm is perceived. That parameter is in function of hub height, layout and distance from the coast. The following Figure 32 represent the graphical visualization along z axis of a 900 MW wind farm composed by 15 MW single turbine located in a point at nearly 10 km from the near coast. In Figure 33 the actual point of wind farm and centre of farm are visualized. To be enlightened how 119 m height tower is barely visible at 5 km and the nearest hub is perceived in only 4 cm and is remarked that the conditions are optimal for the far view so no mist and favourable brightness.

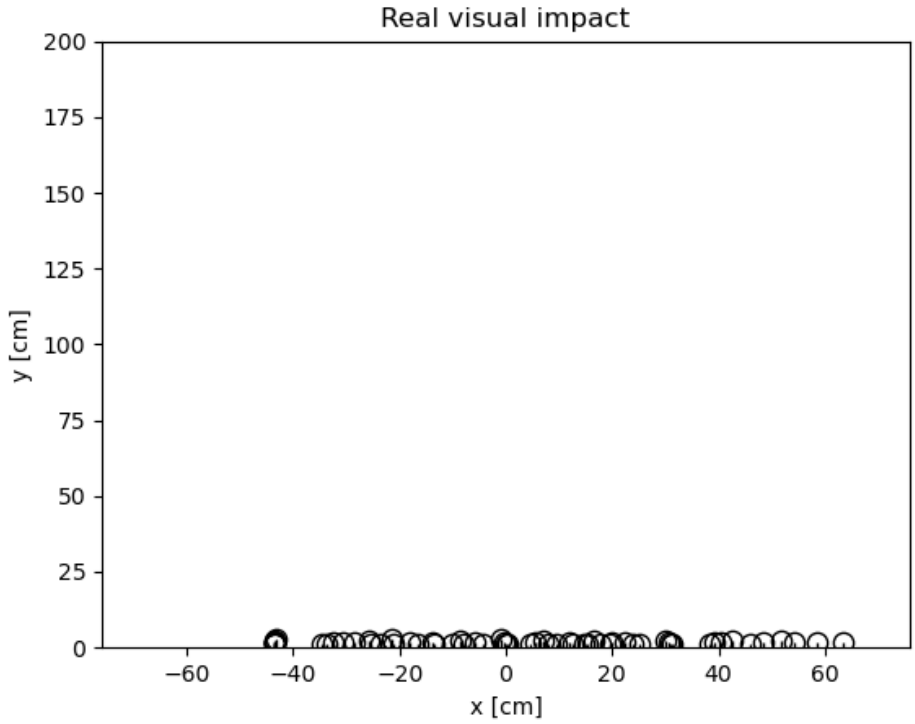

Figure 32 Actual visualization of wind farm located at 10 km from the coast

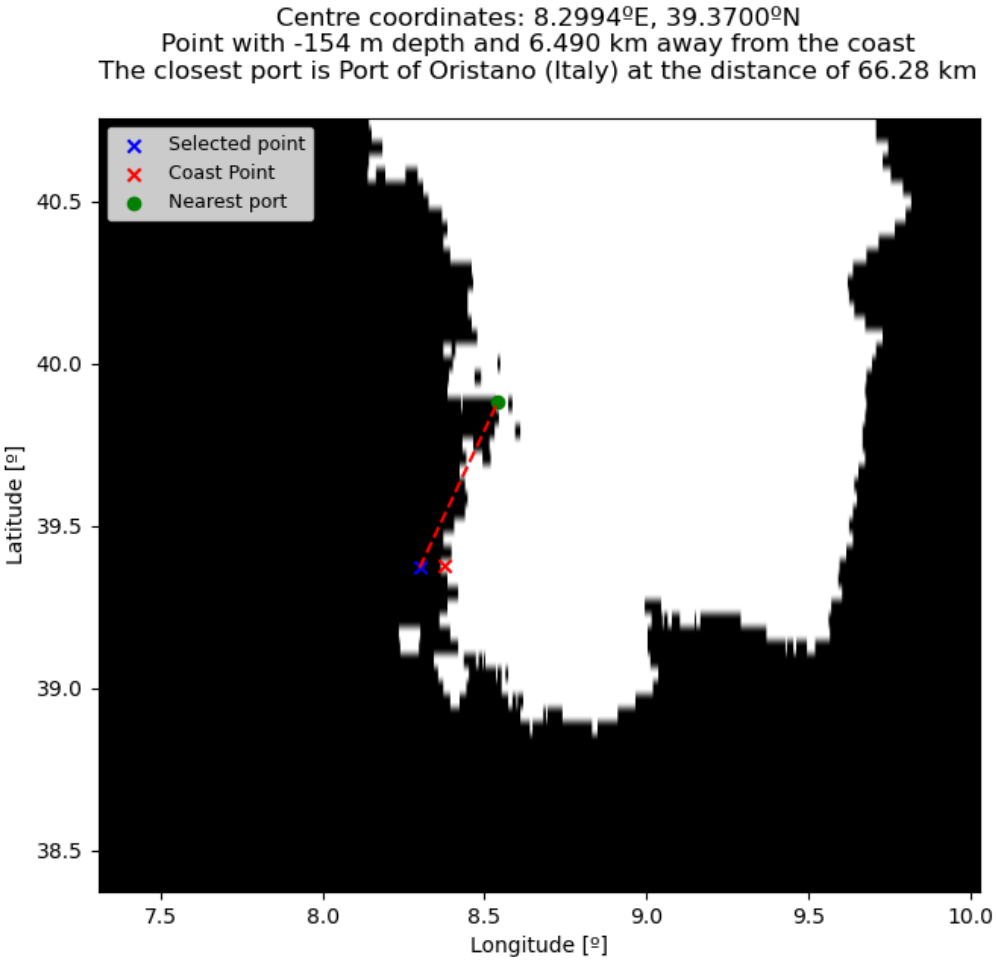

Figure 33 Wind farm and nearest point of view position

Chapter 4

Multi-objective optimization

Multi-objective optimization problem is a problem that has the aim of simultaneously minimize (optimize) two or more functions (a set of objectives) defined as $F(x) = [f_1(x), f_2(x), \dots, f_k(x)]$ where $k > 1$, x_j is a set of decision variables of d-dimension $x_j = [x_1, x_2, \dots, x_d]$ and x is a solution consisting of n decision variables $x = [x_1, x_2, \dots, x_d]$

For optimization applied in this work N_t is the number of wind turbines:

$$\boldsymbol{Minimize}\ LCOE(x_i, y_i) \quad i = 1, \dots, N_t$$

$$\boldsymbol{Minimize}\ Occupied\ horizon\ area(x_i, y_i) \quad i = 1, \dots, N_t$$

where $x_i(S_x, S_y, SD_y, \beta)$ and $y_i(S_x, S_y, SD_{dy}, \beta)$

So x_i and y_i are coordinates for each turbine that are in function of layout parameters presented in 3.1.

Each function is calculated for the same variables and for real application are in conflict, so every function pursues a different objective. Tend to minimize one of them could maximize the others and vice versa so the best solution must be found in between the optimum for each function.

The concept expressed above is the Pareto optimum solution and it's applicated not only in engineering project but also in economy and social sciences. In finding the optimal solution a Pareto front is tracked. Pareto front is the group of solution that minimizes every function of the problem and are non-dominated so it does not exist a solution that is better for all objectives in other words giving two solutions A and B solution A is dominant with respect to solution B if A is better than B in at least one objective function and not worse rather than all other objective functions.

On the Pareto frontier of solutions the one that are nearest to axes origin are best balance for minimum between all functions (green and yellow solutions in Figure 34). Depending on variable the problem the best solution can also be only one.

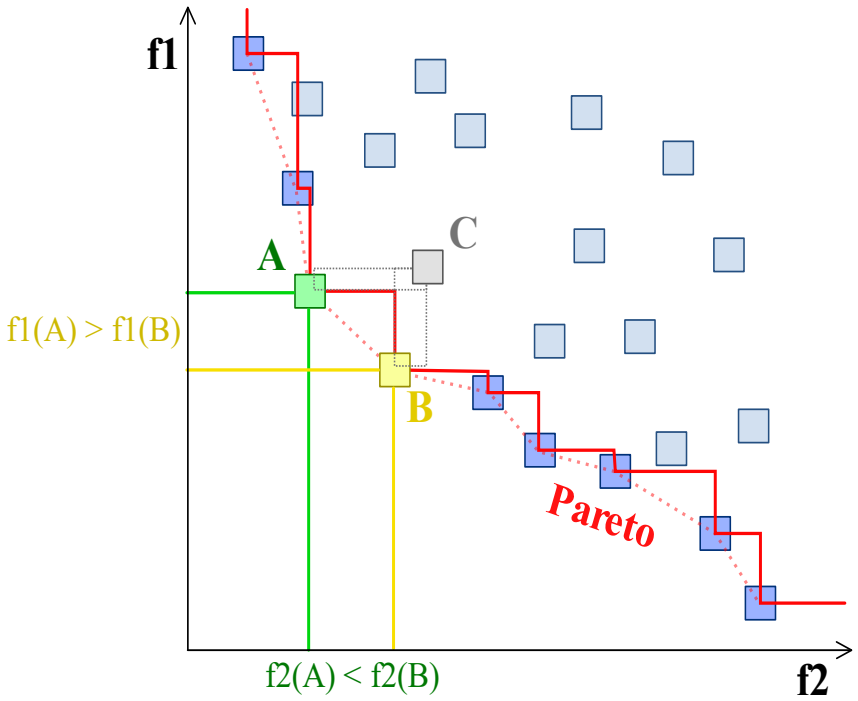

Figure 34 Pareto front example

Approach algorithms to solve this type of problems can be simple or complex here are reported some [75]:

- Weighted sum method: to all functions in the problem a value of weight is assigned deciding how much the function is important in the total problem, then in multiplying the function for the weight the problem is transformed in mono-objective and then solved. This is an easy and computational efficient method that however is not so accurate because of utilisation of weight that exclude to explore of Pareto frontier solution.

- Constraints method: defining objective and also constraints that has to be respected. A single function is than created by the sum of objectives and penalties applied to the function that no respect constraints during optimization. Problem Is then solved like a mono objective optimization that although consider also constraint and so can be more precise than the weighted sum but solution depend strongly on constraints input.

- Weighted metric method: similar to weighted sum method but objectives are sum with taking into account the norm with a reference point. Allows to find each and every Pareto-optimal solution but the reference point has to be calculated previously for every function.

- Benson method: as the weighted metric a reference point is chosen but this time from inside the feasibility area of the solutions, then the non-negative difference between every function solution and the reference point is calculated for each objective is calculated and their sum is maximized. Utilised for also for non-convex Pareto front problem in which Pareto solution doesn't have a continuous curve distribution for example for complex constraints applied.

- Evolutionary algorithm [76]: the one chosen for this implementation are algorithm that use iteration creating a 'population' of variables at every step and guiding the solution towards the Pareto front in utilising stochastic operators. The advantages of EO (Evolutionary Optimization) are multiple: do not require any derivative information, are relatively simple to implement and are flexible and have a wide-spread applicability.

4.1 Evolutionary Optimization Algorithm

For the nature of the optimization problem presented in this work: a non-linear and discontinuous problem, as assessed before, an Evolutionary algorithm is then choice because it permit to explore a lot of probably configurations taking into account all variable and guiding itself towards the solution with metaheuristic method and so they aren't built to solve only one type of problem that make this type of approach flexible.

This presented type of algorithm takes its cue from survival strategies that can be observed in nature for example Genetic Algorithm (that is the one most used evolutionary) is based on survival of the fittest such as Darwin's theory.

Genetic algorithms rely on a population of candidate solutions, called individuals, that represent possible answers to the problem to be solved. Each individual has a genotype, that is a mix of decision variable the characterize the problem. From an initial solution the population change according to a evaluation based on the fittest (objective of problem) and between them genetic operators are applied: mutation and crossover in order to mix the initial 'genetic heritage' of first population. The process is then repeated passing by a selection of new individuals to maintain 'alive' and so able to pass their attributes and individuals that scrap instead based on fittest criteria. This criterion favours the solutions that are more suited to the problem.

Evolutionary algorithms so apply mutation and recombination operators to the genotypes of the individuals, generating new solutions that can be better or worse than the previous ones. These operators

introduce variation and diversity in the population, permitting to explore major part of the solution space. A GA (genetic algorithm) procedure uses more than one solution at a time (population based) in an iteration, this approach differs from classical optimization algorithms which updates one solution in each iteration [76]. The use of a population has several advantages: it provides an EO with a parallel processing power achieving a computationally quick overall search, it allows an EO to find multiple optimal solutions, thereby facilitating the solution of multi-objective optimization problems.

For multi objective function such as the one treated in this tool NSGA – II procedure is used. Non-dominated Sorting Genetic Algorithm is a very popular algorithm among problem optimization that use a selection criterion based on non-dominance that defines a partial preference relation between two multi-objective solutions.

Relying on Pareto concept of dominance, solution x dominates a solution y if x is better or equal to y in at least one objective. A solution x is non-dominated if there is no other solution that dominates it.

As visible in Figure 35 NSGA-II works with two populations of solutions P_t, that is the parents group of solutions and Q_t, that are generated by genetic operators (mutation and crossover) from P_t, that are combined to form a new big population R_t. This is categorized using dominance and non-dominance between population to sort the solutions into different fronts, where the first front F_1 contains the non-dominated solutions, the second front F_2 contains the solutions dominated only by the first front, and so on. The new sorted population since is too big (two times the initial) cannot fit inside the new parent population P_{t+1} and so another selection among the last front is made by calculating the crowding distance as the perimeter of cuboid. The perimeter of the cuboid in formed by using the nearest neighbours in the objective space as the vertices. To guarantee diversity in solution and major exploration of Pareto solution, points with high crowding distance are chosen instead of others [76].

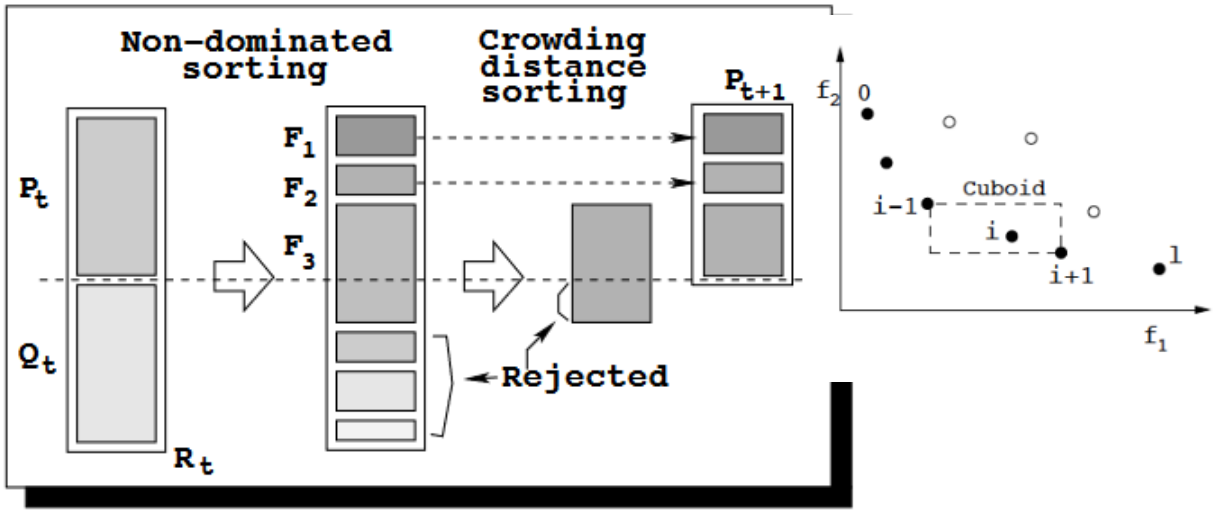

Figure 35 Functioning of NSGA-2

4.2 Pymoo NSGA-II optimization

Talking about problem and function to be optimize, as deeply seen in Chapter 3, two objective functions are defined LCOE and horizon occupation. These two function most of the time are in contrast and the reason is that both depend on the layout of the farm: distancing too much inter array space between turbine and implement a certain angle between array can lead to an increase of power production due to less fluid dynamic losses but can also make inter array cables cost unsustainable or turbines more visible from the nearest point of view from the coast otherwise minimizing the horizon area occupation can lead to worsening LCOE.

To implement NSGA-II algorithm in Python environment a specific library is recalled named Pymoo [77] that insure an user friendly interface and the possibility to set several parameters, that is integrated with other parts of the total script in the following way figured in Figure 36:

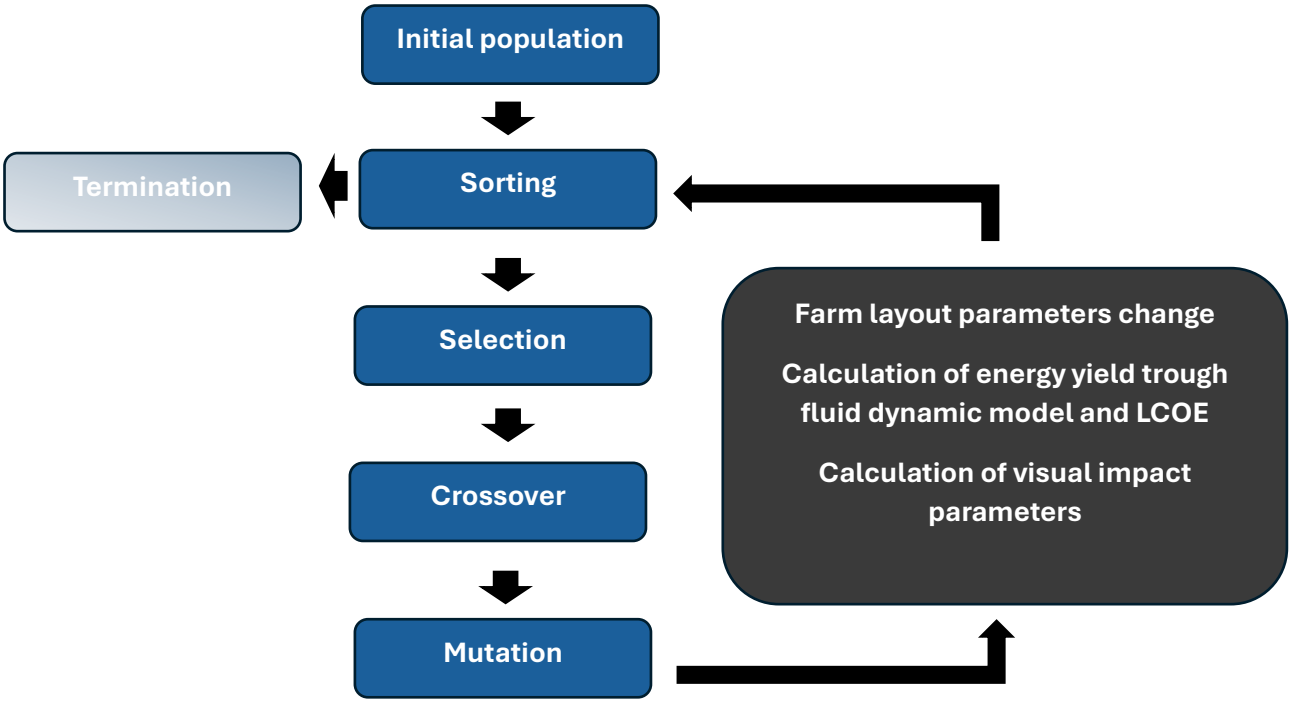

Figure 36 Optimization flow chart

4.2.1 Problem settings

Pymoo first approach is to define the problem class among various type according to characteristics.

The one selected is the "ElementwiseProblem" a class that is optimized for multi-objective optimization, this class allow to evaluate the objective function for every point in the domain of variables independent from the others point and it's used instead of" Problem" class that allow also to parallelize calculation for all variables in the domain in order to optimize computation. It, as well, calculates and it accept constraint as it is explained below.

Once the class is created, there are some variables that has to be initialized:

- n_var: namely the number of free variables on which the optimization work. Is crucial as it determines the layout of farm and distribution of array. All the objective functions values depend on considerations made for how distribute turbine in the area: a very dense arrangement could allow for a better scale economy and maybe a lower visual alteration of landscape, however, it could also imply a worsening in the productivity of the individual turbines due to the shadow effect that they exert on each other. All layout variables have been deeply described in namely four for the optimization.

- n_obj: number of objectives that will be minimized or maximized. NSGA-II method implies more than one objective in this case already treated in 3, LCOE and horizon occupation are chosen to both minimized because the first give an account of economy and energy factors while the second give an account of how will be perceived the farm.

- n_constr: number of constraints assigned to the problem by user. The constraints can be considered in certain values of objectives function or other values inside the problem that depend on objectives. In the case presented in tool only one constrained is considered in a specifical case of max area choice from the user that is one of two choices of procedure (max area, power density and turbine size or nominal total power and turbine size). In the first case an inequality constraint is placed in limiting the space of solution to the max assigned area.

- Boundary conditions: define the upper and lower limits that are assigned to variables because if in one hand is important to explore all possible solutions within the layout in the other hand to avoid waste of time and waste of calculations a reasonable range of values is given in input to the algorithm. This values are findable in sectorial studies [71]. Values are given to function by vector of lower and upper limit as seen in the code snippet below in Figure 37.

```
class Ottimizzazione(ElementwiseProblem):

    def __init__(self):
        super().__init__(n_var=4,
                         n_obj=2,
                         n_ieq_constr=1,
                         xl=np.array([2,3,-20,0]),
                         xu=np.array([8,12,20,0.83])
                         )
```

Figure 37 Problem class initialization code snippet

- Termination criteria: the termination parameter can be of various types, such as a time parameter, a limit of the number of simulations, of generations or a tolerance parameter with respect to the variation of the purpose of the analysis. In this optimization tool, for a matter of repeatability of the experiments we will use the number of generations as a parameter beyond which to stop the simulation through the function *DefaultMultiObjectiveTermination*.

- Seed: genetic algorithm implies a certain level of randomness particularly in initial phase of research of optimum. This randomness is regulated by seed value, an integer number that if is

equal in two subsequent simulations ensure the reproducibility of results. This value will be set to 1 in case study presented in next chapter in order to permit reproducibility.

After the problem definition then the algorithm parameters definition must be initialized. Below a description of parameters and different option are furnished but in the use of tool default options in Pymoo libraries were considered as visible in Figure 38.

```
class NSGA2(
    pop_size: int = 100,
    sampling: FloatRandomSampling = FloatRandomSampling(),
    selection: TournamentSelection = TournamentSelection(func_comp=binary_tournament),
    crossover: SBX = SBX(eta=15, prob=0.9),
    mutation: PM = PM(eta=20),
    survival: RankAndCrowding = RankAndCrowding(),
    output: MultiObjectiveOutput = MultiObjectiveOutput(),
    **kwargs: Any
)
```

Figure 38 Code snippet of NSGA-2 definition

- Pop size: number of results computed for each generation of GA. Population size is fundamental to give algorithm right diversity because large population is one way to explore more possible solutions of optimization. Is also obvious that a large population require a large computational time.

- Sampling: is the way of selection of first population from which starting the generation and sorting works. Sampling according to [78] can be chosen among two way: *FloatRandomSampling* that use a random approach to get first population across the allowed space of solutions or *LatinHypercubeSampling* that divide variables space in ranges that have same probability and then chose solutions avoiding to repeat to use variables from the same space and that guarantee diversity.

- Selection: this function decides which members of actual population have to front crossover and so the individuals that will share their characteristics in order to create new solutions. Selection can be made with *RandomSelection* so in a random way for definition but avoiding the repetition of same solutions to be coupled or with tournament solution that create a “fight” between two solutions and only one is picked up passing through best fit or non-violated constraint criteria. Selection is important for the convergence time because with this operator the algorithm can avoid premature convergence in suboptimal solutions.[79]

- Crossover: is one way of genetic mixing of algorithm. Crossover has the aim of take characteristics from parents solution and mixing to create offspring. Pymoo offer various type of this operator but the one used for simulation is SBX Crossover that is Simulated Binary Crossover since a real binary (with binary variables) crossover can't be done. SBX is indicated for variables in real field and exchange characteristics between two parents solution $p_1\ e\ p_2$ with one point crossover so "cutting" genetic heritage so variables in one point for the two solutions to be crossed and then exchange them. Two factors has to be indicate how many members of population will face crossover (probability) and the distribution factor η (equal to 15 by default) and β_q value that decide how much far offspring $c_1 e\ c_2$ will be far from parents in terms of characteristic. [80]

Equation 4.1 SBX offspring equation

$$c_1 = 0.5\left[(1+\beta_q)p_1 + (1-\beta_q)p_2\right]$$
$$c_2 = 0.5\left[(1-\beta_q)p_1 + (1+\beta_q)p_2\right]$$

Equation 4.2 Equation for Beta parameter

$$\beta_q = \begin{cases} (2u)^{1/(\eta+1)} \\ \left(\frac{1}{2(1-u)}\right)^{1/(\eta+1)} \end{cases}$$

With *u* parameters that is a random number between 0 and 1

- Mutation: the mutation operator randomly modifies a solution to introduce diversity into the population. In the calculations, the PM (Polynomial Mutation) class is used, which uses a polynomial distribution to produce values that are close to the original value. Parameters are chosen in selecting two variables: probability of selection of a variable and distribution parameters η_m that indicate distribution parameter form. Then δ_i is computed as function of η_m and finally new characteristic x_i^I is created by mutating old variable x_i taking into account limits for this variable $x_{max}\ and\ x_{min}$.

Equation 4.3 Delta variable equation

$$\delta_i = \begin{cases} (2u)^{1/(\eta_m+1)} - 1 \; se \; u < 0.5 \\ 1 - \big(2(1-u)\big)^{1/(\eta_m+1)} \; se \; u \geq 0.5 \end{cases}$$

With *u* parameters that is a random number between 0 and 1.

Equation 4.4 Mutated variables equation

$$x_i' = x_i + \delta_i(x_{max} - x_{min})$$

- Survival: survival strategy of the population that is created after the temporary union between parents and offspring populations in NSGA – II is based on Rank and Crowding as has deeply been descripted in 4.1.

Finally, as all parameters is initialized Genetic Algorithm is run through minimize function of Pymoo as visible in Figure 39. Indicators for ongoing optimization is given by interface in terminal dialogue of the code editor through the flag *Verbose* on the done when calling minimize function. Save history flag save instead all information of optimization that are useful to visualize plot of results and to do an evaluation of algorithm work.

```
res = minimize(problem,
               algorithm,
               termination=termination,
               seed=1,
               save_history=True,
               verbose=True,
               )
```

Figure 39 Code snippet of minimize function

4.2.2 Evaluation and convergence

When an optimization algorithm is computed and correctly run is important to evaluate results to understand how fast it had reached solution, how accurate it has been and to make comparison between the chosen approach is the better.

Pymoo give multiple choice to evaluate convergence [81] and results of algorithms that can be distinguished between two way: known Pareto Front and unknown Pareto Front. If Pareto Front solutions are known.

If Pareto Front is known or also approximated then Generational Distance, so the distance between every point in Pareto Front and the nearest point in founded solution, is a good indicator. There is also the Inverted Generational Distance that is just the inverse of the Generational Distance.

When the Pareto Front is unknown then other strategies has to be accounted: Hypervolume and Running metric. Both measure area of calculated objectives.

Hypervolume method measure area between the calculated Pareto Front and a reference point that has to be properly stated. The point must be an ideal point of optimization objective and then the area calculated with the hypervolume is an indicator of how the founded solutions are close to the optimum reference point. Hypervolume value is calculated as $(1 - Area_{sol})$ so better solution tends to 1 when distance from reference and so area tend to zero.

To plot an example a 500 MW farm has been optimized at the coordinates 18.6°E 40.2°N with turbines of 10 MW. Optimization has been computed with a population of 50 and fixed n_{gen} equal to 30. Hypervolume given in Figure 40 has the reference point at coordinates (1,1), these choice for reference point rely on infinitesimal probability of this point to be computed and so represent an utopian point of reference for a comparison with Hypervolume method.

To verify convergence of only one objective function then minimum LCOE for every generation of algorithm has been showed in Figure 41.

Another plotted parameter is the *RunningMetric*. The running metric shows the difference in the objective space from one generation to another and uses the algorithm's survival to visualize the improvement. This metric is also being used in Pymoo to determine the termination of a multi objective optimization algorithm if no default termination criteria have been defined. In Figure 42 Running metric is showed until the final population shows the algorithm seems to have more a less converged, and only a slight improvement has been made.

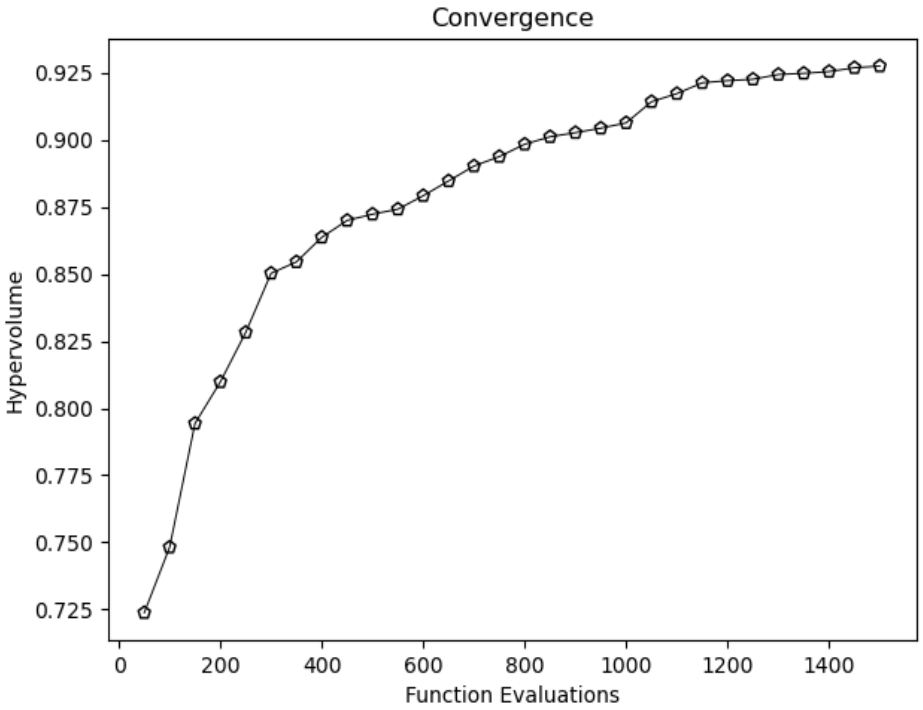

Figure 40 Hypervolume convergence

It should be noted how the solution space tends to converge towards the reference point as evaluations progress. The algorithm explores more solutions with an increasing trend but tend to adjust itself in the latest generation, following an asymptotic trend towards a value of 0.925.

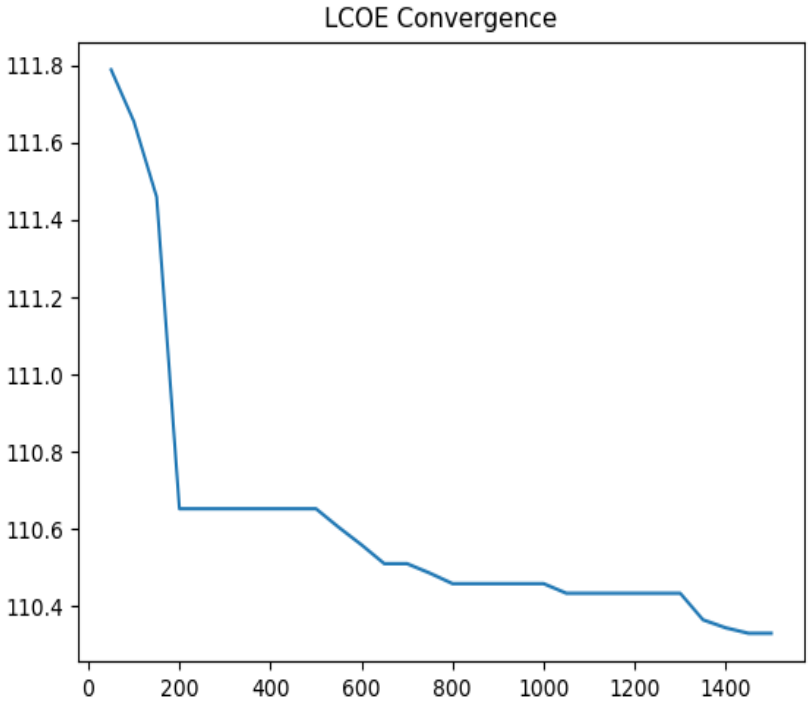

Figure 41 LCOE convergence

As it is visible in Figure 42 with ongoing of generations there is not more improvement e.g between generations 25 and 30 Running metric area follow same asymptotic trend. That is the indices of a good choice in number of population and number of generations.

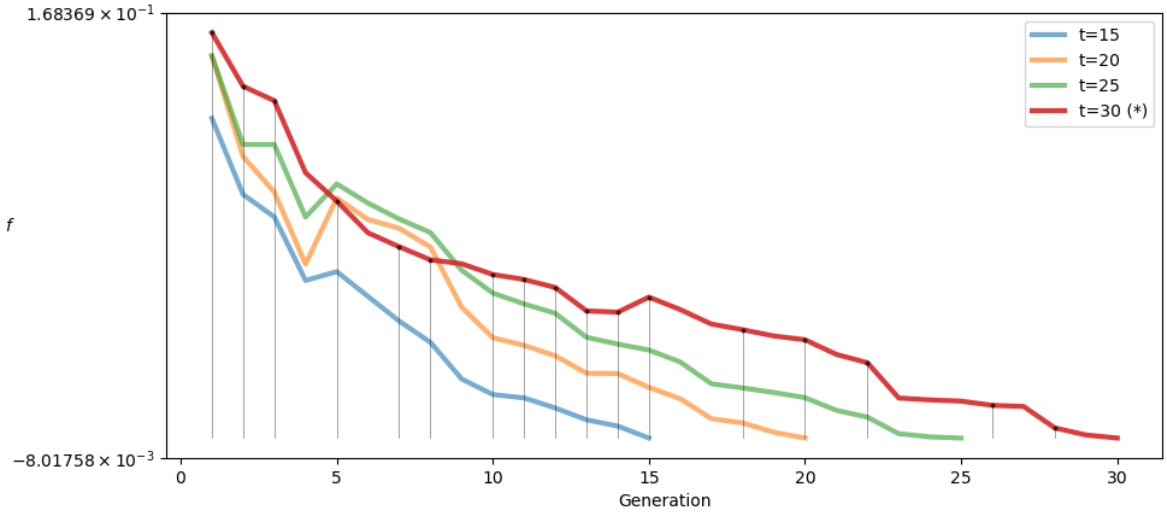

Figure 42 Running metric evaluation

The Figure 43 describes Pareto Front giving an account of how Genetic Algorithm had worked to explore space of results. In order to choose best optimum for user point of view and only one solution between the many non-dominant solution that the optimization had found a norm between the axis origin and every point in Pareto Front has been calculated and then the minimum has been chosen to guarantee a solution that is good for both the two objectives.

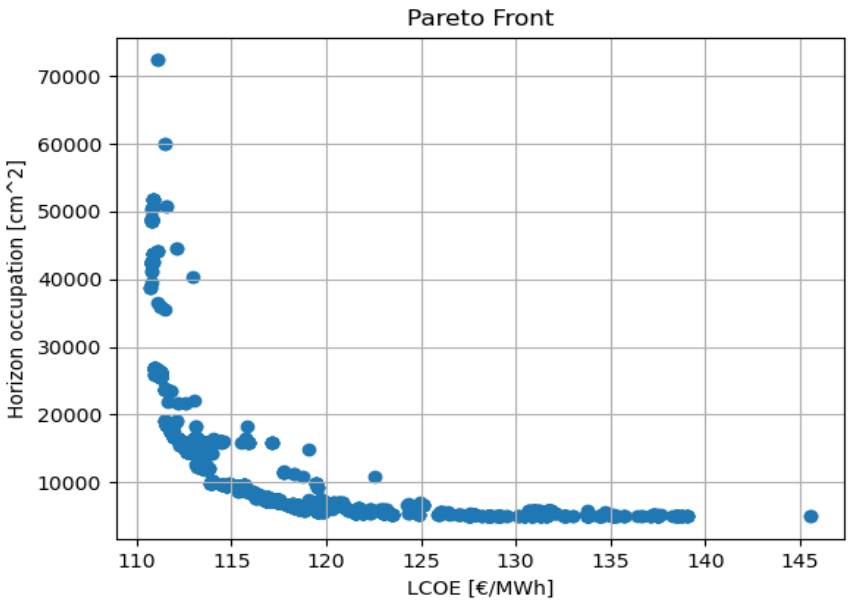

Figure 43 Pareto front

Chapter 5

Results and case studies

In this chapter an example of tool's working with a realistic case study give an account of all the work explained before and, once the functioning of the tool has been clarified, reference with presented projects permit to validate tecno-economical model.

5.1 Identification of suitable wind farm area in MED region

First of all for chosen of site an interactive map is showed in Figure 44 that inform user about feasible point of chosen made about bathymetry and maritime routes constraints chosen from user input that in this case are presented in Table 7.

Map includes coloured points of wind resource in m/s that are inserted in range between minimum and maximum bathymetry and under the maximum maritime routes value allowed. In defining a feasible region, a point then can be manually selected. A coloured legend shows mean wind speed level, that are mean data collected for ten years in region, and, as well, yellow lines for lower bathymetry and red lines for higher bathymetry limit.

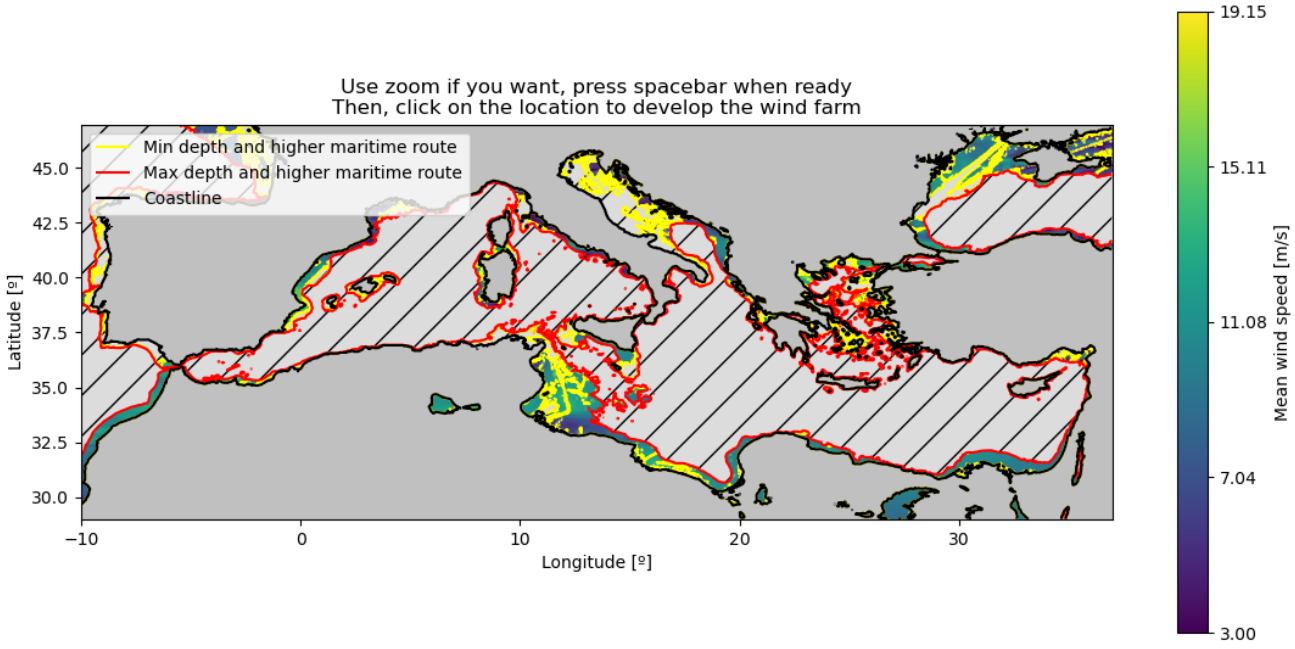

Figure 44 Constraints map in MED region

Users can also select a site by entering numerical coordinates values. It is important to emphasize that, whether though map selection or manual input of coordinates, the tools alerts the user with a textual message if the selected point is too close to the coast, falls below or exceeds the minimum and maximum bathymetric limits, or is located inland.

Since the total occupied area is unknown at the beginning of optimization, since optimization act on spacing between turbines, then a control function of the maximum area that can be occupied after the optimization has been implemented. A textual message warn user that, after the optimization, occupied total area can overcome imposed limits on bathymetry. This type of warning should be also done with distance constraints but it's an idea for future's improvements.

5.2 Case study

To have an idea of how tool is presented to user and the results that can be obtained realistic simulation is made with a site selection through several given input showed in Table 7 of bathymetry, nominal power, coast distance and maximum maritime route. A comparison is made between one optimized result and one default result without optimization.

First of all, through the interactive map of Mediterranean area in Figure 44 is figured out with considering the constraints in Table 7 as defining feasible points:

Table 7 Wind farm characteristics

Turbine size [MW]	**Nominal Power [MW]**	**Minimum depth [m]**	**Maximum depth [m]**	**Minimum coast distance [km]**	**Maximum maritime route [route/sqm/year]**
15	900	30	300	3	50

In Figure 45 focus version of selection map is showed in including selected point description.

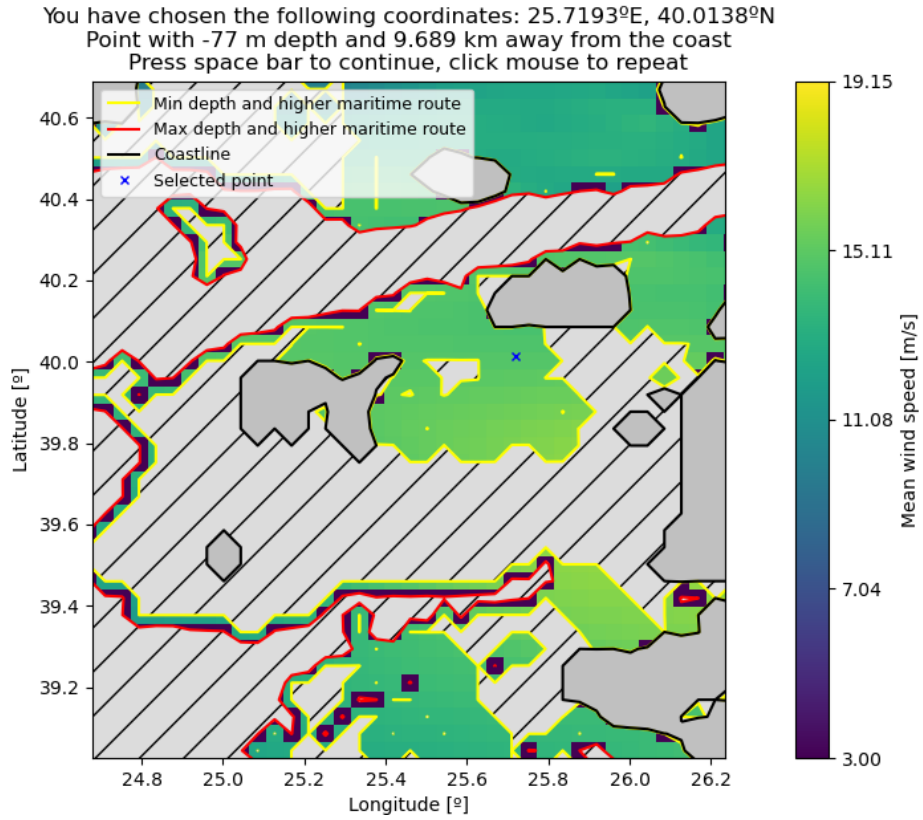

Figure 45 Point selection through map

Simulation starts with collecting wind data and dividing by sectors. In Figure 46 below an overview of wind rose with real wind velocity steps for the site. Main direction in this case is 36° where wind is more frequent as it is visualized, it is evident that the wind speed predominantly ranges between 5.2 and 11 m/s (orange in the graph).

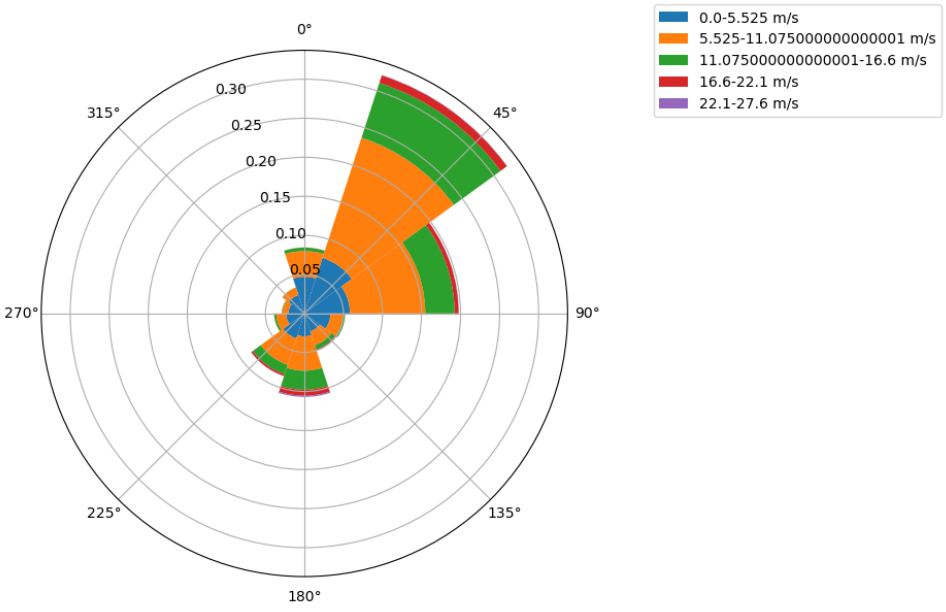

Figure 46 Wind rose for selected point

Simulations have been conducted using 10 years wind data, from 2010 to 2020, to avoid excessive computational time. For a complete simulation and optimization, the tool spend almost 15 mins doubling time in doubling years of wind data considered.

Creating economic and visual impact model require individuation of nearest port to compute installation costs and nearest point of view from coast for individuation of horizon occupation figured out in Figure 47.

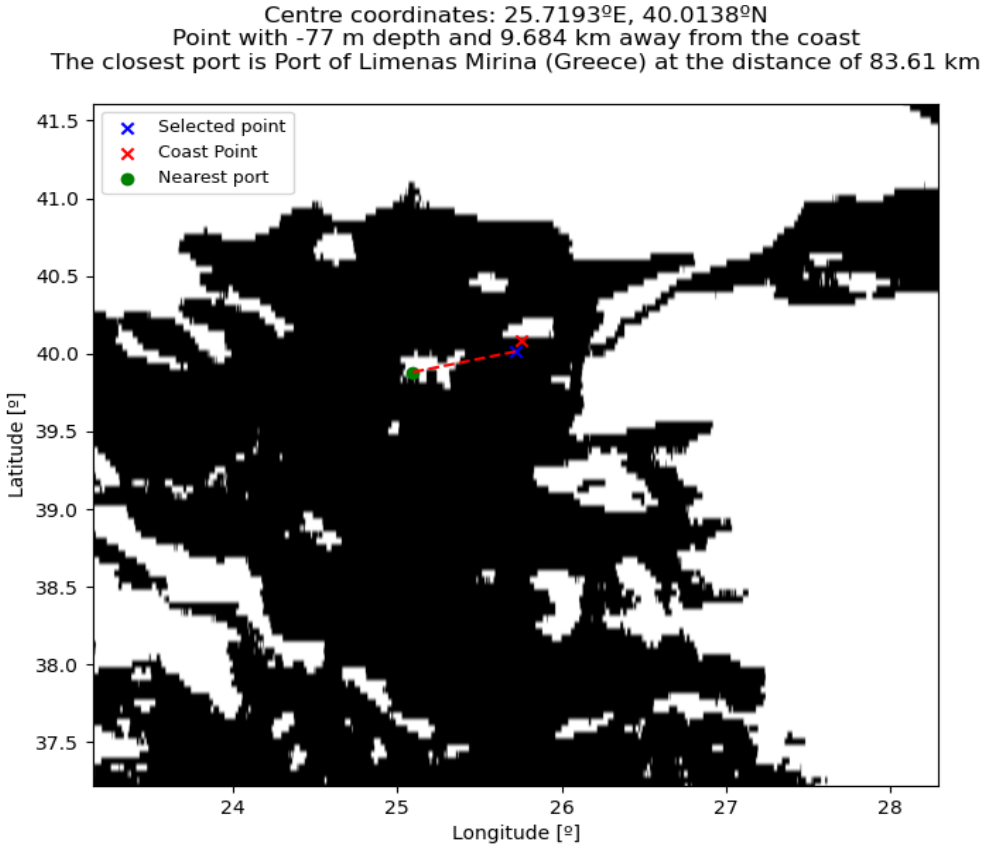

Figure 47 Distance from nearest port and visual point

In Table 8 results are shown, non-optimized layout is referred to a farm with the same distance of each turbine in wind direction and in cross wind direction namely 5*D in this case with no staggered configuration. For Optimized case is clearly visible how optimization has slightly improved LCOE that drop of a -3% due to an increase of AEP +2% and down of Capex + Opex costs -2%. Occupied area that with optimization has been dropped with a -88% resulting in a better turbines distribution and a reduction of cost of grid connection -1,5% (passing from 213 to 112 km of medium voltage inter array cables) to on the total Capex + Opex costs visible in Figure 48. From visual perspective a clear improvement has been made because total horizon occupation has dropped of -46% (as will be shown in Figure 50) despite nearly the same number of distinguishable turbines.

Both objectives of optimization are then reached.

Table 8 Comparison of simulations

	Capex + Opex [M€/MW]	LCOE [€/MWh]	Horizon occupation [cm^2]	Occupied Area [sqkm]	AEP [GWh]	CP [%]	Distinguishable turbines	Wake Loss
Non-Optimized layout	2.71	104.9	171.3	129.4	2846.6	36.1	53	22.3
Optimized layout	2.66	101.8	92.8	29.15	2895	36.7	49	21

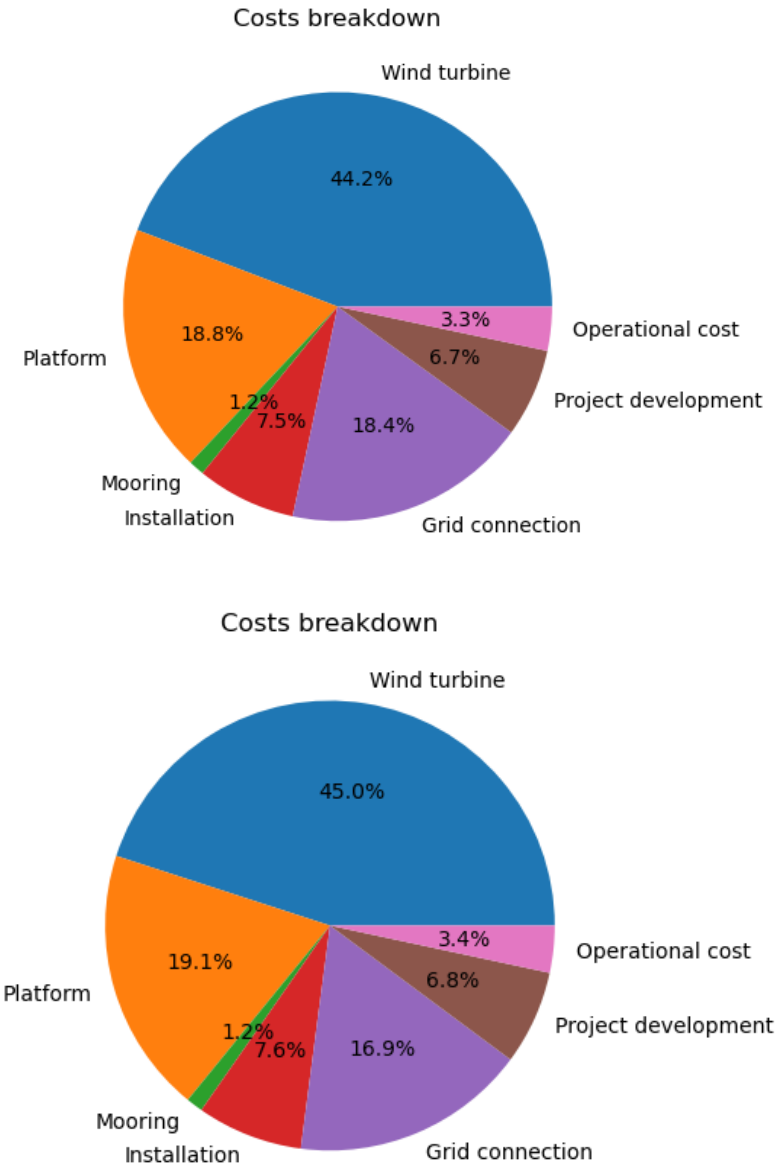

Figure 48 Costs breakdown

For a better view of comparison then the two layouts are shown in Figure 49 (a and b). While the first present a squared layout the second is built with a staggered layout that is better both for avoiding fluid dynamic losses and occupation of horizon as will be seen below.

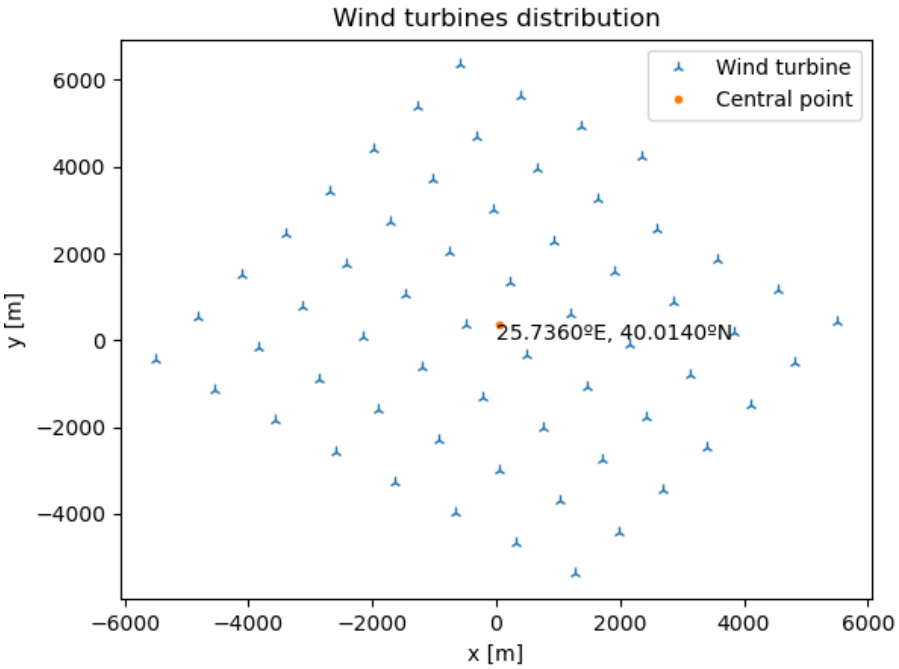

(a)

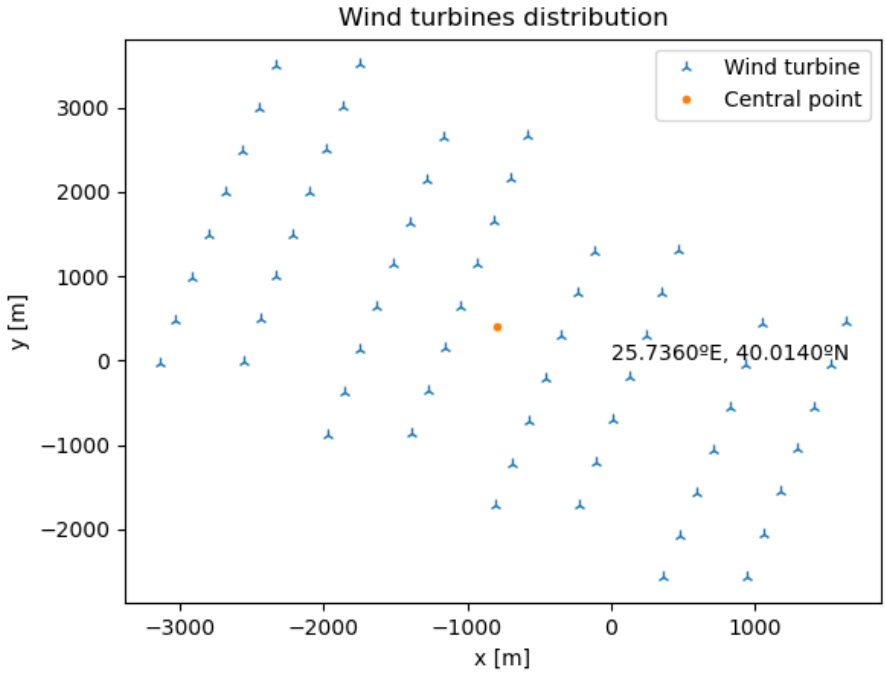

(b)

Figure 49 Farm layout

To visualize improvement in visual impact of farm the visualization in x-z axes is the Figure 50 (a,b). Is clearly visible as in the optimized layout (b) the turbines are more grouped in the centre towards the direction of the land and then less of them are visible. Horizontal max distance between the first and the last turbine visible in x-axes is nearly 110 cm in non-optimized case and 63 cm in the optimized one.

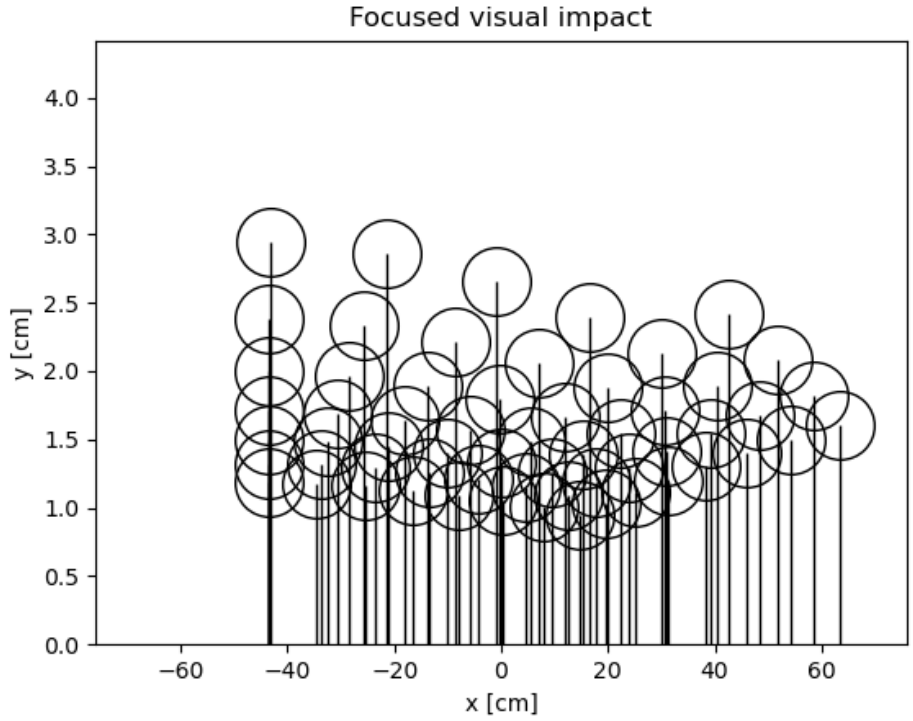

a

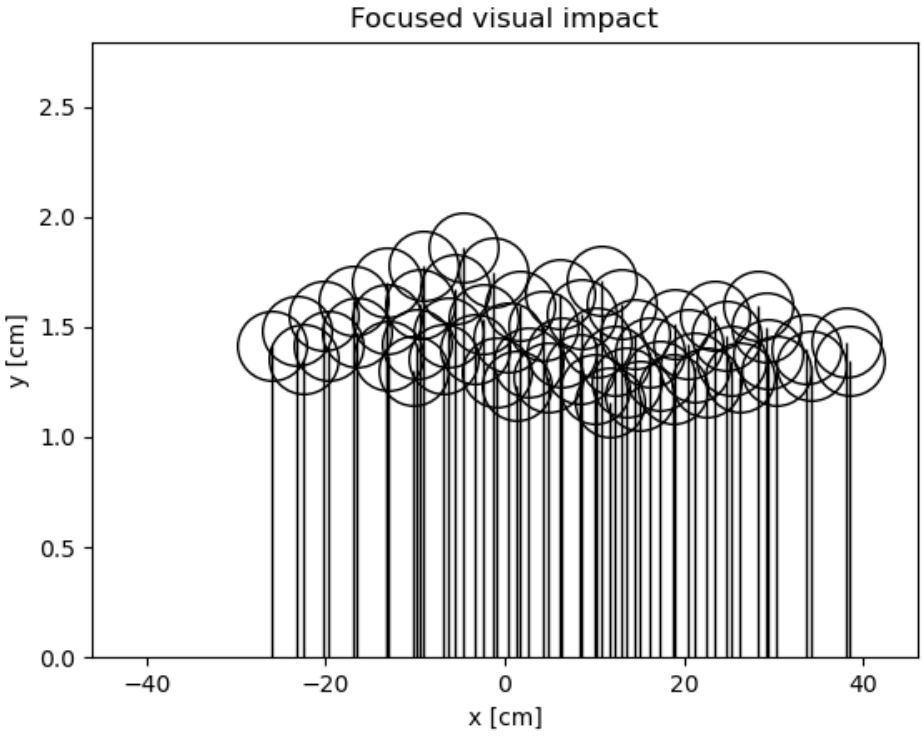

b

Figure 50 Visual impact

Effective wind speed map is plotted for the considered layout comparison in Figure 52. Since the computational cost for this type of plot is very high, due to the calculation for the wake effect model used, only a portion of the entire farm has been considered: 9 turbines have been plotted instead of 60 to give an account of different layout can influence a lot wind velocity within arrays.

The staggered and more spanned layout in Figure 52-b permits to reach higher value of downwind velocity with respect to squared profile in Figure 52-a.

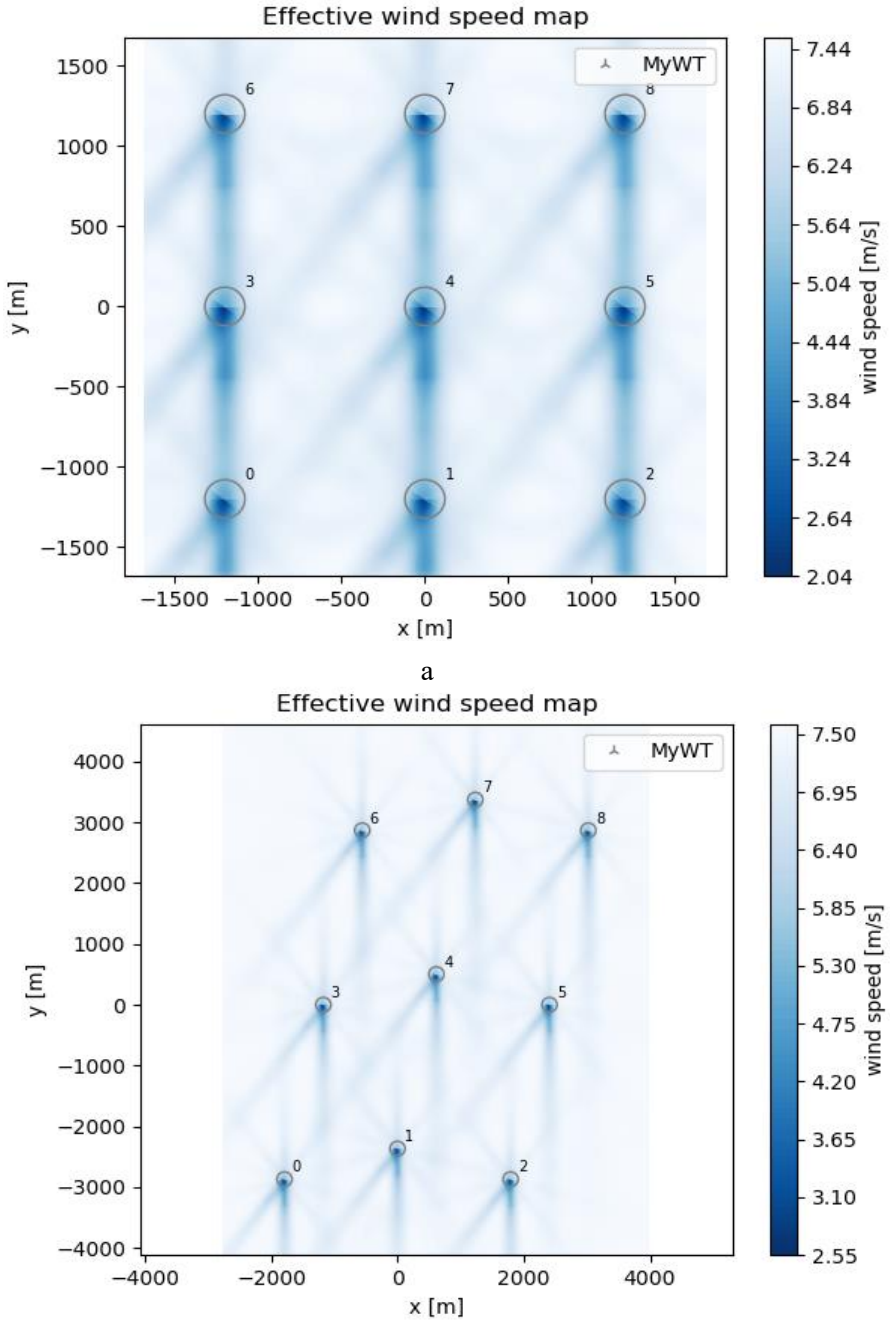

Figure 52 Wake map

5.3 Comparison against wind farm project case studies

Projects chosen for the comparison are all located in Italy and the reason is the availability of data since in the site of the Italy government [82] where all documents about new projects waiting for approval are stored. Since all projects considered are not yet constructed but in state of scoping or under approval data about are not always correct since most projects are not definitive.

In Table 9 informations about projects are reported as well as references and positioned in Mediterranean area in Figure 53.

Table 9 Real presented offshore project in Italy

Project name	Total power (MW)	Longitude	Latitude	ref
Atis Floating wind	864	9.62°	43.32 °	[32]
Nora Energia1	795	8.53°	38.67°	[83]
MedWind	2793	11.38°	37.98°	[31]
Nereus	1800	16.6°	41.798°	[34]
Odra Energia	1350	18.55°	39.85°	[84]
SicilySouth	1200	13.21°	37.07°	[85]
Rimini	330	12.76°	44.12°	[86]

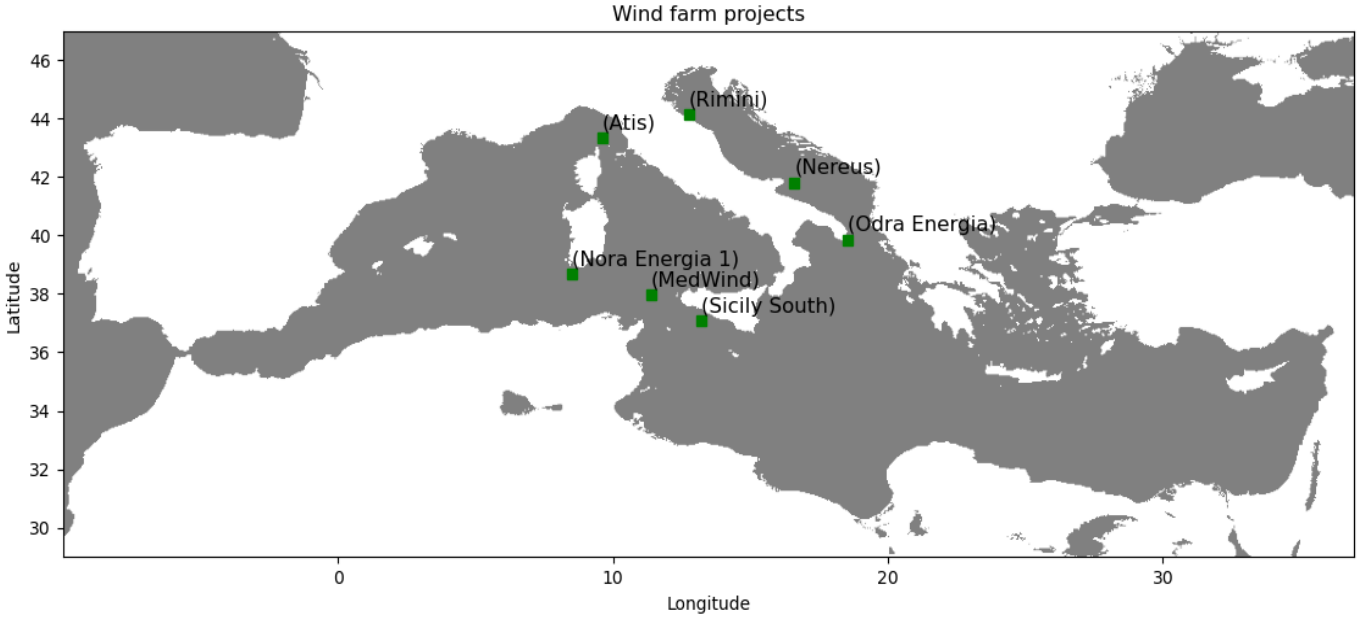

Figure 53 Presented projects in MED area

Wind rose for every point has been visualized in every considered point in Figure 55 for the ten wind direction sector considered in simulation. As assessed before wind profile are comparable within every case except for Rimini showed in Figure 55-Rimini in which the lower wind velocity is clearly visible and affect producibility and LCOE.

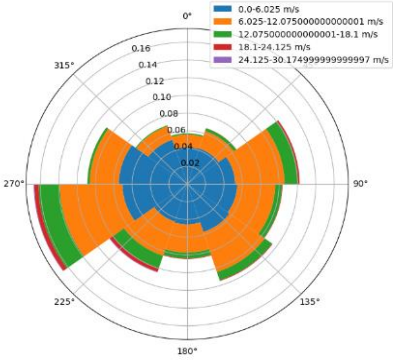

(Atis Floating Wind)

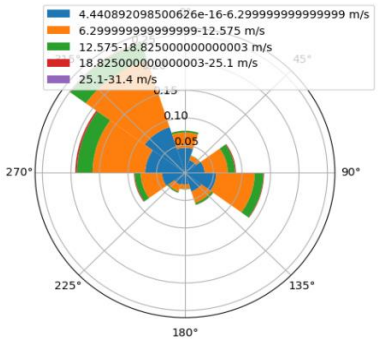

(Nora Energia 1)

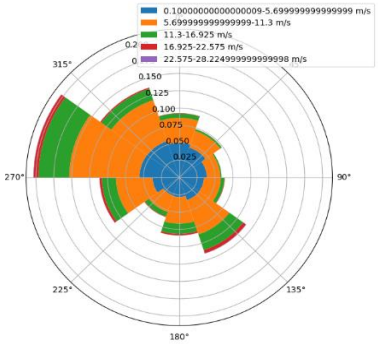

(MedWind)

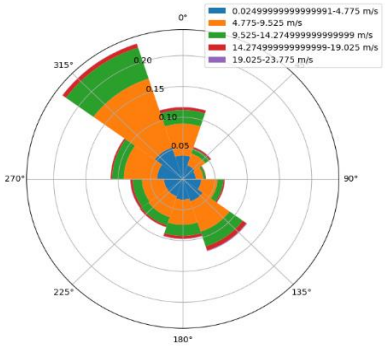

(Nereus)

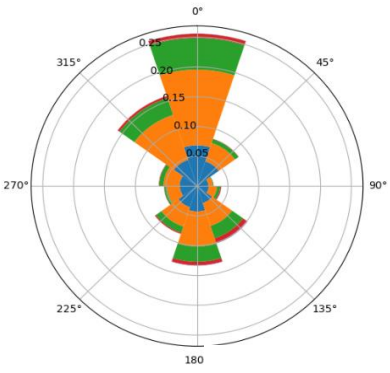

(Odra Energia)

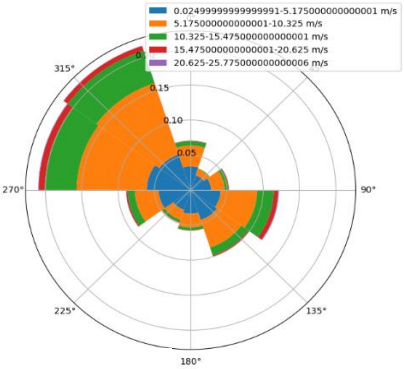

(Sicily South)

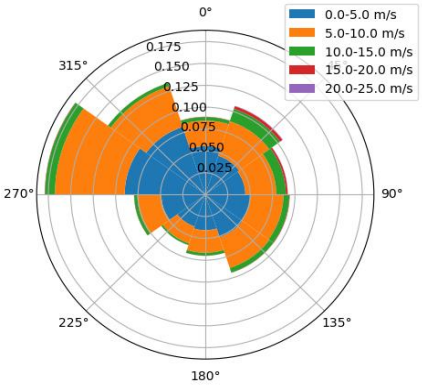

(Rimini)

Figure 55 Wind rose for presented projects

The various simulation will compare data of annual energy production, Capex and Opex, occupied horizon area between optimized and non-optimized layout with a focus on costs distribution.

Table 10 Parameters comparison before and after optimization

	Non-Optimized layout			Optimized layout		
	AEP [GWh]	Opex+Capex [M€/MW]	LCOE [€/MWh]	AEP [GWh]	Opex+Capex [M€/MW]	LCOE [€/MWh]
Atis	2018,7	2,78	145,7	2434	2,84	122,67
Nora Energia 1	2584,6	2,79	104,7	3095,5	2,84	88,59
MedWInd	8004,8	2,87	120,59	9646	3	103,61
Nereus	4329,9	2,77	140	5718,8	2,84	108
OdraEnergia	3389,4	2,74	133,2	4181,7	2,73	107,62
SicilySouth	3221,8	2,79	126,25	3955	2,86	104,67
Rimini	434,4	2,95	262,6	494,7	2,95	235,89

Table 11 Horizon occupation area before and after optimization

	Horizon occupation area [cm^2]	
	Non-Optimized layout	Optimized layout
Atis	4,34	4,46
Nora Energia 1	13,59	10,75
MedWInd	0	0
Nereus	0,38	0,76
OdraEnergia	51,35	38,62
SicilySouth	4,65	4,21
Rimini	14,73	19,56

From results of optimization of all presented case studies can be seen how the algorithm has optimized the two objectives: LCOE and horizon occupation area. Comparison of layouts can be seen in **APPENDIX C**. From economical point of view every found optimized layout is more costly than the non-optimized one (Capex+Opex colums in Table 10) but a net increase in AEP has been noted. The drastic increase in AEP had led to a decrease in LCOE for every considered case study. For what concern horizon occupation area showed in Table 11 and so visual impact from coast optimization led to improvement for Nora Energia 1, OdraEnergia and Sicily South in minimizing the area and worsening for Atis, Nereus and Rimini in which area is increased. MedWind case remain unaltered since project is not visible from cost. In Figure 57 costs breakdown is reported. Is visible how grid connection costs are affected by layout of farms, optimization algorithm tends to spread turbines in order to minimize shade effects and this behaviour increase connection costs for longer cables.

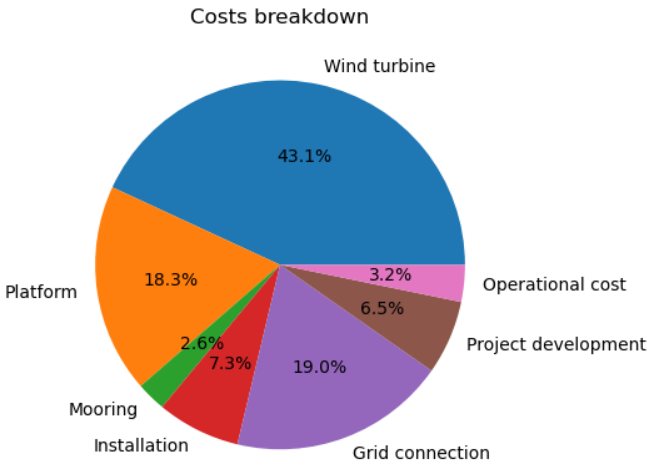

(Atis Floating Wind Non-optimized)

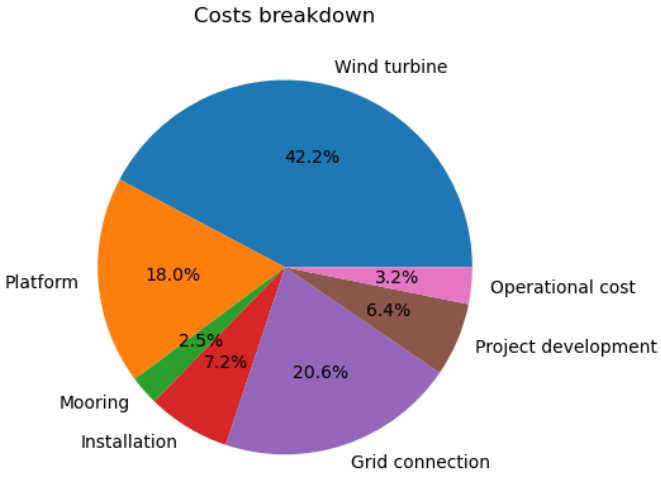

(Atis Floating Wind Optimized)

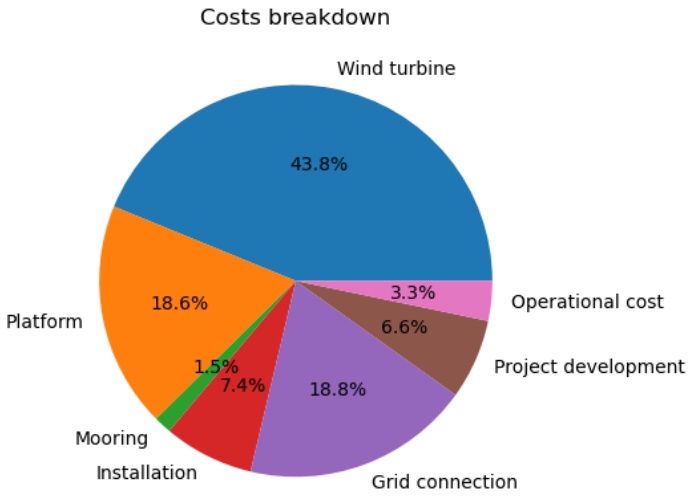

(Nora Energia 1 Non-Optimized)

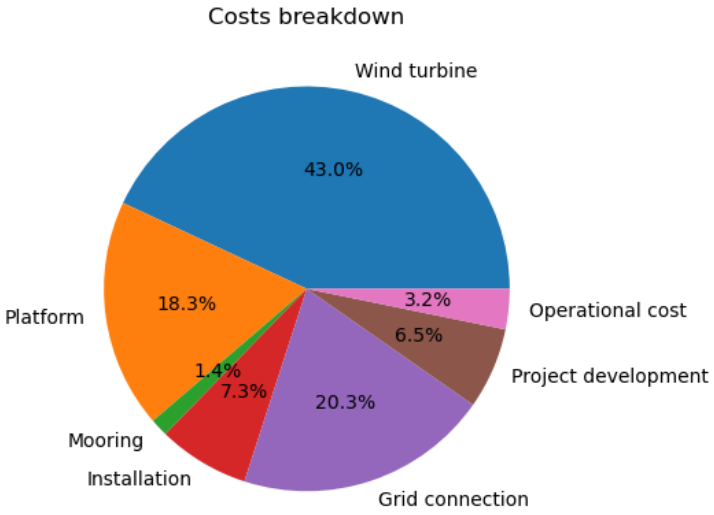

(Nora Energia 1 Optimized)

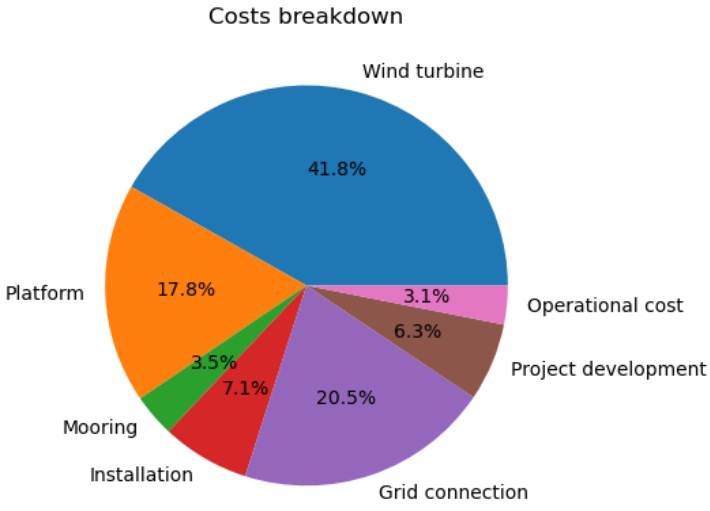

(MedWind Non-Optimized)

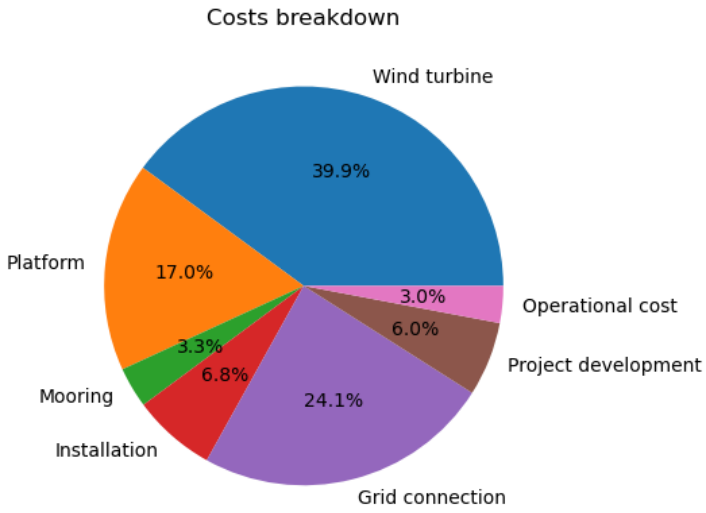

(MedWind Optimized)

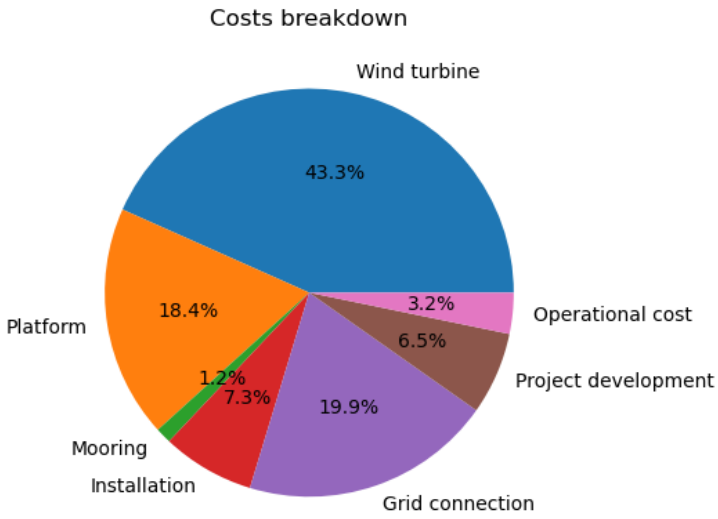

(Nereus Non-Optimized)

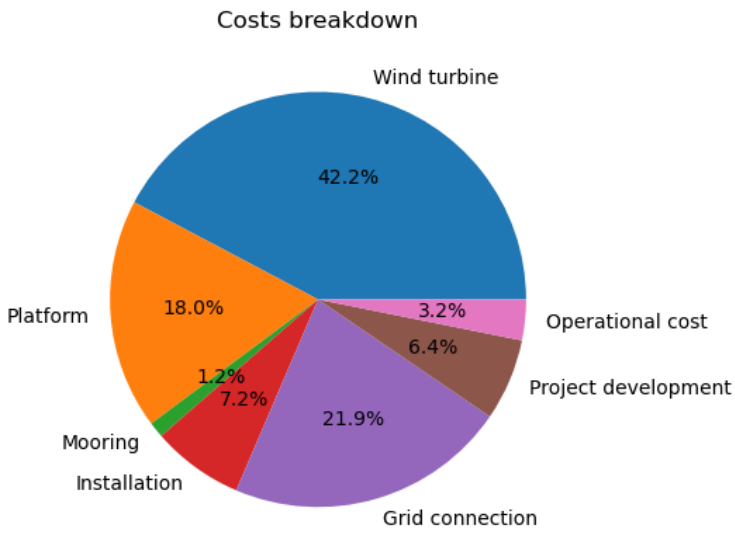

(Nereus Optimized)

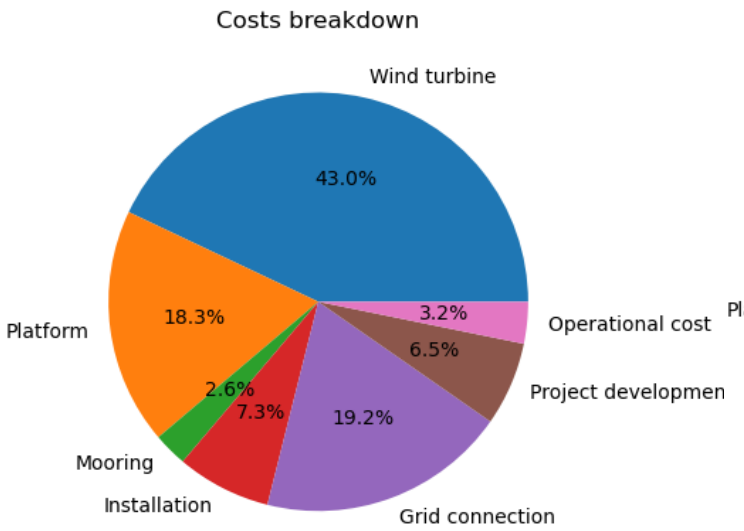

(Odra Energia Non-Optimized)

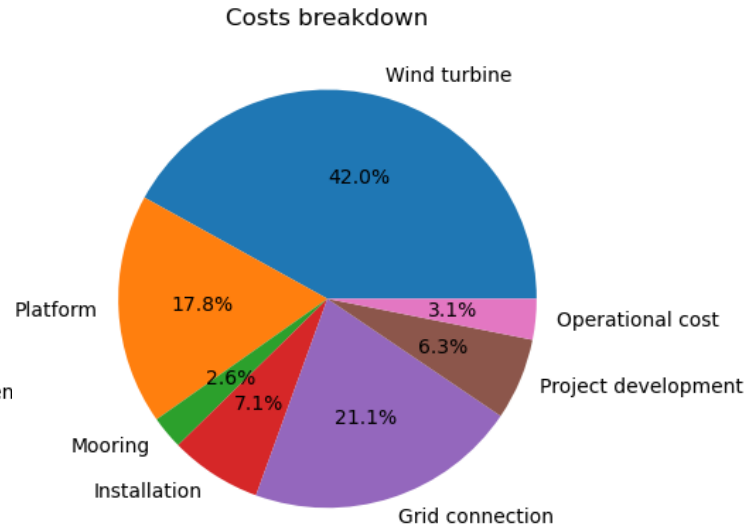

(Odra Energia Optimized)

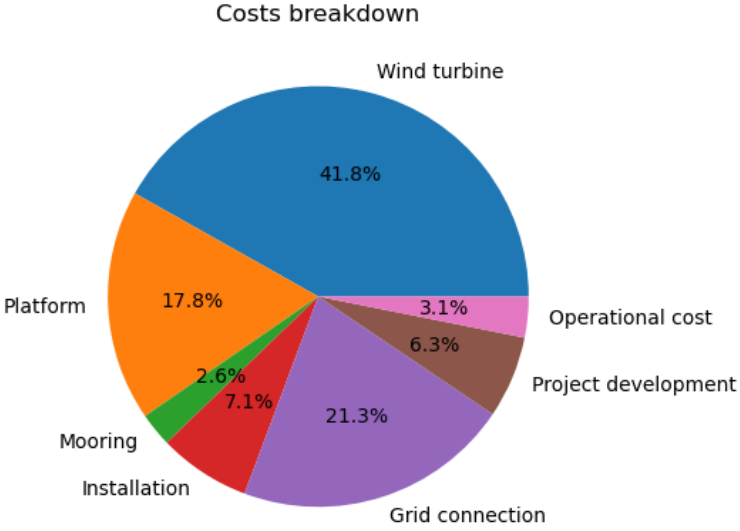

(Sicily South Non-Optimized)

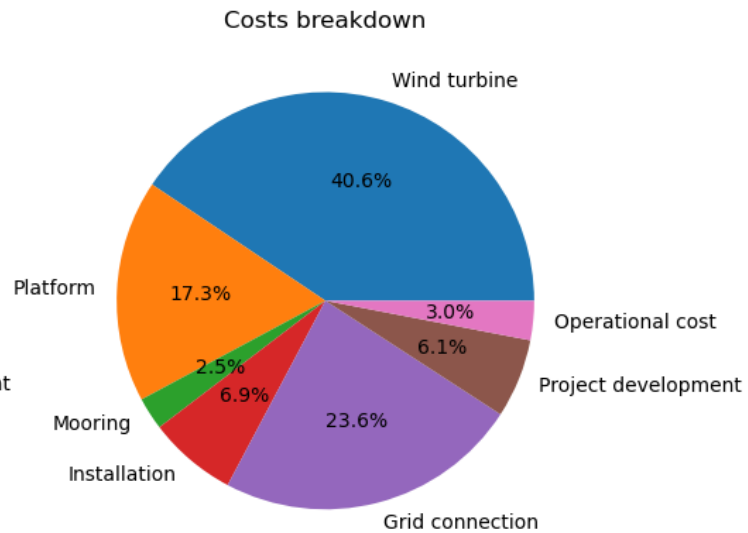

(Sicily South Optimized)

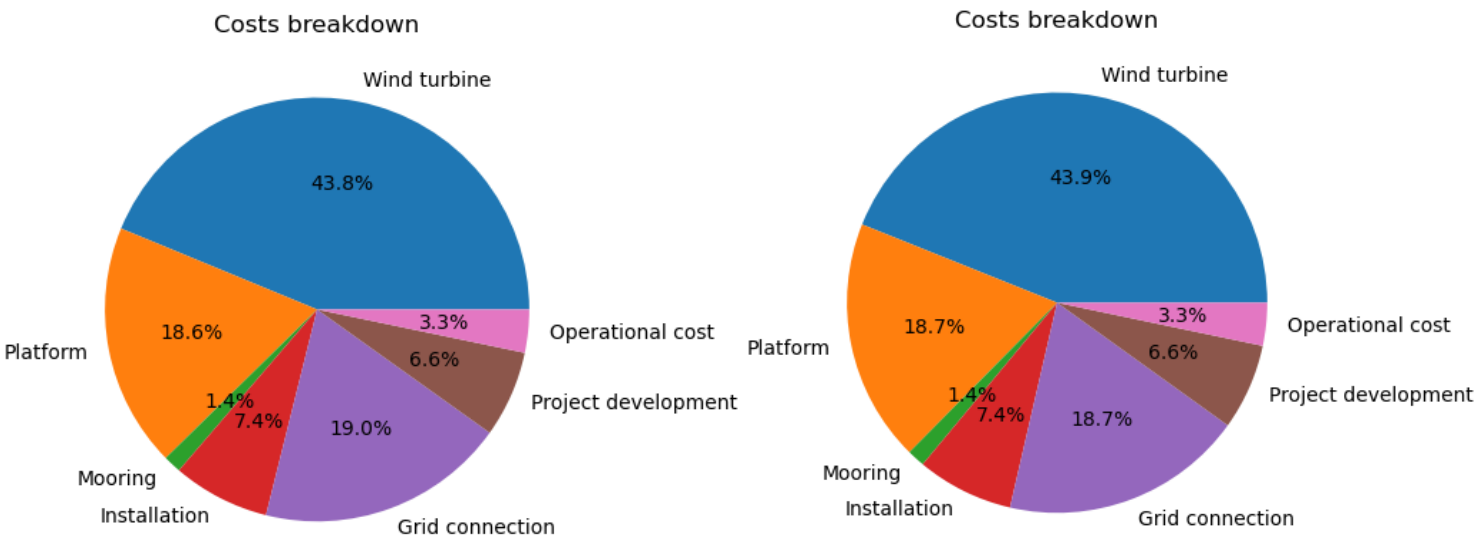

(Rimini Non-Optimized) *(Rimini Optimized)*

Figure 57 Costs breakdown comparison

For every case study a comparison between LCOE and CP has been figured out in Figure 58. The trend for LCOE is almost linear for presented case with a mean of 124,4 €/MWh overcame only by Rimini farm that due to a non-favourable wind velocity in the area has reached an estimated LCOE of 235,9 €/MWh. Data are consistent with the Cp value that present greatest value for Nora Energia 1 43,6% and lowest value for Rimini 17,1%.

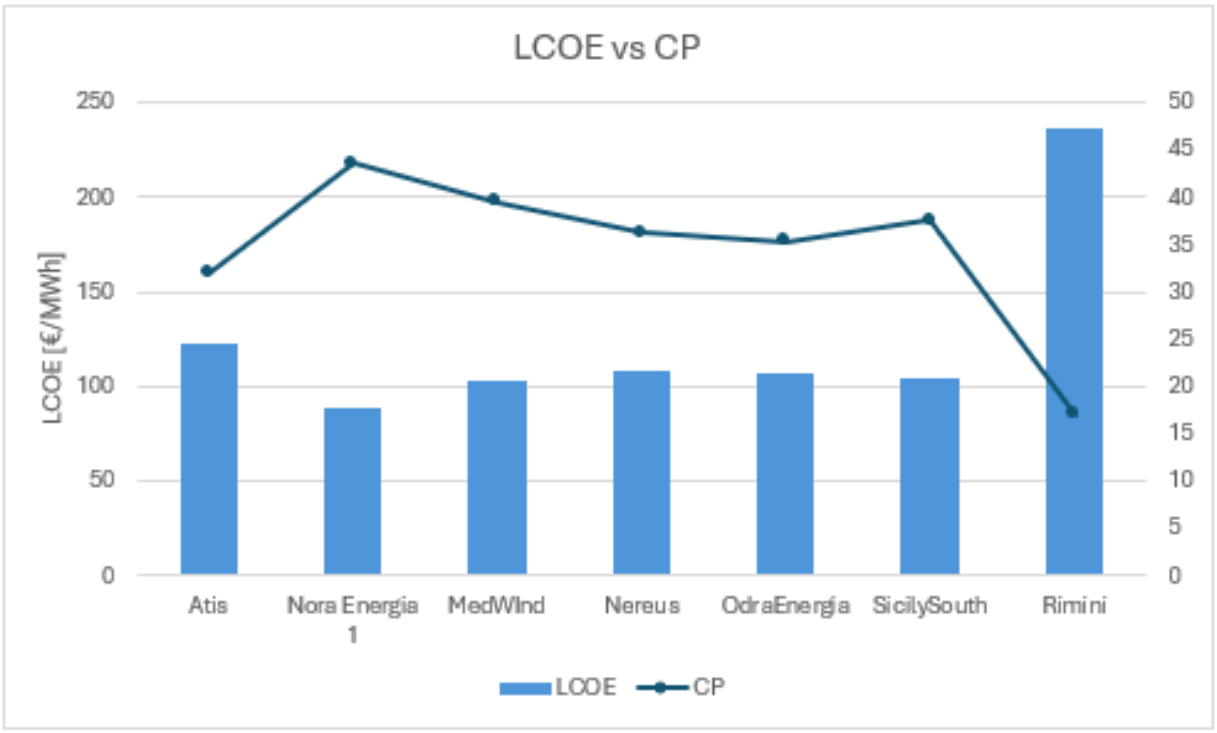

Figure 58 LCOE vs Cp

5.4 Economic model validation

For validation of model purpose, values of cost per installed MW have been chosen because other values like layouts are difficult to retrieve for real projects. Design is strongly influenced not only by efficiency reasons but also from granted areas, seabed condition and marine current that are difficult to take into account in a preliminary simulation like that. Costs estimation on the contrary can be a good term of comparison because they are based on literature despite are not yet the correct one. Among the found cost of presented projects onshore cable cost have been discarded because it is not considered in tool economic model.

In Table 12 below a comparison between costs for optimized tool farm and real farm is made. Is showed how estimation from designer and from tool vary of a mean of 10%.

It's important to note that for not every farm compared an exact simulation has been made because real turbines model utilised are not available in tool constructions: 18 MW model for Atis Floating Wind and 25 MW model for Sicily South has been replaced with 15 MW the max power available in tool and 6.5 MW used in Rimini project with 5 MW.

Table 12 Comparison between estimated costs

Project name	**Estimated cost from designers [M€/MW]**	**Estimated cost from tool [M€/MW]**	**Relative gap [%]**
Atis Floating wind	3.375 [87]	2.863	-16%
Nora Energia1	2.904 [88]	2.764	-5%
MedWInd	3.298 [91]	3.002	-9%
Nereus	3.218 [89]	2.853	-11%
Odra Energia	2.909 [90]	2.683	-8%
Sicily South	3.083 [91]	2.750	-11%
Rimini	3.139 [92]	2.783	-11%

Mean: 10%

Chapter 6

Conclusion

Facing climate change and future's challenges for world population such as growing in energy demand require investments in new energy technologies and worldwide policies to face commune objectives.

As offshore wind is demonstrating to be a good adding to worldly energy mix, the possibility of utilising this technology among the Mediterranean basin countries, that have good unexploited potential, has inspired this tool that claim to be a good starting point for future projects where there is lack of other similar works.

This work has achieved as goal the characterization, as well as possible, and optimization an user defined floating offshore wind farm placed in Mediterranean basin through creations of models defined by Python functions.

Looking at EU, policies against climate change has already push spread of renewables in energy mix and this is valid also for Mediterranean countries that see clean energy as an objective. On the other hand, a still large utilisation of conventional energy commodities (oil and gas) from non-EU North African countries is detected.

Role of offshore wind as a very promising technology among the renewable scenario is claimed: with its large potential and developing technology, energy companies see offshore wind as a very profitable investment. This technology offers a large opportunity for business in this sector due to large unexploited potential that could offer in next future one solution to renewable energy request and a way of valorising maritime areas for example near Mediterranean island and for less developed Mediterranean countries.

From a technical point of view several technologies for offshore wind has been developed to face different sea and wind condition starting with different types of floating platforms (TLP, Spar, Semi-Sub) as well as mooring and anchorage typologies to deal with several type of seabed condition.

The scope of this thesis namely the optimization of layout of offshore wind farm is a crucial step to maximize investments and guarantees low visual impact from the nearest coast. From the very simplest layout (rectangular, radial), optimized layout (staggered, irregular) can meet these goals. In order to optimize layout of wind farms several approaches have been developed and can be found in literature (gradient-based, heuristics and metaheuristics). Such method present pros and cons based on problem typology and number of variables and objectives to be optimized.

6. Conclusion

Talking about economic perspective of offshore wind in MED region, with a focus on exploitable areas and already presented projects under approval state, in this work has been explained how this technology is nowadays untapped in the area due to lack of infrastructure and clear regulatory frameworks that, both with higher costs compared to other regions, make this technology at embryonal state.

Regarding tool construction after site selection in considering user input constraint minimum and maximum bathymetry levels, maritime routes, minimum distance to the coast data collection has been performed in utilising wind and bathymetry grid of Mediterranean as well as turbine power curves for different size. Then models have been created from collected data with PyWake library: *site model* with Weibull wind distribution divided in ten main sectors while *fluid-dynamic model* in choosing different approaches in characterizing air stream behaviour for wake losses estimation. Models varies between the most precise but more computational expensive and the simpler but less precise. Good results have been achieved in case study simulations in utilising *BastankhahGaussianDeficit* conjugate precision and velocity of simulations.

LCOE calculation so minimum price of sellable energy to recover costs within life cycle of plant, with detailed economical model deep description, has been defined for every voice of cost considering various lifetime phase of projects as well as costs for every component that has been estimated. Economic model has better defined the installation costs considering the distance from nearest feasible port for every position. LCOE is a crucial value for wind farm evaluation as it indicates a sort of efficiency for the entire plant.

Important aspect of optimization so study of visual impact has been conducted with creation of a model to investigate parameters of visualization of farm from nearest cost point with the aim of reduce impact for coasts citizens namely horizon occupation area and distinguishable turbines.

Talking about optimization methodology, functions has been created with *Pymoo* library using a Genetic Algorithm. NSGA-2 implemented for this tool carry on a multi-objective optimization: minimize LCOE computed with economical model and minimize visual impact parameter of horizon occupation.

Parameters of layouts design and so distance in wind and crosswind direction (D_x and D_y), angle between nearest arrays (β) and staggering distance (SD_y) has been stated. Distance D_x and D_y are measured in diameters of turbines considered. The objectives of changing layout are reducing as much as possible wake losses that affect heavily energy production and so LCOE value as well as stacking arrays towards the visual point of the coast to occupy less horizon area as possible.

Evaluation of algorithm performance trough convergence indicators such as hypervolume and visualization of Pareto front that represent the ensemble of non-dominated results has been carried on. Through multiple non dominated results found only one layout is then selected that is a good compromise between two objectives.

6. Conclusion

To make an account of entire work of tool first in a map of feasible MED region for fixed input data for bathymetry and for collected wind speed data.

A comparison between a non-optimized (fixed rectangular layout) and an optimized layout has been carried out with a random selected farm has showed better performance in AEP +2% (annual energy production) and lower Capex+Opex that goes from 2.71 to 2.66 M€/MW costs that have minimized LCOE from 104.9 to 101.8 €/MWh, less occupied farm area 129,4 in non-optimized case versus 29.15 sqkm in optimized case as well as less occupied horizon from nearest coast point of view that has decreased from 171.3 to 92.8 cm^2 so every objectives of optimization have been achieved. From the costs breakdown can be seen how percentages of connection costs have changed from 18.4% to 16.9% following the reduction of area of farm that means lower cables utilisation that has been reduced from 213 to 112 km of medium voltage inter array cables length.

Approved presented projects in MED region has been selected to test tool in realistic case. For every case study results of optimization has leaded to an increase of AEP in avoiding fluid dynamic losses (+17% for Atis, +17% for Nora Energia 1, +17% for MedWind, +16% for Nereus, +19% for OdraEnergia, +19% for Sicily South, +12% for Rimini) with respect to a fixed rectangular layout. Costs Capex+Opex have increased (+2% for Atis, +2% for Nora Energia 1, +4.4% for MedWind, +2% for Nereus, nearly same for OdraEnergia, +2.5% for Sicily South, same for Rimini) for the connection costs due to increased cables because major distances between turbines.

LCOE so has been good optimized in lowering every value (-16% for Atis, -16.5% for Nora Energia 1, -14% for MedWind, -23% for Nereus, -19.7% for OdraEnergia, -17% for Sicily South, -10% for Rimini)

Nominal values of LCOE in €/MWh 122.7 for Atis, 88.59 for Nora Energia 1, 103.6 for MedWind, 108 for Nereus, 107.6 for OdraEnergia, 104.67 for Sicily South, 235.9 for Rimini are in range for this type of plants with the exception of Rimini site that present scarce wind source.

For what concern visual impact of farms results of optimization does not always improve parameter of occupied horizon area value but in such case results show good improvement (+2.7% for Atis, -21% for Nora Energia 1, same value for MedWind, +0.5% for Nereus, -25% for OdraEnergia, -9.5% for Sicily South, +24.7% for Rimini)

To show fidelity of constructed model to real cases a validation analysis has been carried on. Chosen evaluation parameters is cost for installed MW because, as assessed before, offshore floating wind farm in Mediterranean are at project phase and so real data about energy production and losses do not exist. Comparison has given good results in terms of fidelity of economic model considering all approximation and assumptions made with estimated costs that are -10% from real estimated costs from project.

6. Conclusion

The multi-objective optimization function presented in this work so a balance between visual impact and LCOE reduction is nearly unique among literature. Other works from literature about offshore wind multi-optimization (i.e minimum LCOE and maximum efficiency, AEP maximization and minimum Capex) with GA algorithm has rejoined different results for case with fixed farm area for example in grid connection share costs and so length of cable that can be half in such case. This evidences how pursuing visual impact minimization or minimization of LCOE can tend to extend too much distance between turbines. Regarding results for other works with visual impact and LCOE minimization algorithms resulting Pareto front shape is comparable. Off course in case of other farms optimizations LCOE values can be lower if algorithm is focused on only minimizing LCOE (mono-objective optimization). However, GA has performed nearly the same compared with other studies since LCOE value between first generation and last generation has changed about 2 €/MWh.

The algorithm has been developed following also time balance, to not weight too much the computational time compromise in grid resolution for bathymetry and consequently for all utilization that has been made of the same grid for example the research for the nearest port facilities.

This tool will be a support in terms of how good placing and optimized layout are fundamental to abate cost, exploit maximum wind potential and give minimum impact to population that live near interested area and to economical regional maritime activities.

6.1 Limitations and further works

Some limitations must be considered while using this tool. The first limitation regards the grid limit, since the base for calculation of bathymetry and distances not all points have been considered but with one point out of ten dividing grid in (432*1128) elements, each element approximate a maritime area of 18.75 sqkm in which the bathymetry is considered uniform. This can be a problem for preliminary studies of a farm that has to considered platform type and mooring depending on sea deep.

Another limitation due to grid resolution is the calculated distance from nearest port facility that influence installation cost. The implemented Dijkstra algorithm is influenced in functioning by grid resolution, a sensitivity analysis has been performed in **APPENDIX A**.

Some improvements that can be made for the tool in future work to better characterize the model could be:

- Improvements in grid resolution that could permit better results in terms of place characterization and on economical evaluation.
- Implementation of new limitations for feasibility limitations to give fidelity to real exploitable areas.
- For visual impact study visualization parameters may be studied in considering most populated areas instead of nearest coast point.
- Study for better characterize costs accounting for onshore cables and national grid connections with individuation on the grid of connection point.
- As floating wind farms become widespread in the Mediterranean basin in the future, it will be beneficial to account for fluid dynamic effects on nearby farms acting on each other.

In conclusion, the journey of this research has reinforced the critical role of innovation in the sustainability sector, affirming that with the right tools and approaches, the harnessing of wind energy can be significantly optimized to meet and exceed global energy needs sustainably

BIBLIOGRAPHY

[1] J. Muñoz Arias, « Technical and economic analysis of offshore wind turbine farms», Master thesis, Politecnico di Torino, 04 September 2023.

[2] L. Baisi, «Estimation and analysis of offshore renewable energy potential for Mediterranean Sea.», laurea, Politecnico di Torino, 2023. [Online]. Available on: https://webthesis.biblio.polito.it/26050/

[3] «MOREnergy Lab - Marine Offshore Renewable Energy», MOREnergy Lab. [Online]. Available on: http://www.morenergylab.polito.it/

[4] A. Cheung, «Energy Transition Investment Trends 2024». January 30, 2024.

[5] «Electricity and heat statistics», ISSN 2443-8219, July 2022, [Online]. Available on: https://ec.europa.eu/eurostat/statistics-explained/index.php?title=Electricity_and_heat_statistics

[6] «Il Green Deal europeo - Commissione europea». [Online]. Available on: https://commission.europa.eu/strategy-and-policy/priorities-2019-2024/european-green-deal_it

[7] «REPowerEU». [Online]. Available on: https://commission.europa.eu/strategy-and-policy/priorities-2019-2024/european-green-deal/repowereu-affordable-secure-and-sustainable-energy-europe_it

[8] WindEurope, «Wind energy in Europe - 2023 Statistics and the outlook for 2024-2030», February 2024. [Online].

[9] P. Bastida-Molina, E. Hurtado-Pérez, M. C. M. Gómez, J. Cárcel-Carrasco, e Á. Pérez-Navarro, «Energy sustainability evolution in the Mediterranean countries and synergies from a global energy scenario for the area», *Energy*, vol. 252, p. 124067, 2022, doi: https://doi.org/10.1016/j.energy.2022.124067.

[10] M.Kreider, F.Oteri, A.Robertson, C.Constant, E.Gill, «Offshore Wind Energy: Technology Below the Water». [Online]. Available on: https://www.nrel.gov/docs/fy22osti/83142.pdf

[11] H. Díaz e C. Guedes Soares, «Cost and financial evaluation model for the design of floating offshore wind farms», Centre for Marine Technology and Ocean Engineering (CENTEC), Instituto Superior Tecnico, Universidade de Lisboa, Lisbon, Portugal, 25 September 2023.

[12] J. Feng e W. Z. Shen, «Design optimization of offshore wind farms with multiple types of wind turbines», *Appl. Energy*, vol. 205, pp. 1283–1297, 2017, doi: https://doi.org/10.1016/j.apenergy.2017.08.107.

[13] Z. Yong, Q.Shengli «A Practical Optimization for Offshore Wind Farm Layout», Renowind Energy Technology (Beijing) Co., Ltd. Beijing, China.

[14] M. Kumar, B. Das, P. Nallagownden, I. Elamvazuthi, e S. Khan, «Optimal Configuration of Wind Farms in Radial Distribution System Using Particle Swarm Optimization Technique», *Bull. Electr. Eng. Inform.*, vol. 7, pp. 286–293, giu. 2018, doi: 10.11591/eei.v7i2.1224.

[15] J. F. Herbert-Acero, O. Probst, P.-E. Réthoré, G. Chr. Larsen, e K. K. Castillo-Villar, «A Review of Methodological Approaches for the Design and Optimization of Wind Farms», *Energies*, vol. 7, fasc. 11, pp. 6930–7016, 2014, doi: 10.3390/en7116930.

[16] D. Guirguis, D. A. Romero, e C. H. Amon, «Gradient-based multidisciplinary design of wind farms with continuous-variable formulations», *Appl. Energy*, vol. 197, pp. 279–291, 2017, doi: https://doi.org/10.1016/j.apenergy.2017.04.030.

[17] J. Park e K. H. Law, «Layout optimization for maximizing wind farm power production using sequential convex programming», *Appl. Energy*, vol. 151, pp. 320–334, 2015, doi: https://doi.org/10.1016/j.apenergy.2015.03.139.

[18] M. Wagner, J. Day, e F. Neumann, «A fast and effective local search algorithm for optimizing the placement of wind turbines», *Renew. Energy*, vol. 51, pp. 64–70, 2013, doi: https://doi.org/10.1016/j.renene.2012.09.008.

[19] K. Chen, M. X. Song, X. Zhang, e S. F. Wang, «Wind turbine layout optimization with multiple hub height wind turbines using greedy algorithm», *Renew. Energy*, vol. 96, pp. 676–686, 2016, doi: https://doi.org/10.1016/j.renene.2016.05.018.

[20] G. Marmidis, S. Lazarou, e E. Pyrgioti, «Optimal placement of wind turbines in a wind park using Monte Carlo simulation», *Renew. Energy*, vol. 33, fasc. 7, pp. 1455–1460, 2008, doi: https://doi.org/10.1016/j.renene.2007.09.004.

[21] S. A. Grady, M. Y. Hussaini, e M. M. Abdullah, «Placement of wind turbines using genetic algorithms», *Renew. Energy*, vol. 30, fasc. 2, pp. 259–270, 2005, doi: https://doi.org/10.1016/j.renene.2004.05.007.

[22] K.Yang and K. Cho « Simulated Annealing Algorithm for Wind Farm Layout Optimization: A Benchmark Study», *Faculty of Wind Energy Engineering, Jeju National University, 102 Jejudaehakno, Jeju 63243, Korea, Published: 20 November 2019*

[23] C. Wan, J. Wang, G. Yang, e X. Zhang, «Particle swarm optimization based on Gaussian mutation and its application to wind farm micro-siting», in *49th IEEE Conference on Decision and Control (CDC)*, 2010, pp. 2227–2232. doi: 10.1109/CDC.2010.5716941.

[24] J.Lee, F.Zhao «GWEC-Global-Wind-Report-2024 ». [Online]. Available on: https://gwec.net/wp-content/uploads/2024/05/GWR-2024_digital-version_final-2.pdf

[25] «Eolico Offshore Galleggiante: opportunità nel percorso di decarbonizzazione e ricadute industriali per l'Italia». [Online]. Available on: https://cdn.qualenergia.it/wp-content/uploads/2023/09/010923_Presentazione-conferenza-stampa-Cernobbio_ITA1.pdf

[26] E. Commission *et al.*, *Study on the offshore grid potential in the Mediterranean region – Final report*. Publications Office of the European Union, 2020. doi: doi/10.2833/742284.

[27] A. E. Gharras e E. Menichetti, «Offshore wind in the Mediterranean», 10 September 2023.

[28] «Beleolico - Renexia». [Online]. Available on: https://renexia.it/beleolico-progetti/

[29] «Provence Grand Large | Découvrez le projet». [Online]. Available on: https://provencegrandlarge.fr/

[30] «EOLMED Project». [Online]. Disponibile su: https://www.bw-ideol.com/en/eolmed-project

[31] «Il Parco Med Wind», Med Wind. [Online]. Available on: https://medwind.it/parco-eolico-offshore-medwind/

[32] «Progetto per la realizzazione di un parco eolico offshore flottante denominato "Atis" - Mar Ligure, Toscana, potenza complessiva di 864 MW - Info - Environmental Assessments and Authorizations - SEA - EIA - IPPC Permit. [Online]. Disponibile su: https://va.mite.gov.it/en-GB/Oggetti/Info/10119

[33] «Il parco», Tibula. [Online]. Available on: https://tibulaenergia.it/ilparco/

[34] «Progetto di un impianto eolico off-shore denominato "Nereus", composto da 120 aerogeneratori di potenza unitaria pari a 15 MW, per una potenza totale d'impianto di 1800 MW, da realizzarsi al largo della Regione Puglia, nel Mar Adriatico Meridionale, incluse le opere di connessione con approdo costiero nel Comune di Barletta (BT). - Info - Environmental Assessments and Authorizations - SEA - EIA - IPPC Permit». [Online]. Available on: https://va.mite.gov.it/en-GB/Oggetti/Info/9734

[35] T. Stehly, P. Duffy, e D. M. Hernando, «2022 Cost of Wind Energy Review», National Renewable Energy Laboratory, December 2023. [34]

[36] R. Ferrari, «Optimization of the spatial disposition of an array of floating offshore wind turbines using a Python genetic algorithm», laurea, Politecnico di Torino, 2023. [Online]. Available on: https://webthesis.biblio.polito.it/27138/

[37] P. Beiter *et al.*, «A Spatial-Economic Cost-Reduction Pathway Analysis for U.S. Offshore Wind Energy Development from 2015–2030», NREL/TP--6A20-66579, 1324526, set. 2016. doi: 10.2172/1324526.

[38] A.Koch, «BalticLINes_CapacityDensityStudy», Federal Maritime and Hydrographic Agency (BSH) [Online]. Available on: https://vasab.org/wp-content/uploads/2018/06/BalticLINes_CapacityDensityStudy_June2018-1.pdf

[39] N. Maslov, C. Claramunt, T. Wang, e T. Tang, «Method to estimate the visual impact of an offshore wind farm», *Appl. Energy*, vol. 204, pp. 1422–1430, 2017, doi: https://doi.org/10.1016/j.apenergy.2017.05.053.

[40] Copernicus Climate Change Service, «CERRA sub-daily regional reanalysis data for Europe on height levels from 1984 to present», 2022. doi: 10.24381/CDS.38B394E6.

[41] «GEBCO data download». [Online]. Available on: https://download.gebco.net/

[42] B. Tozer, D. T. Sandwell, W. H. F. Smith, C. Olson, J. R. Beale, e P. Wessel, «Global Bathymetry and Topography at 15 Arc Sec: SRTM15+», *Earth Space Sci.*, vol. 6, fasc. 10, pp. 1847–1864, ott. 2019, doi: 10.1029/2019EA000658.

[43] U. Kumar, «Reading NetCDF4 Data in Python (codes included)», [Online]. Available on: https://earthinversion.com/utilities/reading-NetCDF4-data-in-python/

[44] Jon Blower, «Lesson 3: Plotting Data from NetCDF file», 17 September 2014, [Online]. Available on: https://notebook.community/jonblower/python-viz-intro/Lesson%203.%20Plotting%20data%20from%20NetCDF%20files/3.%20Plotting%20data%20from%20NetCDF%20files

[45]]K. Hafen, «Read NetCDF Data with Python», Medium, 9 July 2020, [Online]. Available on: https://towardsdatascience.com/read-netcdf-data-with-python-901f7ff61648

[46] «Gridded data, NetCDF — Oceanography with python». [Online]. Available on: https://lijodxl.github.io/OceanographyWithPython/L4-working_with_netCDF.html

[47] «EMODnet Map Viewer». [Online]. Available on: https://emodnet.ec.europa.eu/geoviewer/#!/

[48] «Benvenuto in QGIS!» . [Online]. Available on:: https://qgis.org/it/site/

[49] «WGS84», *Wikipedia*. 26 luglio 2023. [Online]. Available on: https://it.wikipedia.org/w/index.php?title=WGS84&oldid=134643081

[50] «National Renewable Energy Laboratory (NREL) Home Page». [Online]. Available on: https://www.nrel.gov/index.html

[51] «Seventh framework programme of the European Community for research and technological development including demonstration activities(FP7) | Programme | FP7», CORDIS | European Commission. [Online]. Available on: https://cordis.europa.eu/programme/id/FP7/es

[52] «Welcome to PyWake — PyWake 2.5.1.dev61+gc9dea98 documentation».. [Online]. Disponibile su: https://topfarm.pages.windenergy.dtu.dk/PyWake/

[53] «Windenergie-Daten der Schweiz». [Online]. Available on: https://wind-data.ch/tools/weibull.php?lng=en

[54] B. Pérez, R. Mínguez, e R. Guanche, «Offshore wind farm layout optimization using mathematical programming techniques», *Renew. Energy*, vol. 53, pp. 389–399, mag. 2013, doi: 10.1016/j.renene.2012.12.007.

[55] «Site Object — PyWake 2.5.1.dev61+gc9dea98 documentation». [Online]. Available on: https://topfarm.pages.windenergy.dtu.dk/PyWake/notebooks/Site.html#XRSite

[56] «Engineering Wind Farm Models Object — PyWake 2.6.1.dev1+g227be36 documentation».. [Online]. Available on: https://topfarm.pages.windenergy.dtu.dk/PyWake/notebooks/EngineeringWindFarmModels.html

[57] PyWake development team, «Automated validation report for PyWake», DTU Wind Energy, May 2024.

[58] M. Bastankhah e F. Porté-Agel, «A new analytical model for wind-turbine wakes», *Renew. Energy*, vol. 70, pp. 116–123, 2014, doi: https://doi.org/10.1016/j.renene.2014.01.002.

[59] «Qualification of innovative floating substructures for 10MW wind turbines and water depths greater than 50m - LCOE tool description, technical and environmental impact evaluation procedure», Fundació Institut de Recerca en Energia de Catalunya-IREC, 10 June 2016

[60] A. Myhr, C. Bjerkseter, A. Ågotnes, e T. A. Nygaard, «Levelised cost of energy for offshore floating wind turbines in a life cycle perspective», *Renew. Energy*, vol. 66, pp. 714–728, giu. 2014, doi: 10.1016/j.renene.2014.01.017.

[61] «Qualification of innovative floating substructures for 10MW wind turbines and water depths greater than 50m - LCOE tool description, technical and environmental impact evaluation procedure», Fundació Institut de Recerca en Energia de Catalunya-IREC, 10 June 2016 [62]J. Chen e M.-H. Kim, «Review of Recent Offshore Wind Turbine Research and Optimization Methodologies in Their Design», *J. Mar. Sci. Eng.*, vol. 10, fasc. 1, Art. fasc. 1, gen. 2022, doi: 10.3390/jmse10010028.

[63] R. James e M. Costa Ros, «Floating Offshore Wind Market Technology Review», June 2015 [Online]. Available on: https://ctprodstorageaccountp.blob.core.windows.net/prod-drupal-files/documents/resource/public/Floating%20Offshore%20Wind%20Market%20Technology%20Review%20-%20REPORT.pdf

[64] S. Heidari, «ECONOMIC MODELLING OF FLOATING OFFSHORE WIND POWER», Mälardalens högskola eskilstuna västerås, Project in Industrial Engineering and Management with Specialization in Energy Engineering, 06/09/2017.

[65] «Offshore Wind Ports Platform», WindEurope. [Online]. Available on: https://windeurope.org/policy/topics/offshore-wind-ports/

[66] «Algoritmo di Dijkstra», *Wikipedia*. 14 dicembre 2023. [Online]. Available on: https://it.wikipedia.org/w/index.php?title=Algoritmo_di_Dijkstra&oldid=136889292

[67] A. Haugen, «Dijkstra's Shortest Path Algorithm», Medium, 20 Apr 2021. [Online]. Available on: https://antonhaugen.medium.com/dijkstras-shortest-path-algorithm-cb8d0a7ae642

[68] «Shortest Paths — NetworkX 3.3 documentation». [Online]. Available on: https://networkx.org/documentation/stable/reference/algorithms/shortest_paths.html

[69] «Welcome to GeoPy's documentation! — GeoPy 2.4.1 documentation». [Online]. Available on: https://geopy.readthedocs.io/en/stable/

[70] C. Elkinton, J. Manwell, e J. McGowan, «Offshore Wind Farm Layout Optimization (OWFLO) Project: Preliminary Results», in *44th AIAA Aerospace Sciences Meeting and Exhibit*. doi: 10.2514/6.2006-998.

[71] NIRANJAN S. GHAISAS e CRISTINA L. ARCHER, «Geometry-Based Models for Studying the Effects of Wind Farm Layout», Journal of Atmospheric and Oceanic Technology, July 2015, DOI:10.1175/JTECH-D-14-00199.1.

[72] C. L. Archer, S. Mirzaeisefat, e S. Lee, «Quantifying the sensitivity of wind farm performance to array layout options using large-eddy simulation», *Geophys. Res. Lett.*, vol. 40, fasc. 18, pp. 4963–4970, 2013, doi: 10.1002/grl.50911.

[73] «Visione periferica», *Wikipedia*. 16 ottobre 2023. [Online]. Available on: https://it.wikipedia.org/w/index.php?title=Visione_periferica&oldid=136003741

[74] H. SHANG e I. D. BISHOP, «VISUAL THRESHOLDS FOR DETECTION, RECOGNITION AND VISUAL IMPACT IN LANDSCAPE SETTINGS», *J. Environ. Psychol.*, vol. 20, fasc. 2, pp. 125–140, 2000, doi: https://doi.org/10.1006/jevp.1999.0153.

[75] G. Narzisi, «Classic Methods for Multi-Objective Optimization», Courant Institute of Mathematical Sciences New York University, 31 January 2008.

[76] K. Deb, «Multiobjective Optimization Using Evolutionary Algorithms. Wiley, New York», 2001.

[77] J. Blank e K. Deb, «Pymoo: Multi-Objective Optimization in Python», *IEEE Access*, vol. 8, pp. 89497–89509, 2020, doi: 10.1109/ACCESS.2020.2990567.

[78] «pymoo - Sampling». [Online]. Available on: https://pymoo.org/operators/sampling.html

[79] «pymoo - Selection». [Online]. Available on: https://pymoo.org/operators/selection.html

[80] «pymoo - Crossover». [Online]. Available on: https://pymoo.org/operators/crossover.html

[81] «pymoo - Part IV: Analysis of Convergence». [Online]. Available on: https://pymoo.org/getting_started/part_4.html

[82] «Home - Valutazioni e Autorizzazioni Ambientali - VAS - VIA - AIA».[Online]. Available on: https://va.mite.gov.it/it-IT

[83] «Nora Energia 1 - Nora Energia». [Online]. Available on: https://noraenergia.it/noraenergia1/

[84] «Odra Energia, per la produzione di Energia Pulita», Odra Energia.[Online]. Available on: https://www.odraenergia.it/

[85] «Our Projects - Hexicon». [Online]. Available on: https://www.hexicongroup.com/our-projects/

[86] «Marche 1 (Italy) - Wind farms - Online access - The Wind Power». [Online]. Available on: https://www.thewindpower.net/windfarm_en_31058_marche-1.php

[87] B.Coraggioso e M.Molinaroli, «Atis Floating Wind S.r.l. - Relazione Generale», Doc. No. ATI-RIN-TEC-GEN-RPT-0002-R00, lug. 2023.

[88] N.Nobile, «Progetto preliminare per la realizzazione di un parco eolico offshore - Cagliari – Nora Energia 1», Doc. No. P0025305-4-H17-Rev.00, mag. 2022.

[89] JBA01, «Parco Eolico Offshore - Nereus», P0031639-6-H2 Rev.0, apr. 2023.

[90] «Progetto preliminare per la realizzazione di un parco eolico offshore - Lecce - Odra Energia- Stima preliminare delle opere e quadro economico», P0025305-1-H17 Rev.03, dic. 2021.

[91] «PROGETTO DI UNA CENTRALE EOLICA OFFSHORE GALLEGGIANTE NEL CANALE DI SICILIA DENOMINATA “SICILY SOUTH” E DELLE RELATIVE OPERE DI CONNESSIONE ALLA RETE ELETTRICA NAZIONALE - STUDIO PRELIMINARE AMBIENTALE», SS.SCOP.R.11.01, feb. 2023.

[92] ANALISI DEI COSTI E BENEFICI SOCIALI DELLA, REALIZZAZIONE ED ESERCIZIO DELLA, e CENTRALE EOLICA OFF-SHORE “RIMINI”, «ANALISI DEI COSTI E BENEFICI SOCIALI DELLA REALIZZAZIONE ED ESERCIZIO DELLA CENTRALE EOLICA OFF-SHORE “RIMINI”», feb. 2022.

[91] E.Boscarino, «Progetto di una centrale eolica offshore nello stretto di Sicilia e delle relative opere di connessione alla rete elettrica nazionale - Studio preliminare ambientale - Stima preliminare delle opere e quadro economico», R.08.00, 10/10/2020

APPENDIX A

In order to give an account of how precise the search function for nearest port a sensitivity analysis has been performed considering various case among all Mediterranean area. For such comparison only offshore route has been chosen avoiding land.

Wind farm point	**Nearest port**	**Distance algorithm (km)**	**Real distance (km)**	**Relative error**
37° 47’ N 25° 17’ E	37° 27’ N 25° 20’ E	41,56	36,78	+11,5%
38° 0’ N 3° 0’ E	36° 45’ N 3° 5’ E	142,77	139,31	+3%
43° 0’ N 4° 13’ E	43° 42’ N 4° 53’ E	98,43	86,59	+12%
34° 0’ N 30° 0’ E	31° 10’ N 29° 50’ E	280	273,84	+2,2%

Relative error between real and computed distance is going up to 12%. Better results and so calculated distance can be done in rise up resolution of the grid for example in taking 1 point out 5 or 1 point out 2 but this condition will tend to increase time of running of the code. Maybe this will be a work for future improvements.

APPENDIX B

Port (Country)	Longitude	Latitude
Port of Durres (Albania)	19,45	41,32
Port of Alger (Algeria)	3,07	36,77
Port of Mers el Kebir (Algeria)	-0,70	35,73
Port of Mostaganem (Algeria)	0,08	35,93
Port of Bejaia (Algeria)	5,08	36,75
Port of Kyrenia (Cyprus)	33,33	35,35
Port of Famagusta (Cyprus)	33,93	35,12
Port of Pula (Croatia)	13,80	44,88
Port of Rijeka (Croatia)	14,43	45,33
Port of Sibenik (Croatia)	15,88	43,73
Port of Split (Croatia)	16,43	43,50
Port of Zadar (Croatia)	15,22	44,12
Port of Fos-sur-Mer (France)	4,88	43,42
Port of Marseille (France)	5,37	43,32
Port of Antibes (France)	7,13	43,58
Port of Calvi (France)	8,75	42,57
Port of Toulon La Seyne (France)	5,92	43,10
Port of Villefranche (France)	7,32	43,70
Port of Vendres (France)	3,12	42,52
Port of Said Port (Egypt)	32,30	31,27
Port of Alexandria (Egypt)	29,83	31,17
Port of Eleusis (Greece)	23,52	38,03
Port of Perama (Greece)	23,58	37,92
Port of Preveza (Greece)	20,75	38,95
Port of Limin Sirou (Greece)	24,95	37,43
Port of Mikonos (Greece)	25,33	37,45
Port of Limenas Mirina (Greece)	25,07	39,87
Port of Kerkira (Greece)	19,93	39,62
Port of Zakynthos (Greece)	20,90	37,78
Port of Thessaloniki (Greece)	22,93	40,63
Port of Piraeus (Greece)	23,65	37,93
Port of Trieste (Italy)	13,75	45,65

Port of Ravenna (Italy)	12,28	44,50
Port of Catania (Italy)	15,10	37,50
Port of Oristano (Italy)	8,55	39,87
Port of Marghera (Italy)	12,25	45,45
Port of Siracusa (Italy)	15,28	37,05
Port of Sanremo (Italy)	7,78	43,82
Port of Barletta (Italy)	16,28	41,32
Port of Bari (Italy)	16,87	41,13
Port of Monfalcone (Italy)	13,55	45,78
Port of Palermo (Italy)	13,37	38,13
Port of Ancona (Italy)	13,50	43,62
Port of Genoa (Italy)	8,93	44,40
Port of Napoli (Italy)	14,27	40,85
Port of Brindisi (Italy)	17,98	40,65
Port of Livorno (Italy)	10,32	43,55
Port of La Spezia (Italy)	9,83	44,10
Port of Gaeta (Italy)	13,58	41,20
Port of Augusta (Italy)	15,23	37,22
Port of Venezia (Italy)	12,43	45,42
Port of Pesaro (Italy)	12,90	43,92
Port of Gioia Tauro (Italy)	15,87	38,43
Port of Trapani (Italy)	12,50	38,02
Port of Messina (Italy)	15,55	38,20
Port of Bayrut (Lebanon)	35,50	33,90
Port of Benghazi (Lybia)	20,05	32,12
Port of Misurata (Lybia)	15,22	32,37
Port of Tripoli (Lybia)	13,18	32,90
Port of Valletta (Malta)	14,50	35,88
Port of Castelnuovo (Montenegro)	18,55	42,43
Port of Koper (Slovenia)	13,72	45,55
Port of Izola (Slovenia)	13,67	45,53
Port of Al Ladhiqiyah (Syria)	35,77	35,53
Port of Tartus (Syria)	35,87	34,90
Port of Palma (Spain)	2,63	39,55
Port of Escombera (Spain)	-0,95	37,57

Port of Malaga (Spain)	-4,42	36,72
Port of Grao (Spain)	0,02	39,97
Port of Valencia (Spain)	-0,32	39,45
Port of Mahon (Spain)	4,27	39,88
Port of Barcellona (Spain)	2,17	41,35
Port of Algeciras Bay (Spain)	-5,43	36,13
Port of Sfax (Tunisia)	10,77	34,73
Port of Bizerte-Menzel Bourguiba (Tunisia)	9,88	37,27
Port of Istinye (Turkey)	29,05	41,12
Port of Izmir (Turkey)	27,13	38,43
Port of Aksaz Limani (Turkey)	28,38	36,83
Port of Istanbul (Turkey)	28,97	41,02

APPENDIX C

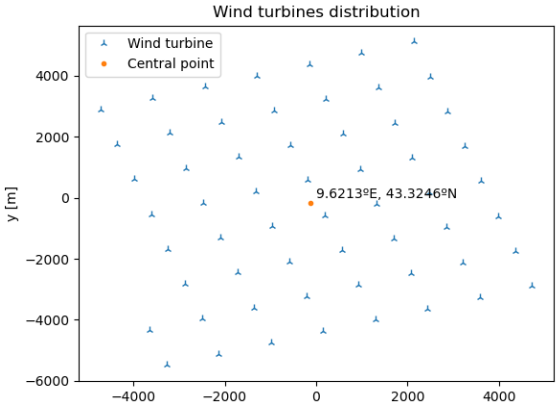

(Atis Non-Optimized layout)

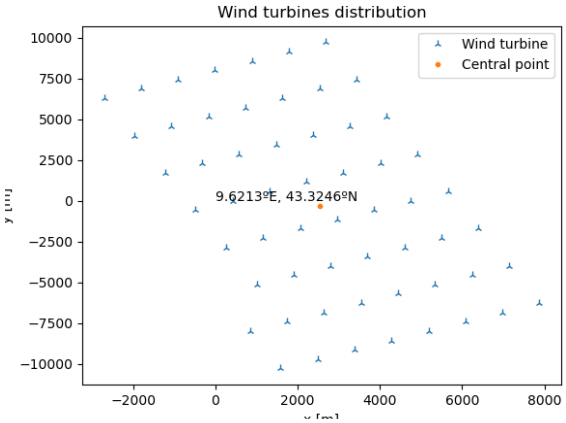

(Atis Optimized layout)

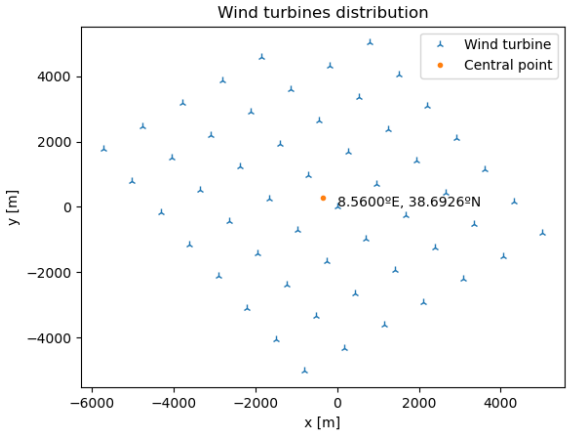

(Nora Energia 1 Non-Optimized layout)

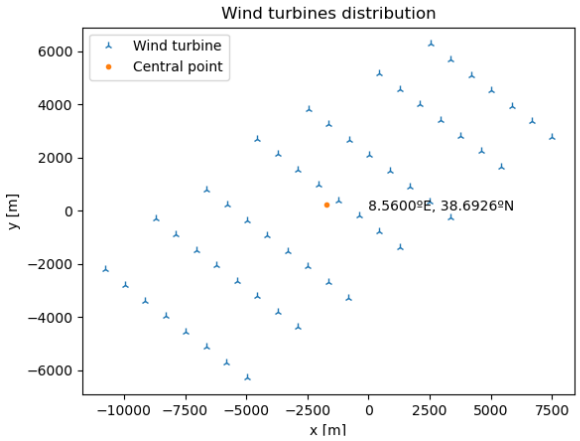

(Nora Energia 1 Optimized layout)

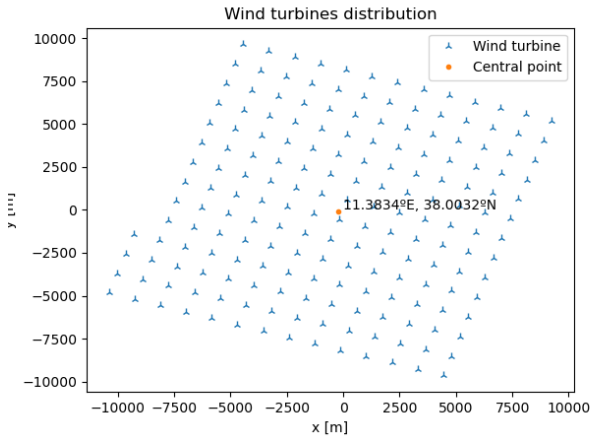

(MedWind Non-Optimized layout)

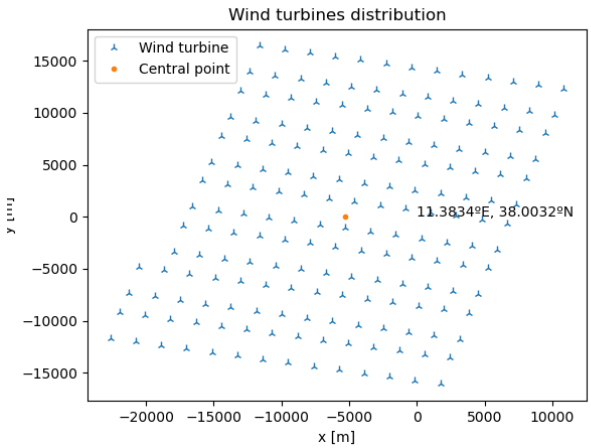

(MedWind Optimized layout)

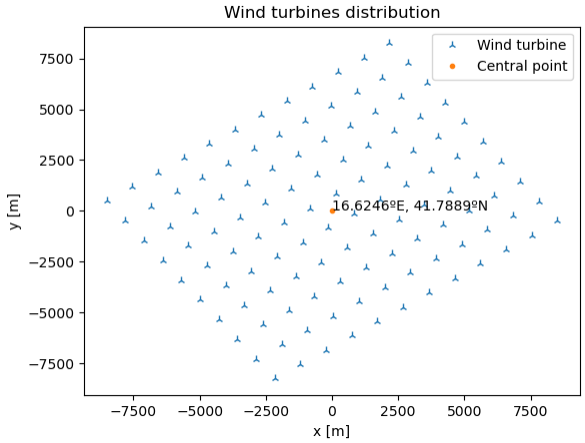

(Nereus Non-Optimized layout)

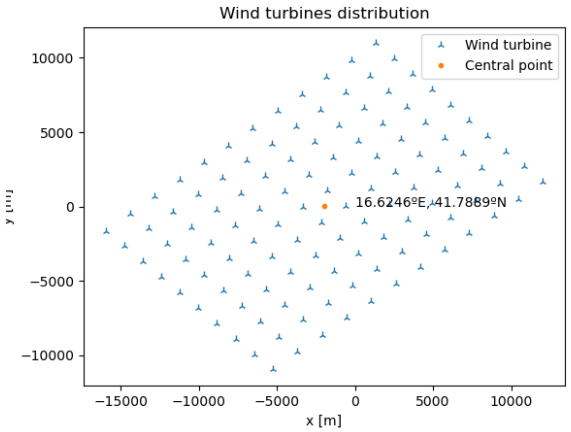

(Nereus Optimized layout)

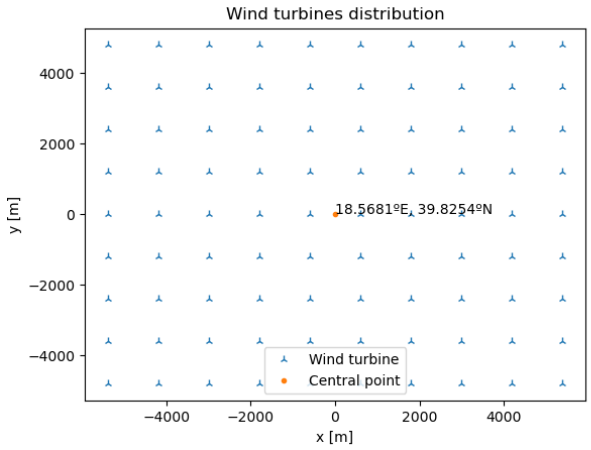

(Odra Energia Non-Optimized layout)

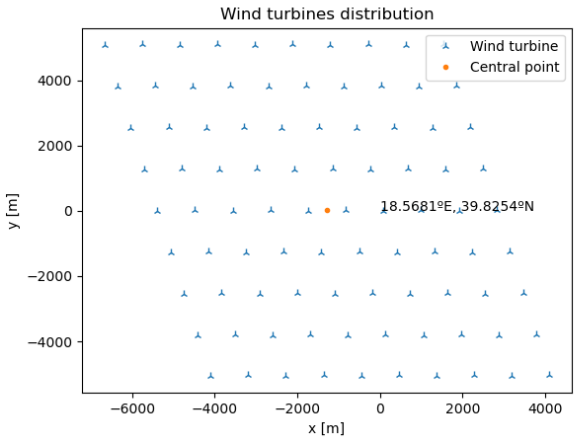

(Odra Energia Optimized layout)

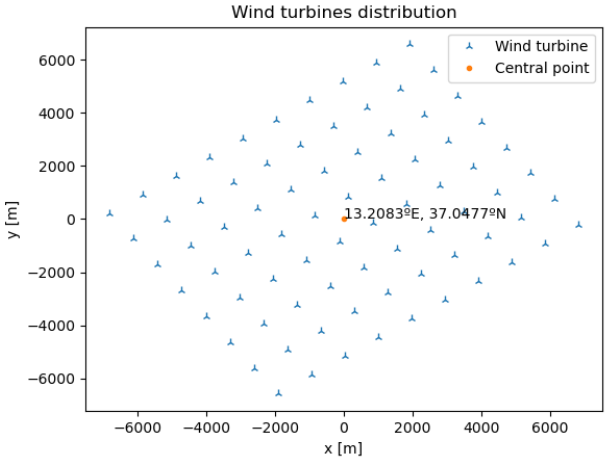

(Sicily South Non-Optimized layout)

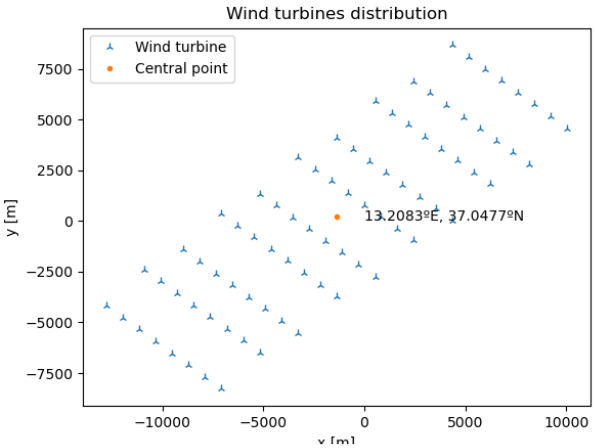

(Sicily South Optimized layout)

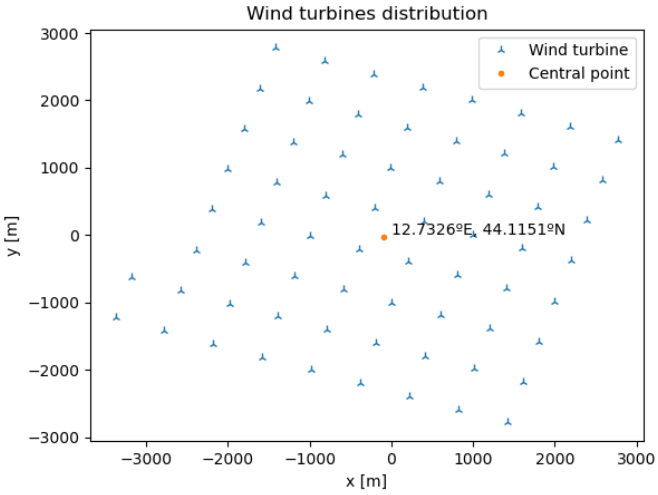

(Rimini Non-Optimized layout)

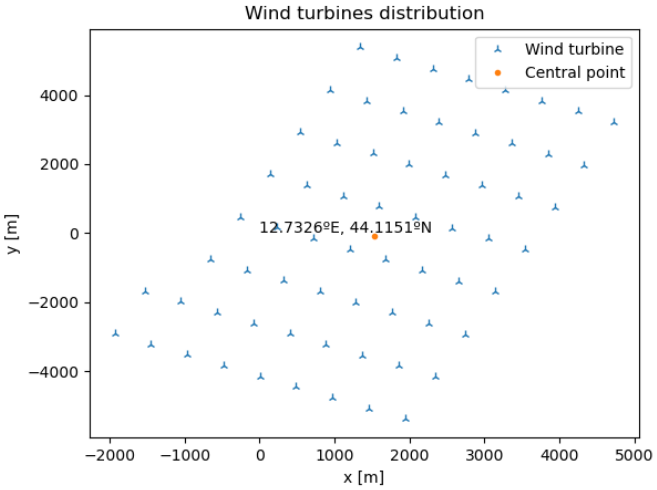

(Rimini Optimized layout)